8.4

ANL/RAS 76-22
VOLUME II

EXPERIMENT NEEDS AND FACILITIES STUDY
APPENDIX A
TRANSIENT REACTOR TEST FACILITY (TREAT) UPGRADE

September 1976

ARGONNE NATIONAL LABORATORY, ARGONNE, ILLINOIS

Prepared for the U. S. ENERGY RESEARCH
AND DEVELOPMENT ADMINISTRATION
under Contract W-31-109-Eng-38

The facilities of Argonne National Laboratory are owned by the United States Government. Under the terms of a contract (W-31-109-Eng-38) between the U. S. Energy Research and Development Administration, Argonne Universities Association and The University of Chicago, the University employs the staff and operates the Laboratory in accordance with policies and programs formulated, approved and reviewed by the Association.

MEMBERS OF ARGONNE UNIVERSITIES ASSOCIATION

The University of Arizona
Carnegie-Mellon University
Case Western Reserve University
The University of Chicago
University of Cincinnati
Illinois Institute of Technology
University of Illinois
Indiana University
Iowa State University
The University of Iowa
Kansas State University
The University of Kansas
Loyola University
Marquette University
Michigan State University
The University of Michigan
University of Minnesota
University of Missouri
Northwestern University
University of Notre Dame
The Ohio State University
Ohio University
The Pennsylvania State University
Purdue University
Saint Louis University
Southern Illinois University
The University of Texas at Austin
Washington University
Wayne State University
The University of Wisconsin

ANL/RAS 76-22

VOLUME II

EXPERIMENT NEEDS AND FACILITIES STUDY

APPENDIX A

TRANSIENT REACTOR TEST FACILITY (TREAT) UPGRADE

September 1976

Reactor Analysis and Safety Division
ARGONNE NATIONAL LABORATORY
9700 South Cass Avenue
Argonne, Illinois 60439

TABLE OF CONTENTS

TABLE OF CONTENTS (Cont'd)

LIST OF FIGURES

LIST OF FIGURES (Contd.)

LIST OF TABLES

LIST OF TABLES (Contd.)

1.0 OVERALL FACILITY MODIFICATION DESCRIPTION

1.1 Summary

The TREAT Upgrade effort is designed to provide significant new capabilities to satisfy experiment requirements associated with key LMFBR Safety Issues. The upgrade consists of reactor-core modifications to supply the physics performance needed for the new experiments, an Advanced TREAT loop with size and thermal-hydraulics capabilities needed for the experiments, associated interface equipment for loop operations and handling, and facility modifications necessary to accommodate operations with the Loop. Section 1.5 summarizes the costs and schedules of the tasks to be accomplished under the TREAT Upgrade project.

Cost, including contingency, is about 10 million dollars (1976 dollars). A schedule for execution of 36 months has been established to provide the new capabilities in order to provide timely support of the LMFBR national effort. A key requirement for the facility modifications is that the reactor availability will not be interrupted for more than 12 weeks during the upgrade.

The Advanced TREAT loop is the prototype for the STF small-bundle package loop. Modified TREAT fuel elements contain segments of graphite-matrix fuel with graded uranium loadings similar to those of STF. In addition, the TREAT upgrade provides for use of STF-like stainless steel-UO_2 TREAT fuel for tests of fully enriched fuel bundles.

This report will introduce the Upgrade study by presenting a brief description of the scope, performance capability, safety considerations, cost schedule, and development requirements.

This work is followed by a "Design Description", Sect. 2.0. Because greatly upgraded loop performance is central to the upgrade, a description is given of Advanced TREAT loop requirements prior to description of the loop concept.

Performance requirements of the upgraded reactor system are given in Sect. 3.0. An extensive discussion of the reactor physics calculations performed for the Upgrade concept study is provided in Appendices. Adequate physics performance is essential for performance of experiments with the Advanced TREAT loop, and the stress placed on these calculations reflects this. Additional material on performance and safety completes Sect. 3.0. Backup calculations on calculations of plutonium-release limits are described in Appendix A-5.

Cost and schedule information for the Upgrade are presented in Sect. 4.0.

1.2 Introduction

1.2.1 Experimental Range

The TREAT Upgrade effort is designed to provide significant and new capabilities for LMFBR safety experiments by upgrading the existing TREAT facility and its supporting facilities. New facilities or a new reactor are not considered; neither is a modification of TREAT which would be so extensive as to involve prolonged shutdown or incur excessive costs.

At present, TREAT is used for tests in the single- to 7-pin size for fuel response to off-normal conditions, margins to failure, failure thresholds and mechanisms, phenomenology of fuel response, immediate postfailure movements, fuel-coolant energetics, and limited information on extended postfailure movements. Both transient overpower (TOP) and transient undercooling (TUC) events have been simulated. Current thermalhydraulics capabilities are limited. The Mark-II TREAT Loop is capable of providing an adequate thermal environment for up to 7 plutonium-bearing irradiated fuel pins, but the pumping capability is not sufficient to produce the prototypic test-train pressure drops and flow rates needed for simulating postfailure conditions. The gas-driven R loop, which also currently accommodates up to seven pins, does provide prototypic pressure drops and flows, but is restricted to fresh, uranium oxide fuels. Thus extensive, model-dependent analytical extrapolations are needed to provide the postfailure movement of many-pin bundles, particularly of irradiated fuel.

The Advanced TREAT loop, which is the prototype for the "small bundle" STF loop, will provide geometric capability for 37 advanced oxide-fuel pins with good thermalhydraulics for simulation of postfailure conditions. Thermalhydraulics performance improves for 19 pins, and the capability of the vehicle can be stretched to up to 91 FTR/CRBR-type pins. The loop is to accommodate irradiated, plutonium-bearing samples. The upgraded TREAT core will provide capability for tests on up to 19 pins of fissile content typical of that in the outer regions of FTR or PFR. It will also have capability for experiments on 61 fullyenriched pins. Over the full range of test sizes, the upgraded TREAT will provide a significant improvement over the current TREAT in sample radial power flattening.

Table 1.1 summarizes the principal ranges of LMFBR Safety Tests to be accommodated in the TREAT Upgrade. Experiments in which the details of

Table 1.1 Principal Types of Tests in Upgraded TREAT

Size	Fuel	Test Category
1-7 Pins	Prototypic Irradiated	Phenomenology of fuel behavior
		Margins to failure
		Failure mechanisms
		Fuel and coolant movements associated with failure
		Fuel-coolant energetics
7-19 Pins	Prototypic Irradiated	Postfailure cluster voiding and fuel movement
		Post HCDA damage limits
		Fuel-coolant energetics
37-61 Pins	Fresh Fuel	Recriticality limits - development of transition phase
		Recriticality limits - transition-phase boilup and dispersal

It sounds like 91 will fit but meaningful tests cannot be run on 91. True?

initial cladding failure-location, timing, size, and propensity for multiple failures are important require fuel previously irradiated under prototypic or near-prototypic conditions. Experiments in which gross postfailure extended fuel motion is the major objective are planned as tests with fresh UO_2 fuel. Decay heat is simulated using TREAT neutrons by programming a low-power "tail" to follow the disruptive power transient proper.

It is expected that the range of LMFBR safety experiments to be conducted with advanced fuels will generally parallel those with the current oxide fuels: TOP, TUC (including TUCOP), and simplified versions of these incidents for studying phenomenology of fuel response. Energetic fuel-coolant-interactions appear at present to be possible with advanced carbide and nitride fuels. Scoping tests will be begun using the Mark-II loops. Data from those tests will be used to determine the quantities of advanced fuels that can be accepted for Advanced loop tests.

Sample energy requirements for advanced fuels are expected to be similar to those for oxides, since the sample enthalpies corresponding to the carbide or nitride liquidus are lower than that for the oxide liquidus. More heat may be lost from the advanced fuel pins during heatup, because of their higher values of fuel thermal conductivity, but this effect can be accommodated by programming of experiment power-flow profiles.

1.2.2 TREAT Upgrade

1.2.2.1 Modified TREAT Fuel

The TREAT driver is a highly thermal graphite-moderated core with carbon-to-^{235}U atom ratio of 10,000:1. Typical experimental vehicles produce large flux depressions and harden neutron spectra in the sample regions. However, even in these cases, it is necessary to provide neutron filters in order to obtain even relatively flat radial power profiles.

TREAT capabilities for LMFBR safety tests will be upgraded by placement of a region of modified TREAT fuel elements around the test hole. Control rods and rod drives will remain unchanged. However, it is recognized that the four rod pairs now located in the inner ring of TREAT rod positions may be moved away from the high-temperature modified elements to outer rod positions not currently occupied. The modified elements will be designed to run in air at temperatures up to 1200°C, and will have TREAT-type graphite fully enriched uranium fuel with higher ^{235}U loadings (i.e. lower C-to-^{235}U atom ratios) to harden the neutron spectrum emerging on the test vehicle, as

well as to prevent power depressions near the vehicle. These elements will be clad with a high-temperature alloy proven for high-temperature service in air and will be handled in the same fashion as the existing TREAT driver fuel. Additional modified elements will be designed of stainless steel-UO_2, to be loaded into TREAT fuel positions near the test hole to provide a wider range of experimental capabilities for fully enriched sample fuel.

1.2.2.2 TREAT Facility Modifications

Minor modifications in the TREAT reactor will be made to accommodate the Advanced TREAT loop. These changes consist of opening up the slot in the rotating top plug to admit the loop, removing the grid-plate insert, and lowering a shielding plug below the grid plate to provide room for bottom plenum pins.

The TREAT crane will be upgraded, and the building roof will be raised for handling of the Advanced TREAT loop cask. In addition the building will be extended to provide space for loop receipt, loading, checkout, and storage fuel; element storage; and test-section cutting operations after tests with fresh, uranium-bearing fuel. Driveway and door modifications will be made to accommodate the SLSF transporter for transfers to and from TREAT.

A TREAT cooling ~~emergency~~ backup or redundant power system will be provided.

1.2.2.3 Interface Equipment and Support Facilities

Interface equipment necessary for the loop experiments will be provided. This consists of two loop-control consoles, one for the loop assembly and prooftest support facility, and one for operations at TREAT; ~~two ALIP power supplies;~~ two ALIP cooling modules; a loop-handling cask; equipment for loop loading at TREAT; equipment for cutup at TREAT of tests with fresh uranium-bearing pins; and additional hodoscope detectors to fill out coverage of the test region in TREAT.

Existing support facilities will be upgraded for the test-train assembly, for loop assembly, and for loop proof testing. HFEF will be used for loading previously irradiated fuel into test trains, and for cutting up previously irradiated fuel. Major pieces of equipment designed for the SLSF Project will be used for the operations. The "TREAT Upgrade" program will provide additional fixtures and equipment where needed.

1.2.3 Advanced TREAT Loop

The Advanced TREAT loop design provides a flexible vehicle for performance of safety experiments producing coolant boiling, fuel melting, and fuel failure. It will accommodate sample pins with bottom or top plena.

Geometrical capability was set at 37 advanced oxide pins. With the Annular Linear Induction Pump (ALIP) selected, this sample size results in a bypass-ratio capability of 2:1. This same geometrical loop envelope has capability for 61 pins with 1:1 bypass and 91 FTR/CRBR-type pins without bypass flow. For smaller clusters, higher bypass flow ratios are obtainable. Instrumentation capability is to match that currently available in TREAT vehicles: test-section thermocouples, pressure transducers, flowmeters, and acoustic sensors, as well as fuel-motion detection with the fast-neutron hodoscope.

The loop design includes capability for tests on previously irradiated, plutonium-bearing fuel samples.

Fig. 1-1 illustrates schematically the Advanced TREAT loop concept. The entire vehicle is inserted into the TREAT reactor from the top and is supported from the TREAT rotating plug. The loop primary is designed to be removable from the reusable secondary containment/ALIP assembly (SCALIP). The test train, tailored to specific experiment requirements, is concentric with the primary, and serves as a flow divider as well as holder for the test fuel and instrumentation. Flow out of the ALIP is downward and then divides into two streams: one flows downward along the outside of the test train to the bottom of the loop, where it turns and flows upward through the test fuel bundle in the test train. Flow is monitored by inlet and outlet flowmeters, and by inlet and outlet pressure transducers. The other flow stream is the bypass, which flows back upward along the outside of the test train and meets the test-section flow at the loop plenum. The bypass capability not only reduces the dependence of loop test-train pressure drop upon events in the test region, but also provides a flow path for simulating LMFBR conditions for flow expulsion out the subassembly inlet.

1.3 Performance

Two reference cases were selected to represent the range of experimental capabilities provided by the TREAT upgrade:

(1) 19 advanced, mixed-oxide fuel pins, with fissile content typical of the outer enrichment zones of FTR or PFR. This configuration is typical of tests for failure and its immediate consequences, using prototypic samples irradiated under prototypic conditions.

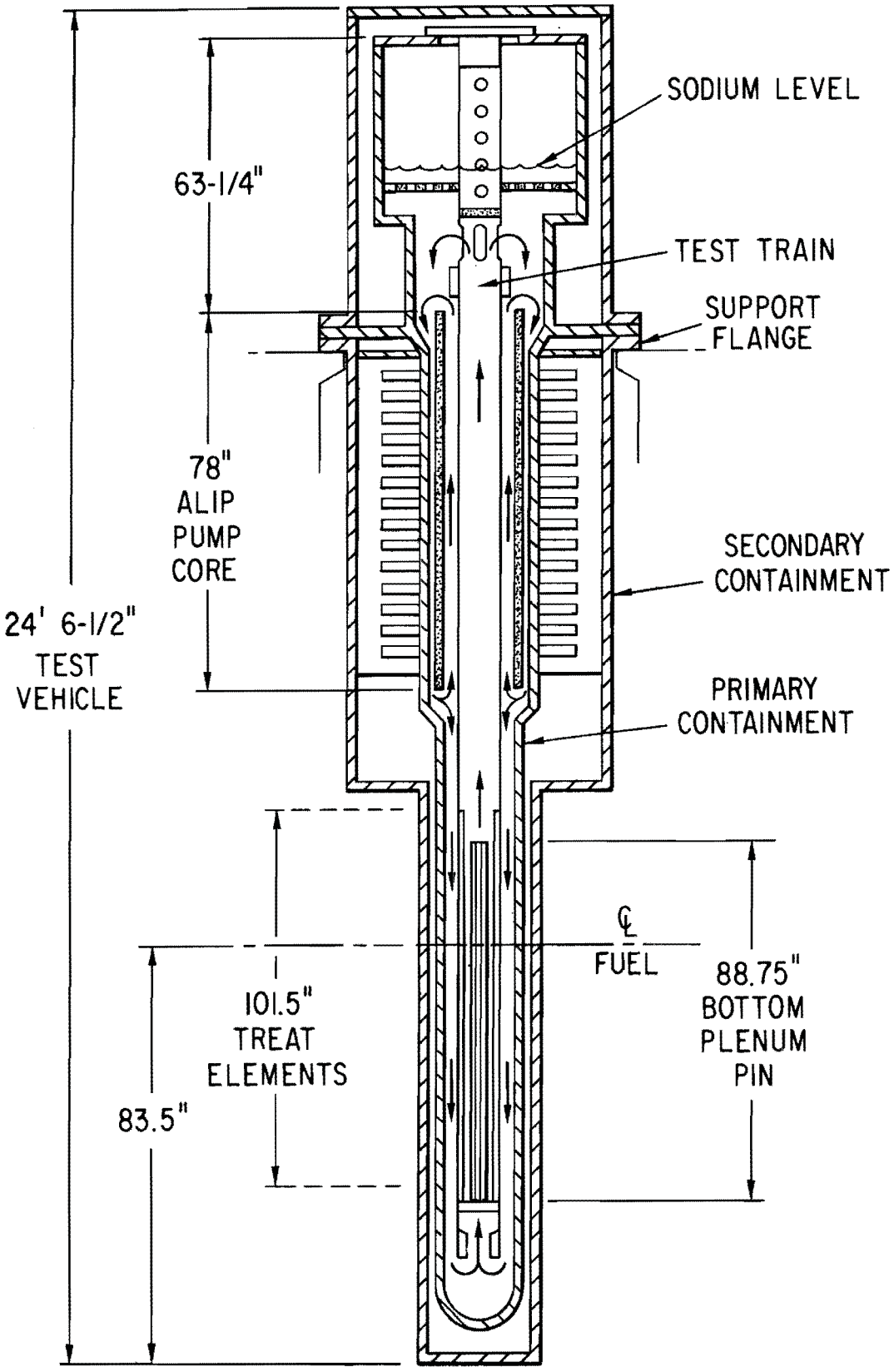

Fig. 1-1 Schematic Diagram of Advanced TREAT Loop Concept

(2) 61 FTR/CRBR-type uranium oxide fuel pins containing fully enriched uranium. This configuration is typical of tests for the phenomena associated with larger bundles and extended fuel motion. The quantity of fuel in this configuration is the same as that for 37 advanced oxide pins.

The upgrade will provide adequate energy capability to carry prototypic irradiated fuel well beyond the failure threshold, in 7-1 and 19-pin-size clusters. Nearly flat radial power profiles are provided. For a 19-pin cluster surrounded by a cadmium filter, cluster-averaged sample energies on the reactor midplane of up to about 2500 J/g are calculated, and the pin-averaged maximum-to-minimum radial power ratio is calculated to be about 1.17.* It should be noted that this is without radial grading of enrichment in the test bundle. With fully enriched fuel, much larger total energies are possible, and the cluster of 61 FTR/CRBR-type, fully enriched pins is calculated to have adequate energy capability for performance of experiments extending into the transition phase of extended fuel movement. With a cadmium filter, cluster-averaged sample energies on the reactor midplane of 4800 J/g are calculated, and the pin-averaged maximum-to-minimum radial power ratio is calculated to be about 1.26.** Again, it should be noted that this is without grading enrichment.

Both cases are based on a temperature rise in the TREAT driver fuel from room temperatures to 600°C (maximum cladding temperature of about 600°C), and a temperature rise in the modified fuel from room temperature to 1100°C (because of the details of fuel design, this produces a maximum cladding temperature of about 1050°C). For both fuel types the cladding oxidation in air is the limiting phenomenon. The modified element cladding has a significant service capability in air at 1200°C. The regular driver-fuel cladding has a limited capability for service at 700°C. Thus, significant margins exist between the performance maximum temperatures and temperatures acceptable for a limited number of "anticipated (accident) transients."

Calculations predict that both the prompt-neutron generation time and the reactor feedback will be reduced. The net effect will be that the minimum

---

* Without a neutron filter to harden the sample spectrum, the pin-averaged radial maximum-to-minimum power ratio is calculated to be approximately 1.4.

** Without the filter, the pin-averaged radial maximum-to-minimum is about 1.4.

reactor period for a "step input" of reactivity at low power will remain about 23 ms. Control-rod worths will be reduced by the modification. However, because of the reduction in reactor feedback, the reduced transient rod worths are expected to be adequate to perform shaped transients in the modified TREAT.

1.4 Safety

No change will be made in the maximum operating temperature limit of 600°C for the TREAT driver fuel. As noted above, it is planned that shaped transients will be run up to the 600°C core limit. This means that credit will be taken for a plant-protection-system-initiated scram to ensure that malfunction of the transient rod system in a shaped transient does not raise the driver temperature above 600°C. No change will be made for temperature-limited transients initiated at low power by a "step input" of reactivity; for these bursts, reactivity input will be limited to that amount which will produce a maximum driver temperature of 600°C in the absence of control-system action.

The temperature limit for modified TREAT fuel is set at 1100°C. This will produce a maximum cladding temperature of about 1050°C. Driver-fuel cladding will be protected from the high temperature of the modified fuel by thermal buffers.

Performance of tests with plutonium-bearing fuels will be limited to meterological conditions for which it is possible to assume complete release from the loop without violating dose limits at the INEL site. Calculations show that adequate meterological conditions can be specified for performance of tests on any quantity of mixed-oxide LMFBR pins which can be accommodated in the Advanced TREAT loop test section. A meterological restriction is currently in effect for TREAT. However, an additional limit in the Technical Specifications, of 150 g plutonium maximum, will have to be lifted.

Analyses have been made of reactivity changes resulting from sample compaction. For tests with a modified region consisting only of graphite-matrix fuel, the calculated reactivity change is small. Reduction of the total transient reactivity available for an experiment by the compaction reactivity change within a single-zone, graphite-matrix modified fuel region will reduce the sample energy available by less than 8%.

1.5 Cost and Schedule

The TREAT Upgrade cost estimate is based on a 36-month program with Title I Engineering assumed to start at the beginning of CY 1978. Ongoing conceptual-design work (in particular, work on the Advanced Test Vehicle, the Modified TREAT fuel, and the Loop Handling Cask) should be completed by this date. The schedule calls for completion of the TREAT Upgrade by the end of the first quarter of FY 1981.

Costs have been estimated according to the following categories:

1. Test Vehicles include provision for one advanced test vehicle consisting of one loop, pump, and associated instrumentation, as well as complete outfitting and prooftesting. Also included is one model test train, a calibration test vehicle, and two ALIP cooling modules.

2. The Interface Equipment includes provision of a Loop Handling Cask, 2 Control Consoles, 2 ALIP Power Supplies, and additional Hodoscope Detectors.

3. TREAT Modifications and Support Systems include modifications to the TREAT building and crane, the Reactor Grid Support and Rotating Plugs, TREAT cooling system, and additional equipment for the TREAT Data Acquisition System (DAS). A new Loop Operations Support Facility building addition to TREAT is also needed and included here, as is filling and surfacing an area north of the TREAT building.

4. The Safety Analysis Report category includes estimated costs for preliminary and final safety analysis reports.

5. Finally, the Modified TREAT Fuel category includes costs estimated for providing modified fuel and special assemblies needed for the upgrading of the TREAT reactor.

The summary conceptual cost estimates both with and without contingency is given in Table 1.2. These costs, including contingency and escalating, total $12,748,000. These projections are cash flow and obligations for the TREAT Upgrade are shown in Table 1.3, based on the three-year summary schedule and an expenditure limit of $1,500,000 for FY 1978.

The summary schedule corresponding to the above cost estimate is shown in Fig. 1.2.

1.6 Development Requirements

The choice of a graphite-urania fuel for the TREAT Upgrade effectively means that a fuel-development program is not required. Because the fuel will be heated to a peak temperature of 1100°C during a transient test, it is

TABLE 1.2 ENFS Study TREAT Upgrade Conceptual Cost Estimate Summary $X(000)

Description	Title I	Title II	Title III Eng.	Const.: Matl. Fab., Proc.	Subtotal	Contingency %	Cont.	Total
Test Vehicles (Total)	209	568	303	879	1959	30	588	2547
Adv. Test Vehicle	184	481	240	464	1369		411	1780
Model Test Train	5	27	41	250	323		97	420
Calibration Test Vehicle	18	40	18	85	161		48	209
2 ALIP Cooling	2	20	4	80	106		32	138
Interface Equipment (Total)	92	217	105	1121	1535	30	460	1995
1 Loop Handling Cask	82	189	98	782	1151		345	1469
2 Control Consoles	2.5	6.5	1	104	114		34	148
2 ALIP Power Supplies	2.5	6.5	1	60	70		21	91
Hodoscope Detectors	5	15	5	175	200		60	260
TREAT Modifications (Total)	75	167	98	1499	1839	30	552	2391
Filling & Surfacing	-	-	-	100	100		30	130
Building Mod.	33	33	21	585	672		202	874
Loop Support Operations Facility	30	60	60	228	378		113	491
Building Crane	5	45	5	400	455		137	592
Shielding/Rotating Plug Modifications	1	4	2	27	33		10	43
Reactor Grid Support Modifications	3	10	3	35	51		15	66
TREAT Cooling System Modifications	2	10	5	35	52		16	68
Data Acquisition System Modification (TREAT)	1	5	2	90	98		29	127
Modified TREAT Fuel	100	400	100	1370	1970		591	2561
Safety Analysis Report	138	164	91	-	393	30	118	511
	614	1516	697	4869	7696	30	2309	10005*
Engineering Cost		2827						2743
Escalation								12748
Total with Escalation								

* Without Esclation, FY 1976 dollars.

how are hodo detector costs?

Table 1.3 TREAT Upgrade - Cash Flow and Obligations
(Thousands of Dollars)

FY	78	79	80	81	Total
Schedule Title I					
Schedule Title II					
Schedule Title III					
Cost Title I	614				614
Cost Title II	392	1124			1516
Cost Title III		2473	2473	620	5566
Cost (Current)	1006	3597	2473	620	7696
Contingency, %	30	30	30	30	30
Cost Incl. Cont.	1308	4676	3215	806	10005
Escalation, %*	14.6	23.8	33.6	44.4	
Cost Inc. Above	1500	5789	4295	1164	12748
Obligations	2118	7012	2818	800	12748

* Assumes 10/1/76 start and ∿3 year Upgrade program.

ENSF STUDY

TREAT UPGRADE

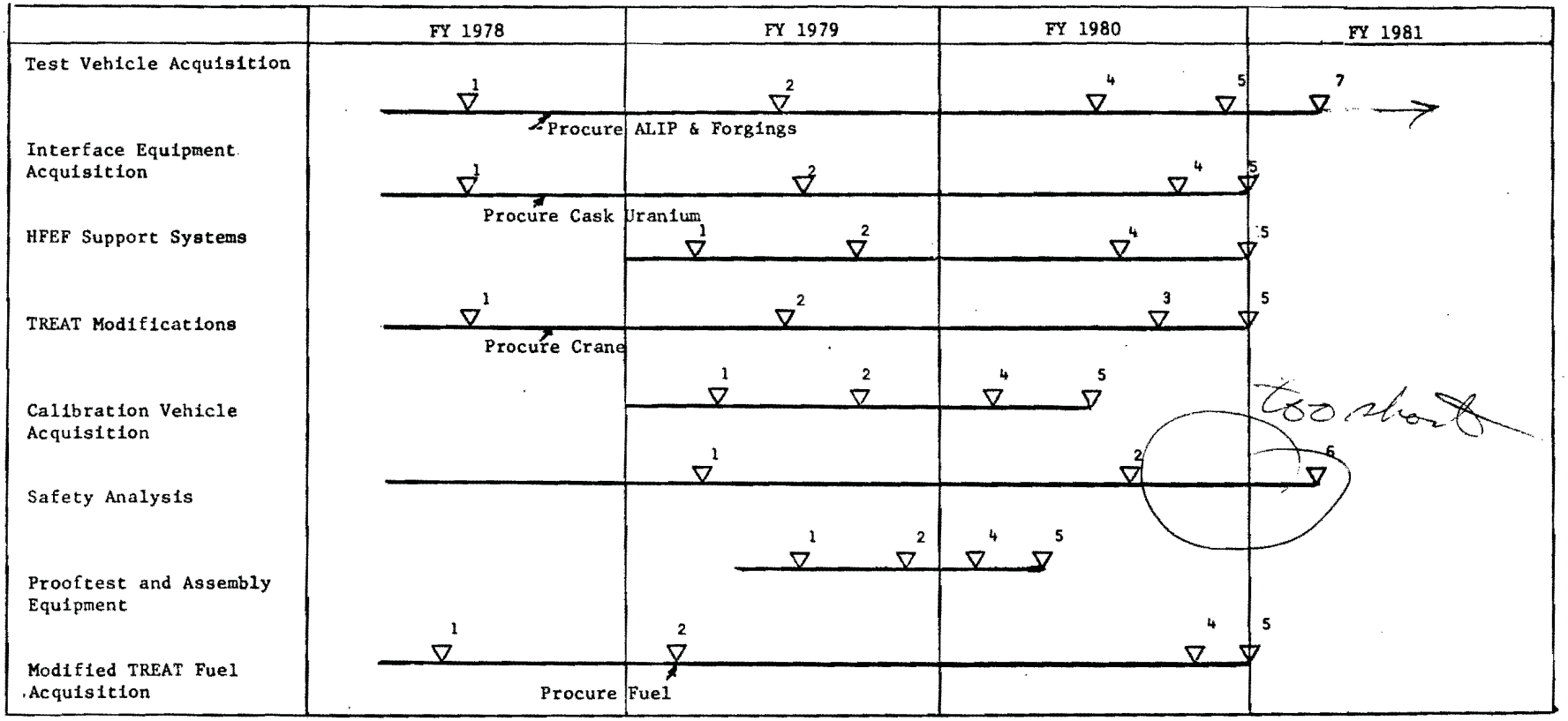

1 Complete Title I

2 Complete Title II

3 Complete Construction

4 Complete Fabrication/Procurement

5 Complete Assembly/Installation and Checkout

6 Final Review and Approval

7 Conduct Test

Time not shown for physics & temp measurements prior to 7 - 3 to 6 mos req'd.

Fig. 1-2 Summary Schedule

necessary that the thermal design of the modified fuel assure that no overheating exists in nearby Zircaloy or aluminum materials, or the test vehicle. The thermal-analysis calculations will be verified by thermal testing of an electrically heated prototypic assembly. Thermal cycling of the test assembly will also be done to verify that acceptable performance can be achieved under cyclic heating of the modified fuel. The test assembly will be cycled in an air atmosphere and the integrity of the Armco 18 SR cladding monitored to verify the good oxidation resistance of this material (see Fig. 1-3).

During the detailed design phase a UO_2-stainless steel fuel assembly will be designed for use in the TREAT positions immediately around the test vehicle.

The possible dispersion of fission products is a concern. It was concluded during the development of the TREAT fuel, however, that dispersion of fission-product activity resulting from a fuel-can rupture will be small even at temperatures approaching the melting point of Zircaloy (~1800°C).*

---

* Hazards Summary Report on the Transient Reactor Test Facility (TREAT), D. R. MacFarlane, G. A. Freund, and J. F. Boland, ANL/RAS 5923, p. 54 (Oct 1958).

OXIDATION RESISTANCE

The following comparison is based on laboratory tests of weight gain versus temperature and data available in the literature. The upper limit of 2200 F (1204 C) on Armco 18 SR is based on 100-hour tests in still air in which 18 SR exhibited weight gains of 33 mg/sq. in. versus over 800 mg/sq in. for Type 446. At 2000 F (1093 C), these rates were 25 mg/sq in. for 18 SR and 50 mg/sq in. for Type 446.

what rates?

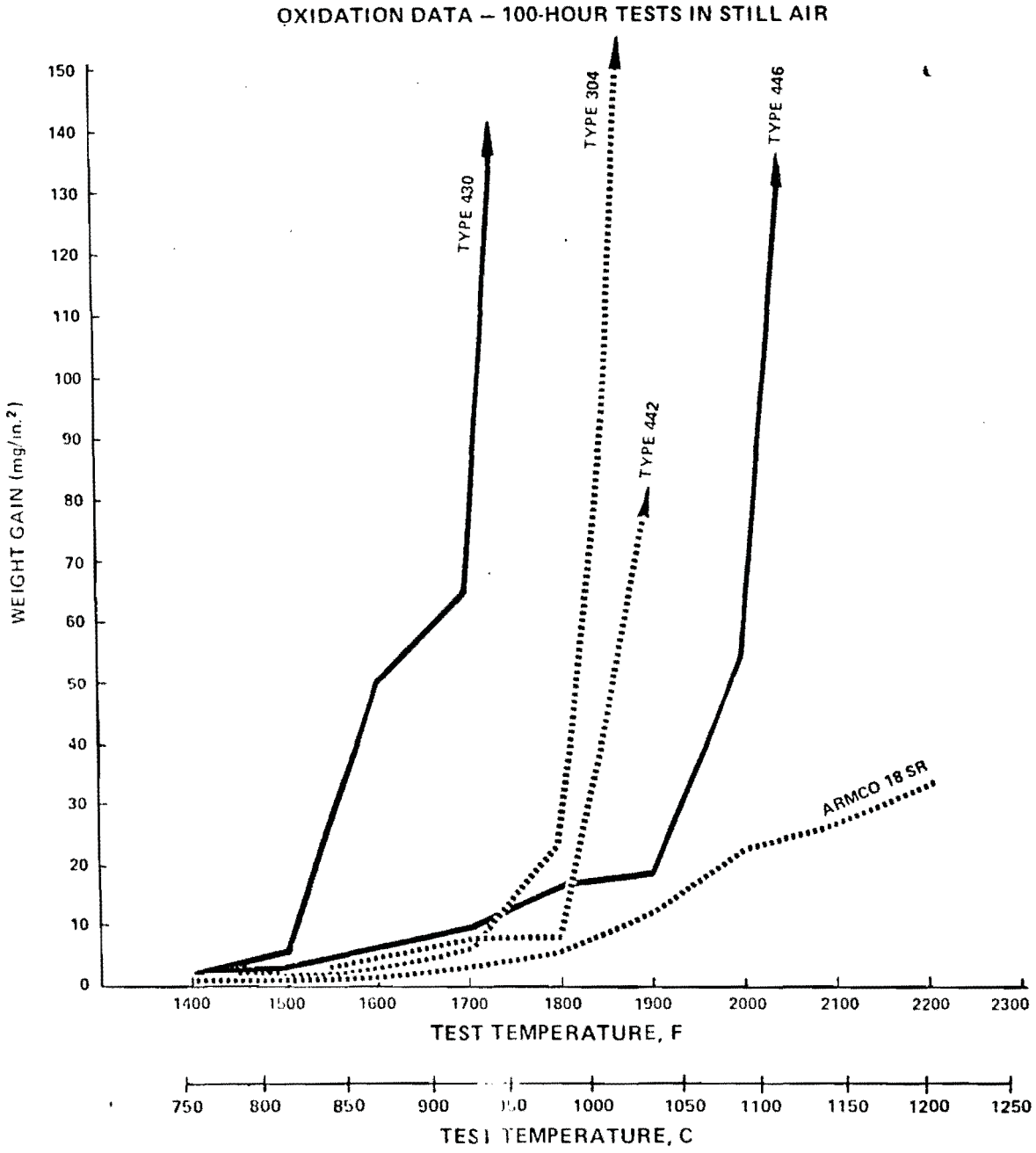

Fig. 1-3 Oxidation Resistance

2.0 DESIGN DESCRIPTION

2.1 TREAT Modifications

2.1.1 Current Envelope and Limits of Modifications

2.1.1.1 Reactor Configuration

The TREAT reactor is basically 6.7 m (22 ft) square by 4.57 m (15 ft) high. The depth from the top of the reactor shielding to the top of the rotating plug is 889 mm (36 in.), and the center line of the reactor core is 889 mm (36 in.) above the building floor. The grid plate is 1219 mm (48 in.) below the core center line or an equivalent of 305 mm (12 in.) below the floor level. Figure 2-1 illustrates the basic dimensions of the reactor, existing envelope perimeters, and the proposed modification limits for an enlarged envelope. The drawing shows the location of the radiography facility adjacent to the TREAT reactor.

2.1.1.1.1 Existing Envelope in TREAT. Fig. 2-1 illustrates the current envelope shape and size. The envelope extending from the top of the grid plate to the top of the rotating plug is approximately 3.92 m (12 ft 10-1/2 in.) long, plus the height above the rotary plug.

The in-pile section of the envelope (reactor fuel-element region) can have a number of geometrical combinations of shapes for the cross section. The most common TREAT geometry is a 102 x 204-mm (4 x 8-in.) cross section. [It is noted that a 204-mm (8-in.)-dia. envelope is also available within a 204-mm square.] The in-pile section is approximately 2.604 m (8 ft 6-1/2 in.) long [including 51 mm (2 in.) of clearance above the TREAT fuel elements].

A cross section 204 x 508 mm (8 x 20 in.) is feasible from a point 51 mm (2 in.) above the TREAT fuel elements, up and through, to the top of the rotating plug. This section is approximately 1.32 m (52 in.) long. Combining this with the in-pile length of 2.60 m would provide an existing envelope length of approximately 3.92 m (12 ft 10-1/2 in.). The 204 x 508-mm configuration is derived from the existing slot in the rotating plug. The slot is 204 mm wide and extends 254 mm (10 in.) either side of the centerline in the length dimension.

Any additional height above the top of the rotating plug is controlled by the available crane-hook height above the reactor. The required height above the plug varies with experiment and its

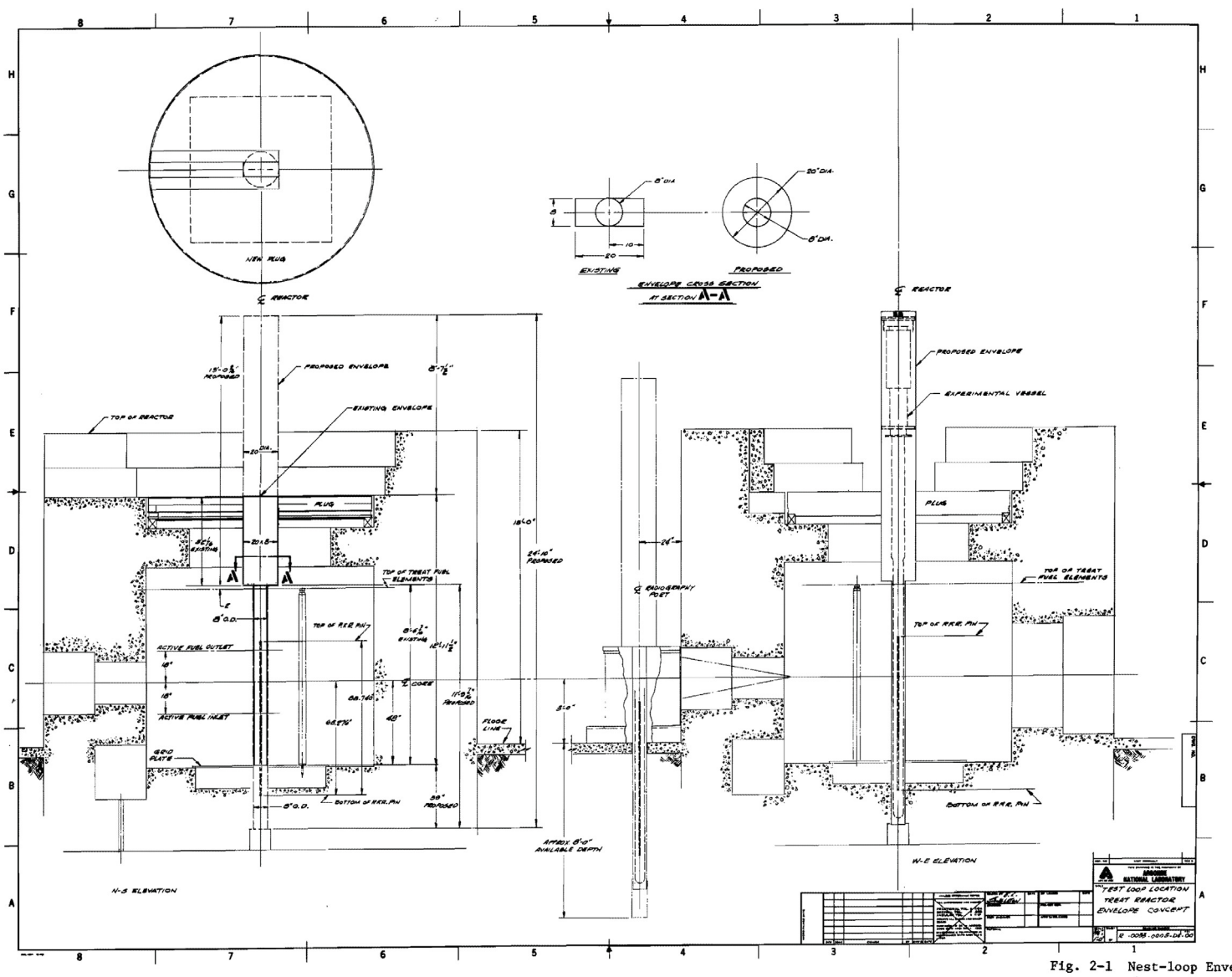

Fig. 2-1 Nest-loop Envelope Shown in the TREAT Reactor

design requirements. To illustrate, some existing loops have utilized an additional envelope (Secondary containment for R-Series tests) above the reactor in the proportions 2.44 m (8 ft) wide x 3.05 m (10 ft) long x 2.74 m (9 ft) high.

2.1.1.1.2 Proposed TREAT Modification for Extended Envelope Limits. The proposed envelope concept is also illustrated in Fig. 2-1. There are three principal areas on the TREAT reactor requiring rework or modifications to provide the size of envelope required: (1) the 508-mm (20-in.)-dia opening in the center of the rotating plug; (2) modification of the 279-mm (11-in.)-square center section of the TREAT grid plate; (3) provision of a new through-hole plug at the bottom of the reactor.

The rotating plug will be reworked to open up the center area. The 204-mm (9-in.)-wide slot (at the centerline intersection) will be opened to a 508-mm (20-in.) dia circle and the remainder of the slot will not be affected. A new group of shielding blocks will be required in two areas: (1) in the 104-mm slot adjacent to the 508-mm (20-in.)-dia circle and (2) in the area between the rotating plug and the top of the reactor.

The out-of-pile section will extend from 51 mm (2 in.) above the TREAT fuel elements to 1.71 m (5 ft 7-1/2 in.) above the top of the reactor. This section will be 3.96 m (13 ft) long and will have a 508-mm (20-in.) diameter. The upper end of the envelope is shown on Fig. 2-1 and is 2.629 m (8 ft 7-1/2 in.) above the rotating plug.

The in-pile section will extend from 51 mm (2 in.) above the TREAT fuel elements to 991 mm (39 in.) below the grid-plate surface. The 279-mm (11-in.)-square center-section insert of the grid-plate will be replaced by a new insert designed to accommodate a 204-mm (8-in.)-dia opening for the loop.

The modification will include removal of the upper section of the through-hole plug in the bottom of the TREAT reactor and also a portion of the lower section of the plug. Currently the plug is 914-mm (36 in.) long with the upper section being 204-mm (8-in.) in diameter and 457 mm (18 in.) long; the lower section has a 279-mm (11-in.) diameter and is 457 mm (18 in.) long. The envelope will penetrate 204 mm (8 in.) into the lower section of the plug. There is adequate space below the reactor to install a new plug (or shield) of length equal to 914 mm, but stepped 279 mm (11 in.) in diameter by 254 mm (10 in.) long, and 330 mm (13 in.) in diameter by 660 mm (26 in.) long.

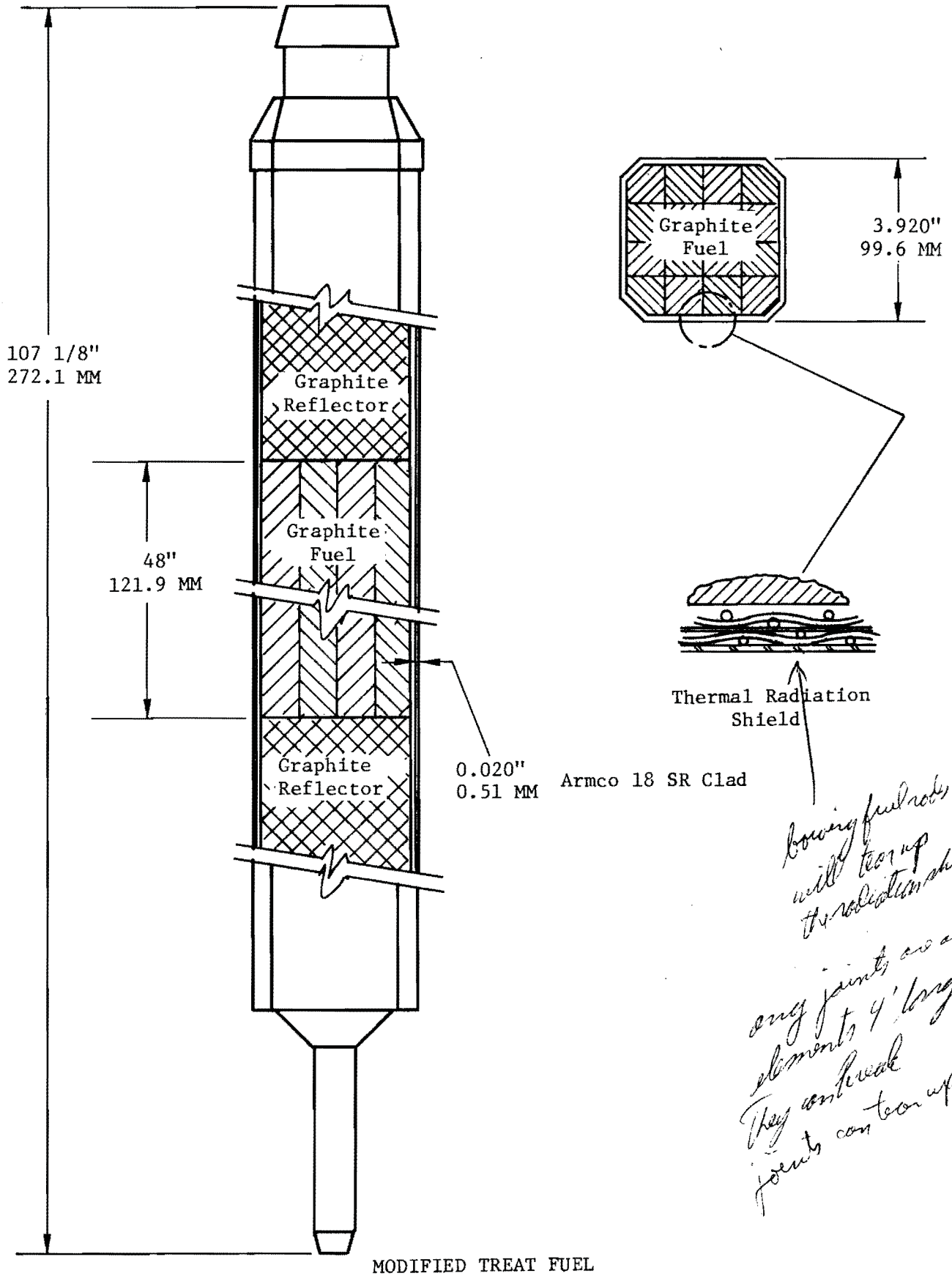

Fig. 2-2 Modified TREAT Fuel Concept

A new plug support will be required, but it does not appear to be a design problem.

The overall length of the envelope is 7.569 m (24 ft 10 in.) with an out-of-pile length of 2.629 m (8 ft 7-1/2 in.) (508 mm diameter, 20 in.) and an in-pile length of 4.941 m (16 ft 2-1/2 in.) (204 mm diameter, 8 in).

2.1.1.2 Reactor Facility

The loop-handling cask for the Advanced TREAT Loop will have a maximum loop plus cask weight of 27,270 kg (30 tons). The length of the cask and use of an appropriate crane will require the building height to be increased approximately 12 m (40 ft).

The envelope for the new TREAT fuel-handling cask will be within the envelope for the SLSF transporter. However, use of the 25.6-m (84-ft)-long SLSF transporter will require grading and surfacing of the area on the north side of the TREAT Reactor Building back to the new security fence.

A review of operations currently conducted in the TREAT facility indicates that the above capability will require additional space in the form of a building extension of one additional column span. This addition will include the storage pits, which means that there will be no interference with operations in the existing building while the pits are being excavated. This will enable erection of a new facility (Loop Support Operations - LSO Facility) inside of the TREAT Reactor Building for the assembly, disassembly, filling, and repair of Advanced TREAT Loops. Inside of this facility, which will operate at a pressure negative to that of the TREAT Reactor Building itself, will be two storage pits for loops plus two storage pits for test trains.

The modified TREAT core will require fabrication of 100 additional fuel/converter elements. These additional elements will be stored in 100 storage pits located as close as possible to the reactor itself to minimize the time in moving the elements between the pits and the reactor.

2.1.2 Reactor Configuration

2.1.2.1 Modified Fuel and Axial Reflector

All modified TREAT fuel elements will fit within the envelope of the current TREAT driver fuel elements. They are handled in the same fashion as the driver fuel and have the same cooling mode.

There are two types of modified elements, both with the same cladding, ARMCO 18 SR steel, and the same operating temperature limit, 1100°C. This cladding material was selected because of the resistance to oxidation by high-temperature air and because of the relatively low parasitic neutron capture compared with Inconel. The cladding provides a vacuum environment for the modified fuel bodies. It is not required to restrain the fuel or to hold internal pressure. The operating temperature limit is fixed at 100°C below the maximum temperature (1204°C), at which cladding-oxidation data for exposure are available. Manufacturer's data show a weight gain in 100 hr of 5.3 mg/cm^2, which corresponds to oxidation of ∿0.02 mm.

For tests on samples with prototypic enrichment, the modified fuel region will be loaded with graphite-matrix fuel. Stainless steel-UO_2 elements, similar to those proposed for the STF will be loaded into the inner portion of the modified fuel region for use in certain tests with fully enriched pins.

A graphite-urania fuel having higher concentration of enriched uranium than the TREAT driver fuel was selected for the TREAT Upgrade because such fuel can satisfy the new capability needed for TREAT tests employing the Advanced TREAT Loop and does not require a fuel-development program. This fuel has the following inherent advantages for a reactor designed to absorb heat from large thermal-neutron-flux integrals applied over very short periods of time:

(1) The high heat-absorbing capability of the graphite moderator provides an effective heat sink for transient-generated heat without dependence on coolant during the transient.

(2) The excellent thermal-shock resistance of graphite will sustain the high rates of heat input of the transient.

The experience with the TREAT fuel assemblies containing a lower concentration of urania and operating at 600°C has been excellent. The modified fuel will be operated at temperatures of 1000 to 1100°C and will have a graded uranium concentration within an assembly. This has required certain design features and changes in clad material as described below, but the basic configuration is similar to that for the existing TREAT fuel.

The modified TREAT fuel concept is shown in Fig. 2-2. The assembly consists of upper and lower graphite reflector sections, and a central uranium oxide-bearing graphite fuel section. The 1.219-m-long fuel

section (4 ft long) contains sixty-four 305-mm (12-in.)-long, 23 mm x 23 mm 0.9-in. x 0.9-in.) nominal fuel blocks canned in ARMCO 18SR, 0.51 mm (20 mils) thick. The can outside dimension is 99.57 mm (3.92 in.) square with 15.9-mm (0.625-in.) chamfered corners. A thermal insulation barrier is placed within the can to reduce the rate of radial heat flow. This feature was provided for two reasons: first, it reduces the temperature rise in the coolant air leaving the modified fuel region; second, it reduces the heating of Zircaloy-clad elements adjacent to the high-temperature modified region.

The upper and lower graphite reflector sections, each about 600 mm (~2 ft) long, are contained in a similar fashion and are maintained in good thermal contact with the fuel by means of a load spring so that axial heat transfer is enhanced. Both the fuel and reflector regions are evacuated, and the thermal insulation barrier extends the full length of both top and bottom reflectors in order to reduce heating of the aluminum-clad reflectors of TREAT driver fuel adjacent to the modified fuel region. Part of the upper and lower reflectors will be poisoned with boron to limit the power density at the ends of the modified fuel.

A gripping fixture of steel is joined to the upper reflector section, and a support and alignment pin, also of steel, will be joined to the lower reflector section to complete the fuel assembly. An orientation device will be designed to assure proper location of the assembly in the core.

The complete fuel assembly will be slightly under 2.74 m (9 ft) long, with a nominal cross section of 99.57 x 99.57 mm (3.920 x 3.920 in.), and weighs 45.45 kg (100 lb). The wide chamfers at the corners combine with those of adjacent assemblies to form 15.9-mm (0.625-in.)-square coolant passages through the assembled core. The clearances in the core are: nominal 2 mm (80 mils) between the adjacent ARMCO 18 SR cans, and nominal 2.1 mm (84 mils) between the steel can and graphite-fuel blocks.

Fabrication techniques should require no development work. The fuel blocks can be made using methods similar to those used in making the original TREAT fuel. However, the fuel blocks will have to be outgassed at higher temperatures, since the operating temperatures will be higher.

The reference loading of modified fuel consists of a 9 x 9 array. This will require approximately seventy-three assemblies, with some specially shaped assemblies required around the test position. In order to have a sufficient number of spares, it is estimated that approximately 100 assemblies will be fabricated.

Design Parameters for the TREAT Reactor with a 9 x 9-array modified fuel zone are given in Table 2.1.

2.1.2.2 Special Modified Assemblies

Special modified fuel assemblies will be built to provide an approximately hexagonal clearance hole at the reactor center for the secondary containment of the advanced test vehicle.

Two types of modified assemblies are required. One type would be simply half an ordinary assembly with approximate dimensions of 51 x 102 mm (2 x 4 in.). Three of this type are utilized, with the fourth position taken by an empty can of the same dimensions in line with the hodoscope (TREAT north). The second type would be an assembly of approximately 102 x 102 mm (4 x 4 in.), with one corner chamfered approximately 40-mm (1.6-in.) at 45°. Four assembles of the second type complete the inner array.

2.1.2.3 Modified Grid Plate

The center of the TREAT grid plate has a 279-mm (11-in.)-square removable section. A new section will be made having a 203.3-mm (8-in.) center hole to accommodate the secondary containment of the advanced test vehicle.

The new TREAT fuel assemblies (9 x 9 assembly array at the reactor center) will have graded enrichments; consequently, a preferential insertion orientation must be maintained. One method to guarantee proper insertion would be to drill piloting holes in the TREAT grid plate for each fuel assembly and have key pins on the base of the fuel assembly.

This spacer a bit sparse!

2.1.2.4 Modified Shielding

Three principal shielding areas will require new design or modifications: (1) the 200-mm (8-in.) slot in the rotary plug, (2) around the secondary containment during a test, and (3) the through-hole plug at the bottom of the reactor.

2.1.2.4.1 Possibly four to eight of the shielding blocks in the region around the 200-mm (8-in.) slot adjacent to the 510-mm (20-in.)-dia envelope circle (or centering ring) will have to be modified. The modifications will involve shaping or contouring of the block segments adjacent to the centering ring collar.

2.1.2.4.2 The concrete shielding blocks in the area of the North/South slot in the top of the reactor will have to be redesigned to accommodate the contour of the secondary containment. This modification is expected to be straightforward and should present no difficulties.

TABLE 2.1. Design Parameters for TREAT Reactor with a Modified Fuel Zone

TREAT Core	
Maximum size (361 fuel assemblies)	1.93 m square by 1.22 m high (6 ft 4 in. square x 4 ft high)
Modified Fuel Zone	
Nominal size (∿73 fuel assemblies plus some special slotted assemblies without fuel)	0.915 m x 0.915 m square by 1.21 m high (3 ft x 3 ft square x 4 ft high)
TREAT Fuel Assemblies	
Overall dimensions	100.57 mm square x 2.74 m long, with 15.9-mm chamfered corners. (3.920 in. square x 8.94 ft long, with 0.625-in. chamfered corners).
Modified Fuel Assemblies	
Overall dimensions	99.57 mm square x 2.74 m long with 15.9-mm chamfered corners. (3.92 in. square x 8.9 ft long, with 0.625-in. chamfered corners).
TREAT Fuel Section	
Configuration	6 graphite-urania blocks clad with Zircaloy-3, 0.634 mm thick.
Block dimensions	96.5 mm (3.800 in.) square x 203 mm (8 in.) long.
UO_2 content	0.248 wt-%
Carbon-^{235}U atomic ratio	10,000/1
^{235}U enrichment	93.24%
Dispersion	-325 mesh (44 μ, max)
Boron content	7.6 ppm
Iron content	0.1% max

TABLE 2.1 Design Parameters for TREAT Reactor with a Modified Fuel Zone (Contd.)

Modified Fuel Section	
Configuration	Graphite-urania blocks clad with ARMCO 18SR, 0.5 mm (0.020 in.) thick; 0.51-mm reflective insulation between fuel and clad.
Carbon-^{235}U atomic ratio	∿4301/1 to ∿500/1
^{235}U enrichment	93+%
TREAT Reflector (Top and Bottom)	
Composition	Graphite
Length	610 mm (2 ft)
Cladding	6063 aluminum, 1.27 mm (0.05 in.) thick
Assembly	Riveted to ends of fuel section
Permanent Reflector	Graphite, 610 mm (2 ft) thick min
^{235}U Loading (nominal core with modified fuel	7.45 kg
Modified Fuel Reflector (Top and Bottom)	
Composition	Graphite with poison material
Length	
Top	595 mm (23.5 in.)
Bottom	558 mm (22 in.)
Configuration	Similar to modified fuel section
TREAT Coolant	Air at atmospheric pressure
Control Rods	
Configuration	Tubular, of 43.5-mm (1.75-in.) OD
Absorber	Carbon steel tube packed with B_4C powder
Absorber length	1.5 m (5 ft)

TABLE 2.1. Design Parameters for TREAT Reactor with a Modified Fuel Zone (Contd.)

Zircaloy follower material	Zircaloy tube filled with graphite
Zircaloy follower length	1.5 m (5 ft) interchangeable with absorber section
Steel follower material	Steel tube filled with graphite
Steel follower length	
Pneumatic	2.262 m (7 ft 5 in.)
Hydraulic	2.110 m (6 ft 11-1/4 in.)
Pneumatic Control-rod Drives	Compressed gas actuated scram, with lead screw-driven magnetic latch for intermediate positioning and relatching. Integral pneumatic-hydraulic dashpot.
Number of drives (max)	16 (2 rods per drive)
Regulating speed	2.5 mm/s (6 in./min)
Scram time	∿280 ms
Hydraulic Control-rod Drives	Hydraulic-operated rod drives using a phosphate ester base fluid, operating at 20.7 MPa (3000 psi), and a hand-operated needle valve to limit the low flow rates for slow-speed operations.
Maximum Rod Speed in Slow-speed Operation	3.00 m/min (120 in./min)
Maximum Rod Speed in High-speed Operation	4.25 m/s (170 in./s)
Number of Drives	2
TREAT Maximum Operating Conditions	
Transient	Unshaped / Shaped
Fuel temperature	600°C / 600°C
Reactor period	0.023 s / 0.050 s
k_{ex}	4.7% / 6.2%

TABLE 2.1 Design Parameters for TREAT Reactor with a Modified Fuel Zone (Contd.)

Steady state	
Power level	120 kW
Coolant outlet temperature	250°C
Time to cool hot-spot temperature after transient	~2 hr
Flux data in central void	
Neutron	5.6×10^6 fissions/g ^{235}U-W-s 5.0×10^6 nvt/W-s ($\sigma_f^{235} = 440$)
Gamma	2.2 r/h/W 6.0×10^3 R/MW-s
Modified Fuel Zone	
Transient	Unshaped / Shaped
Fuel temperature	~1100°C / ~1100°C
Reactor Period	0.024 s / 0.050 s
Time to cool hot-spot temperature after transient	~4 hrs
TREAT Physics Constants	
Mean prompt-neutron generation time	~$6\text{-}9 \times 10^{-4}$ s (depends on loading)
1% k_{ex}	383 in-hours
β_{eff}	0.0072
Isothermal temperature feedback	-0.017% k_{ex}/°C
TREAT with Modified Fuel Physics Constants	
Mean prompt-neutron generation time	-4×10^{-4} s
β_{eff}	~0.007

TABLE 2.1. Design Parameters for TREAT Reactor with a Modified Fuel Zone (Contd.)

Change in reactivity due to change in temperature from cold to hot	∿3.8%
Cold	∿30°C
Hot modified fuel zone	1050°C max.
Driver zone	600°C max.

2.1.2.4.3 Modification of the through-hole plug at the bottom of the reactor, also appears to be a straightforward change from the existing design. The existing length of penetration [914 mm (36 in.)] of the plug within the reactor will be reduced by 660 mm (26 in.), leaving a segment approximately 254 mm (10 in.) long of the 279-mm (11-in.)-dia section intact. The original 914-mm length can be retained by adding 660 mm externally below the bottom of the reactor. The diameter in this region would be approximately 330 mm (13 in.). Although a new support fixture will be required, there does not appear to be any design or major installation problems.

can be shortened by using higher density material

2.1.3 Reactor Physics Characteristics

2.1.3.1 Performance Requirements

Sample energy and radial power distribution requirements are discussed in Sect. 3.1. They are summarized in Table 2.2. Reactor physics calculations performed for the TREAT upgrade study are described in Appendicies A1 through A4. For comparison, calculated performance values are also given in Table 2.2. The calculated values were obtained with the Advanced TREAT loop, a "light" cadmium filter on the loop, and a full 9-element by 9-element equivalent modified fuel zone optimized for energy deposition in the 19-pin prototypic-enrichment advanced oxide cluster. In each case, the total sample energy calculated is that for the average across the cluster at the core midplane. These calculated energy values have each been reduced by 8% from the values calculated for the total temperature swing allowable, in order to provide margin to accommodate a potential reactivity increase due to sample compaction. Physics calculation results on compaction reactivity are described in Appendix A3. Implications of results from those calculations are discussed in Sect. 3.4.

(compaction

For the calculational model employed in the TREAT Upgrade study, a minimum reactivity of 11% in the cold, clean system is needed to cover experimental requirements.

← misleading since the breakdown of requirements is not presented

2.1.3.2 Selection of Modified Core Physics Design

BS Because of the requirements to avoid a fuel-development program and to avoid changes of significance in TREAT, only two types of modified TREAT fuel elements were considered: an air-cooled graphite-matrix fuel, and an air-cooled stainless steel-matrix fuel. Either type was to be loaded with ^{235}U to the maximum permitted by temperature limits on the cladding, in order to provide the maximum contribution possible to sample performance. The

TABLE 2.2 Summary of Required and Calculated* Sample Energies and Radial Power Distributions

Fuel Type	Sample Size	Sample-energy Requirement	Calculated Sample Energy
Prototypic Enrichment, Irradiated Fuel Pins	19 Advanced Oxide Pins	2040 J/g	2500 J/g
Fully enriched, Fresh UO_2 Fuel Pins	61 FTR/CRBR pins (Same sample mass as 37 advanced oxided pins)	2840 J/g	4800 J/g
Radial, Pin-averaged power ratio			
Maximum-to-average desired		1.10-1.15	
Maximum-to-average calculated for clusters of pins with a single fissile-atom loading		1.05 1.10	19-pin case 61-case

* With cadmium filter on Advanced TREAT loop, 9-element x 9-element zone of graphite-matrix modified TREAT fuel, optimized for energy deposition in 19 prototypic-enrichment advanced oxide pins.

fuel inside an element was subdivided so that the fuel loading could be graded within an element, thus raising the average loading in the element for a given maximum temperature. For the calculation model used in the TREAT Upgrade study, the nominal 25-mm-square segments used for internal grading in the modified elements increased sample energy levels by about 4% over a segment size of 50 mm square. The actual advantage including detailed three-dimensional neutron-flux distribution effects should be somewhat larger than 4%.

The following three basic modified core-region configurations were calculated (see attached Appendices): (1) a single zone of stainless steel-matrix fuel, (2) a single zone of graphite-matrix fuel, and (3) a two-zone region with graphite-matrix fuel adjacent to the driver and stainless steel-matrix fuel adjacent to the test hole. Configuration (1) produced a relatively hard neutron spectrum and a flat radial power profile $\bar{<}1.05$. Because of the hard spectrum, sample energy generation was essentially insensitive to the number of pins and was essentially proportional to the fissile-atom loading. Thus, for the range of sample size considered for TREAT (61 pins or less), energy generation in the prototypic-enrichment fuel sample was $\sim$1100 J/g, well below energy requirements. Modified TREAT reactivity calculated in a typical case was also too low. Configuration (1) did generate high sample energy for fully-enriched fuel, $\sim$4500 J/g (uncorrected to provide margin for reactivity addition due to sample compaction). Configuration (2) in the 9 x 9-element geometry reference case exceeded requirements for sample energy for both reference samples of Table 2.2, and gave acceptable radial power flatness. The reference configuration (2) case with Inconel cladding gave a marginal value of 11% reactivity. With ARMCO 18 SR the reactivity was about 13%. Configuration (3) represents a wide range of possible modified zones, with potential for good energy generation in fully enriched fuel, flatter radial power profiles than those of configuration (2), and lower reactivity than configuration (2). On the basis of these considerations, the core physics design is based on configuration (2), with a 19-pin prototypic-enrichment advanced oxide sample. ARMCO 18 SR provides reactivity margin for accommodating stainless steel-matrix fuel in the region immediately surrounding the test hole for use with tests with fully enriched fuel. Because the graphite-matrix fuel produces a somewhat softer neutron spectrum, a cadmium filter is incorporated with the loop, yielding the radial maximum-to-average values quoted in Table 2.2.

Evaluation of material properties led to selection of clad cadmium oxide as a filter material capable of use to 1400°C.

2.1.3.3 Kinetics

The reactivity swing calculated from room temperature to the full temperature limit is about -3.8 for the reference configuration as designed for tests with prototypic-enrichment fuel. For this configuration, limiting-case calculations of reactivity addition from sample collapse (taken as 91 fully enriched FTR/CRBR pins with a loop having a filter) show a potential reactivity addition of as much as 0.3%. Reducing the reactivity available for experiments by 0.3% to provide margin for potential reactivity increase due to sample collapse will reduce the available swing to about 3.5% (see Sect. 3.4). Currently the two pair of the transient rods in TREAT are worth a total of about 8%. One pair of transient rods is on the inner ring, adjacent to the planned high temperature elements. Though it would be desirable to leave these transient rods in their current positions, it is recognized that the presence of the high-temperature zone of modified fuel elements may require movement of rods to unoccupied positions in the outer rod ring. Thus, it has been conservatively assumed that this move will be necessary for the purposes of the Upgrade study. Moving rods outward in TREAT will reduce their worth. The modification also will have the effect of reducing rod worths. This latter effect is estimated (see Appendix A-4) to reduce rod worths to about 75% of the unmodified value. Taking both effects into account, it is expected that transient rods in the outer rod ring with the modified TREAT will have adequate worth to conduct experiments with the calculated reactivity swing due to reactor heating.

The minimum period for the current TREAT (for a temperature-limited burst) is about 23 ms. For the modified TREAT, the change in prompt-neutron generation time is compensated by the change in feedback, and the minimum period is calculated to remain about 25 ms.

2.1.4 Reactor Thermal Hydraulic Characteristics

No change is planned in the TREAT reactor cooling system, which is shown schematically in Fig. 2.3. The modified elements to be loaded into TREAT have the same geometrical envelope as the driver elements they replace. Cooling is provided by ambient air which enters the reactor cavity through filters on the top of the reactor, flows downward through coolant channels

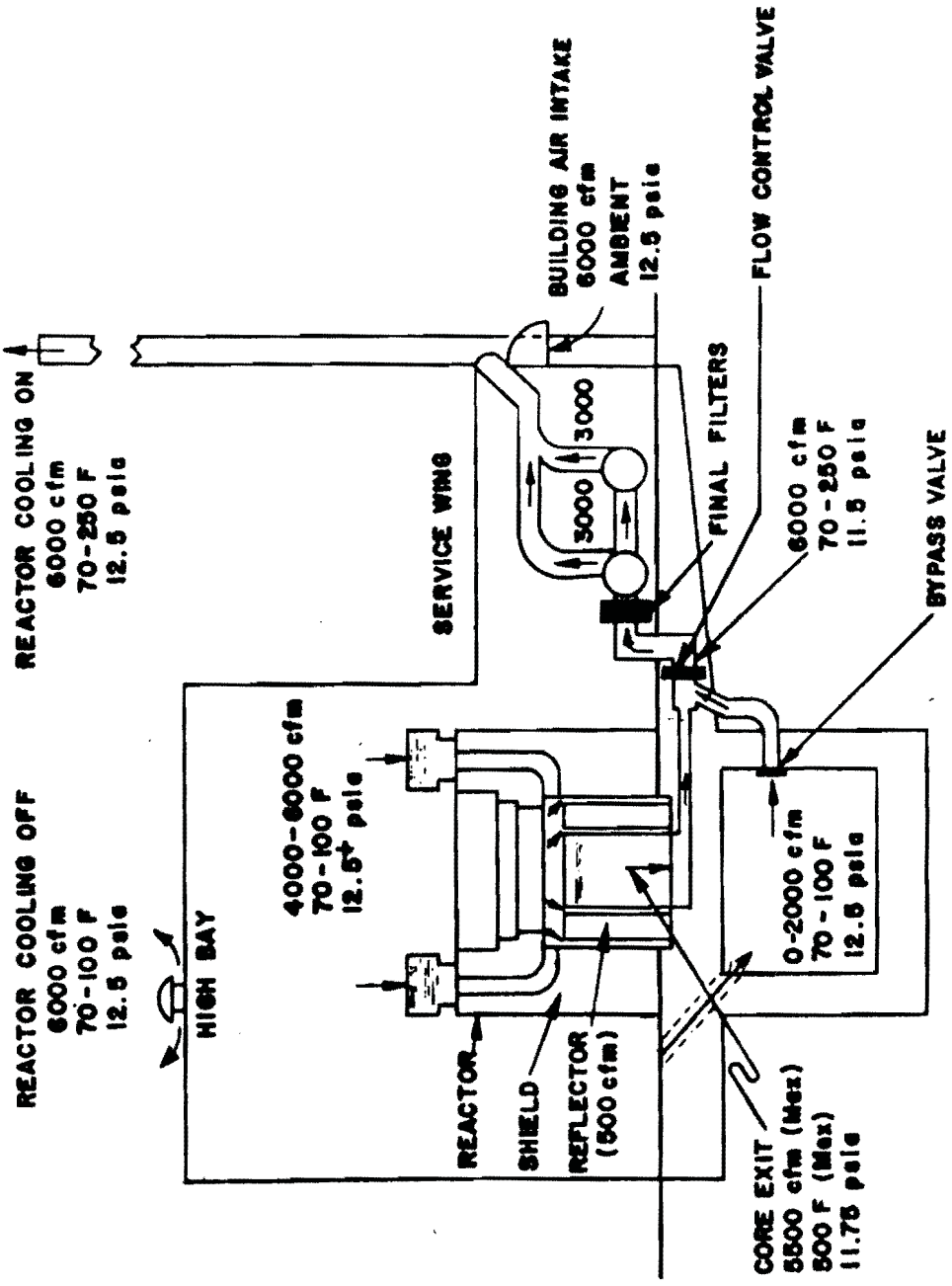

Fig. 2-3 TREAT Cooling and Ventilation System

formed at the corners of the chamfered TREAT elements, through the grid plate at the bottom of the reactor cavity, through duct work into filters at the blower positions, and then is exhausted through the TREAT stack. Additional air enters the exhaust system through openings in the shielding and from the subpile room. During operation of the reactor cooling system, the building exhaust is turned off (see Fig. 2-3).

Thermal performance of the modified TREAT elements has two criteria to be met:

(1) Do the higher-temperature modified elements overheat the adjacent TREAT driver elements?

(2) Do the higher-temperature modified elements heat the coolant air enough to damage the aluminum cladding of the lower reflectors of adjacent driver elements? (3) Grid plate (4) Control rod thimbles

These two questions have been addressed in the current study by two provisions in the modified element design. The outer row of modified elements has been derated in temperature, and all the modified elements have a radial thermal barrier to retard heat transfer to coolant and adjacent elements. Heat transfer from adjacent elements is both radial (across gaps into cooler elements farther from the core center) and to the coolant. It is the purpose of the thermal barriers and the outer lower-temperature ring of modified elements to retard horizontal (radial) heat transfer from the modified zone region sufficiently to prevent local overheating of the driver-element core and reflector cladding. It should be noted that, when radial and axial power distributions are taken into account, the heat generated in a maximum design transient can be absorbed adiabatically and isothermally in the core without exceeding 600°C.

2.1.5 Facility Features

2.1.5.1 Site and Building Description

TREAT is located at the ANL East Area (Site 16) of the National Reactor Testing Station. Site 16 is located approximately 17.7 km (11 miles) from the NRTS east boundary and 6.4 km (4 miles) north of U.S. Highway 20. The TREAT complex comprises reactor and control buildings located 1.3 km (4250 ft) and 0.53 km (1750 ft), respectively, northwest of the EBR-II containment vessel. The topography permits an unobstructed view between the two buildings.

Certain building services and utilities are interconnected with the EBR-II service system. Water is supplied from the EBR-II fire loop by a 10.2-cm (4-in.) main. Power is supplied by a 13.8-kV electrical distribution feeder from the EBR-II power-plant switchgear.

Reactor Building

The existing Reactor Building is an aluminum-sided, steel-frame structure which features a high-bay section and adjacent service wing. The high-bay section [with a 10.7-m (35-ft) ceiling] contains the reactor, fuel-storage pit, instrument room, and basement subpile and equipment rooms. The high-bay area, including the top and three faces of the reactor shield, is serviced by an overhead 15-ton crane. At the southwest corner of the Reactor Building is an instrument shop.

The control-rod-drive mechanisms are located in the subpile room, which measures 4.88 m square by 4.06 m high (16 ft sq by 13-1/3 ft high). The adjacent room, 5.49 x 6.10 x 5.49 m high (18 x 20 x 18 ft high), provides space for data-recording and -reduction equipment. Access is gained by a stairway from the main floor into the data room and through a door into the adjacent subpile room. There is also an escape ladder from the subpile room. Provision has been made for ventilating the subpile room with the reactor cooling blowers in the event exceptional air changes are required. An equipment hatch is available for moving large items in and out of the basement area using the 15-ton crane.

The service wing [with a 3.96-m (13-ft) ceiling] contains the existing reactor cooling blowers and normal building services, and provides access to the thermal-column face of the reactor. The north section of the service wing contains electronics equipment and a mechanical workshop area.

One of the "ground rules" for the TREAT Upgrade Program required that any building-modification work should be completed within 12 weeks reactor downtime to minimize the impact upon the TREAT Experimental Program. To provide identical crane coverage to that presently available, the reference design requires that the entire "high bay" area of the TREAT Reactor Building will have to be raised 12.2 m (40 ft). This must be done to allow the longer cask for the advanced TREAT loop to be moved the full length of the reactor building. The reference design of the new cask plus loop (see Fig. 18) weighs approximately 30 tons.

The 15-ton crane will be removed from its rails. New footings for the high-bay area will be required, and this will require the floor to be broken up between each existing footing for an excavating operation. After excavation is completed, new footings will be poured, followed by the pouring of new "piers."

The existing roof structure will then be sequentially removed while additional vertical structural sections are installed. After installing the new structural sections for the walls in a sequential manner, the roof structure can be installed along with the crane rails at their new height. Whether the building siding and roofing is installed sequentially or in one process upon completion of the structural work is a detail that will be left for the job planning stage.

The area in back of the TREAT Building will require filling and surfacing to accommodate the SLSF Transporter. However, as shown on Fig. 2-4, it should not be necessary to modify the new security fence surrounding the TREAT Reactor Facility.

2.1.5.2 Reactor Building and Crane

The combined weight of the cask loaded with loop is 30 tons. Due to the longer loops required for the TREAT upgrade program, a loop-handling cask approximately 7.92 m (26 ft) in length will be required. Fig. 2-5 presents a schematic outline of such a cask being handled in a modified TREAT Reactor Building. The existing 15-ton crane will be reinstalled to permit simultaneous use of the two cranes.

The present height of the 15-ton crane rails in the TREAT Reactor Building is 8.38 m (27 ft 6 in.) above the floor, and the crane rails for a 30-ton crane will be installed at a required rail height of 16.4 m (53 ft 9 in.).

To be able to move the loop-handling cask between the TREAT Reactor Building and HFEF/N, use of a "transporter" will be required. Since the estimated weight of the TREAT loop-handling cask plus the loop will not be greater than 30 tons, and its "envelope" will be somewhat smaller than the envelope of the SLSF Loop Handling Machine (LHM), use of the SLSF Transporter has been assumed. Figure 2-4 shows the SLSF transporter backing into the North truck door of the TREAT Reactor Building.

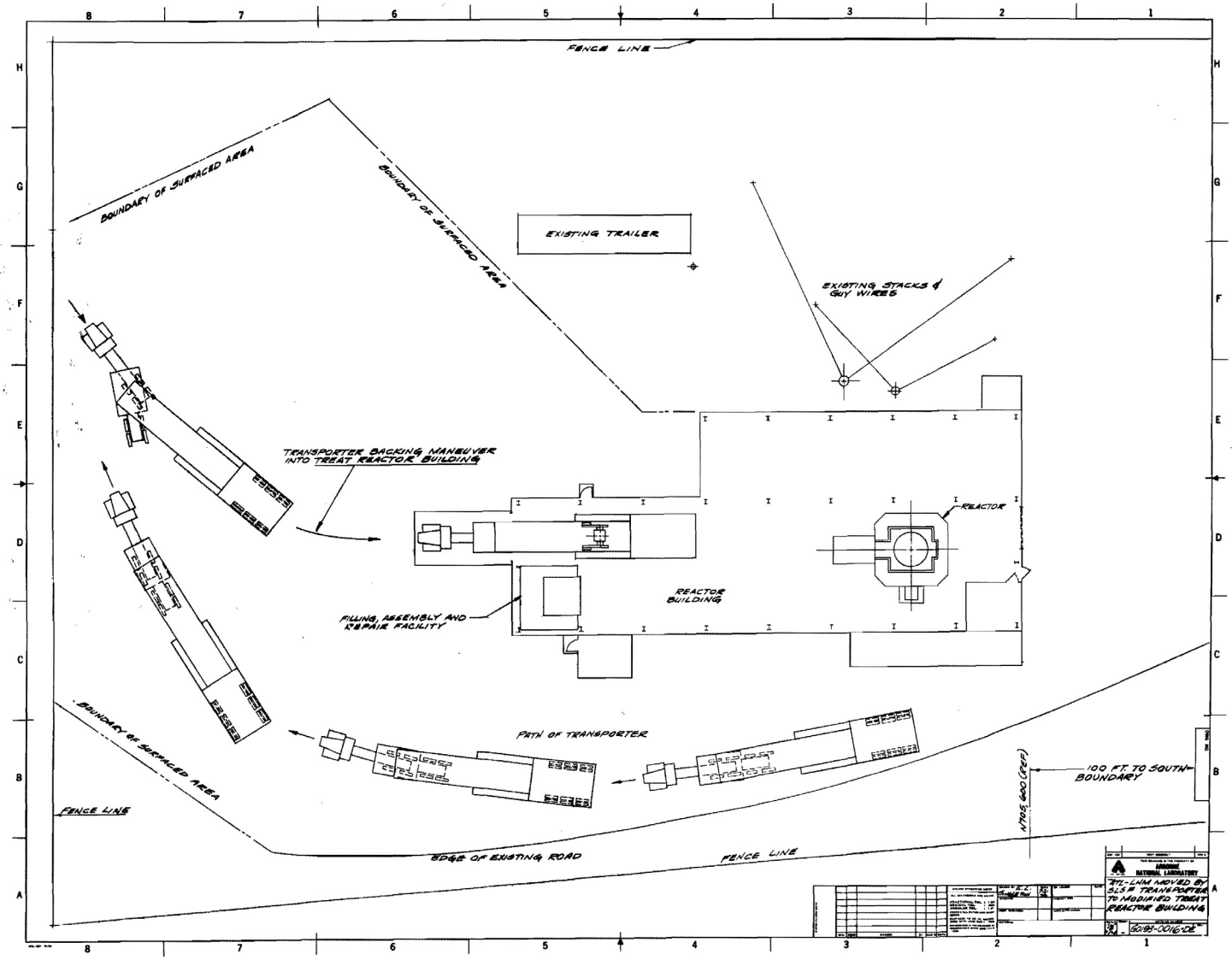

Fig. 2-4 Cask and Loop Moved by SLSF Transporter

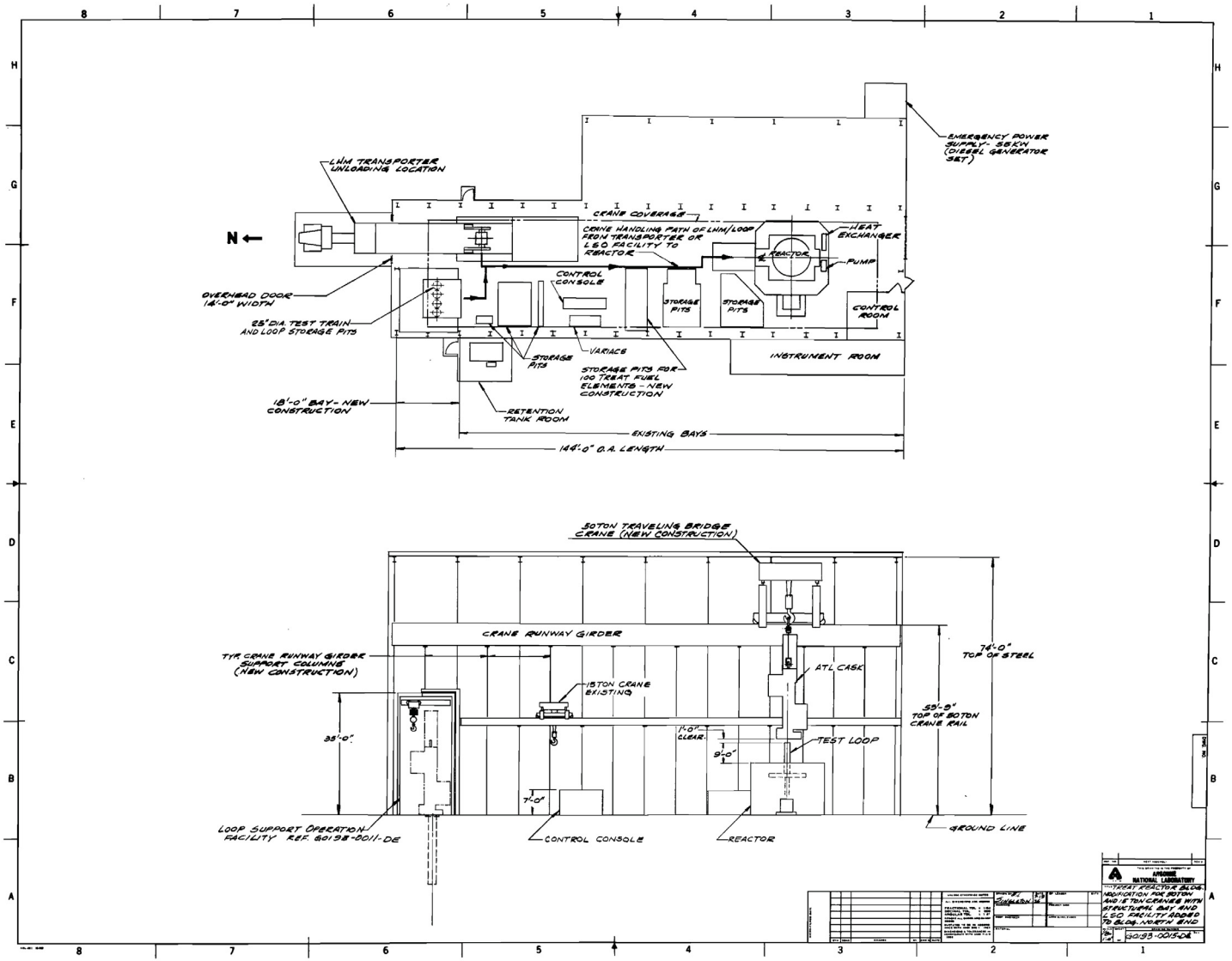

Fig. 2-5 TREAT Reactor Building Modification

2.1.5.3 Fuel- and Loop-Handling Systems

The sequence of operations involved in preparing Advanced TREAT vehicle experiment hardware for a test and in posttest disassembly and examination requires utilization of various parts of the Support Facilities complex (see Vol. VII). However, several of the operations would require portions of the proposed HFEF expansion, which will not become fully available until approximately 3 yr. after the TREAT modifications have been completed. Therefore the TREAT Upgrade Project includes the addition of specific features to the Loop Support Operations facility of the proposed TREAT building addition which will close the schedular gap and permit timely support of all experiment operations involving the ATL.

The overall sequence of experiment operations is schematically illustrated in the flow charts of Figs. 2-6 and 2-7. The following discussion highlights the role of the various facilities that support the Advanced TREAT loop.

It is assumed that the preirradiated mixed-oxide fuel pins will be designed so that remotely performed modifications to the pins in the HFEF/N Decon Cell will not be required.* After irradiation (PFR, FFTF, etc.), the fuel pins will be shipped to HFEF/N, and then they will be remotely assembled into a test train in the Decon Cell at HFEF using equipment designed for the SLSF Project. The remotely assembled test train will be installed into its primary containment using a loop storage hole at TREAT. Transfer to TREAT will be accomplished using the TREAT loop-handling cask.

Because of the cooling time for these irradiated pins and the small bundle size (19 or less), a gas-cooled transfer cask is not required for shipment between HFEF and TREAT.

Each primary and secondary containment will be assembled and checked out at ANL/E using existing facilities. In addition, each primary vessel will receive a hot, high-pressure prooftest prior to shipment to the INEL.

After installing the test train into its primary and secondary containments at TREAT, the loop will be neutron-radiographed in the radiography facility prior to test performance. After this radiograph has

---

* It is expected that HFEF will have a capability for installing wire-wrap spacers by November 1977.

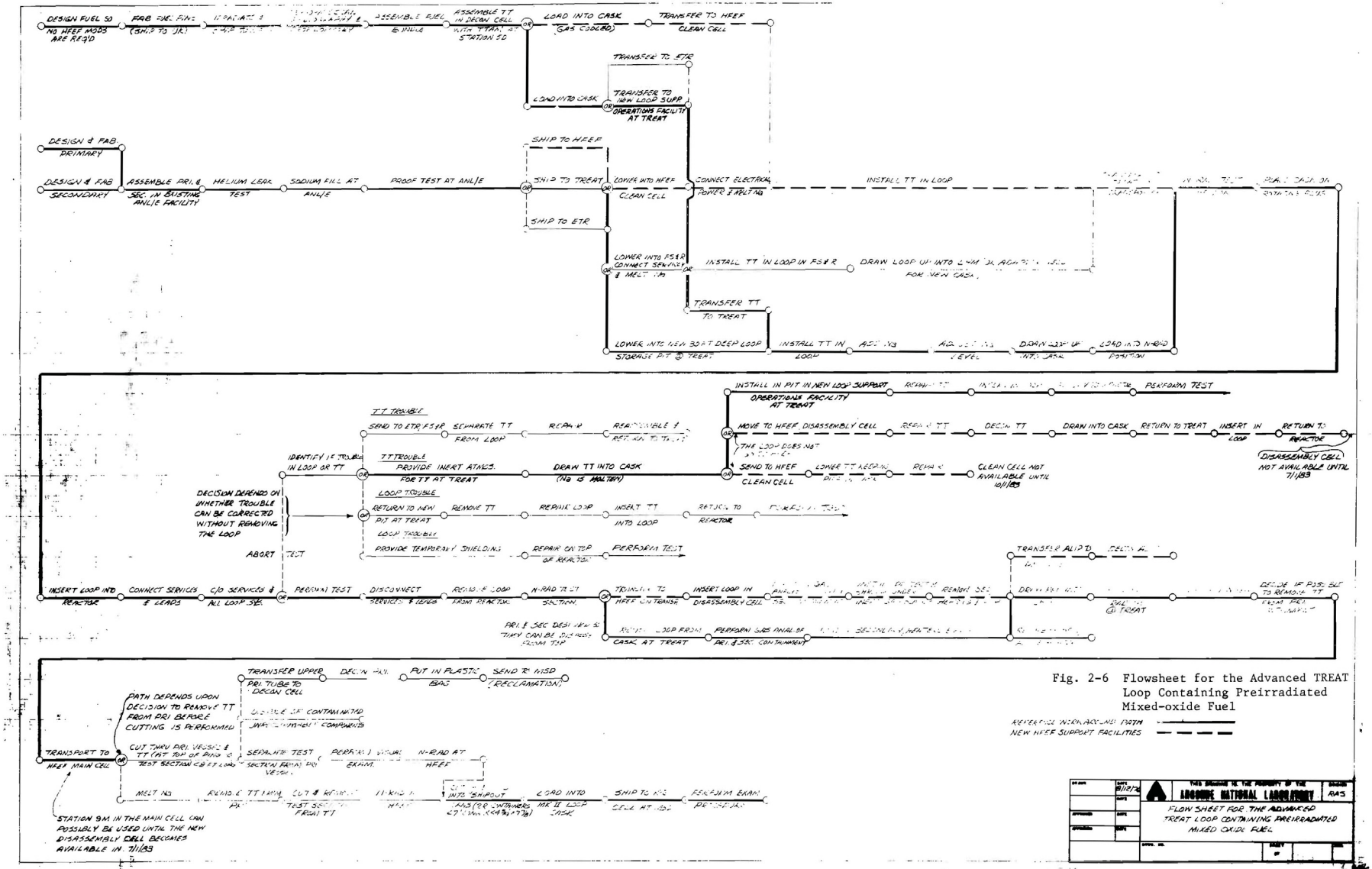

Fig. 2-6 Flowsheet for the Advanced TREAT Loop Containing Preirradiated Mixed-oxide Fuel

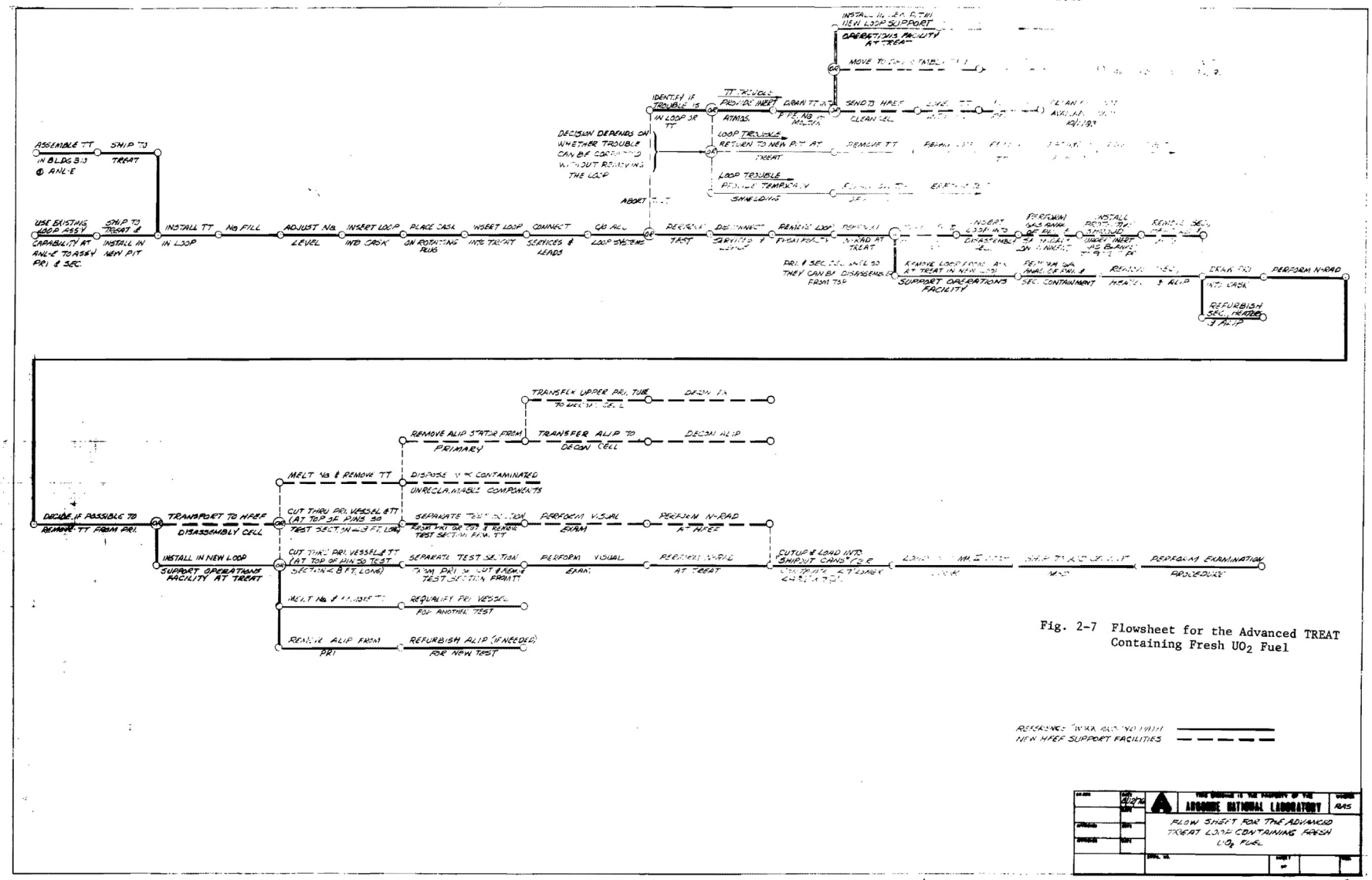

Fig. 2-7 Flowsheet for the Advanced TREAT Containing Fresh UO_2 Fuel

been taken of the test section, the loop will be inserted into the TREAT reactor for test performance. Prior to test performance, all test-train and loop instrumentation and operating systems will be given in a final checkout. If test performance (see Figs. 2-6 and 2-7 for the proposed plans for handling an aborted test) is successful, the loop services and leads will be disconnected, the loop removed from the reactor, and another neutron radiograph will be taken using the TREAT radiography facility. Following neutron radiography, the loop will be moved to a new storage hole inside the TREAT Building, where the loop primary will be lifted out of the secondary. Performance of this task in the TREAT Building eliminates the need for protecting against alpha contamination and virtually assures ready reuse of the ALIP, secondary containment vessel, instrumentation and heaters.

Continuing the handling sequence of a loop containing preirradiated mixed oxide, the primary-vessel test section will again be neutron-radiographed at TREAT. After taking a radiograph of the test train through the primary vessel, the primary with its test train will be transported to the Main Cell at HFEF/N. If the last "picture" shows that the test train can be separated from the primary vessel, the test train will be removed from the primary vessel in HFEF and neutron radiography performed in the new radiography facility at HFEF. If the test train cannot be removed in one piece from the primary, the test section will be cut away from the primary vessel by remote machine operations in the Main Cell. After performing a visual examination, neutron radiography will be performed in the new facility at HFEF.

Upon completion of neutron radiography, the test section will be cutup and loaded into a "shipout can." The shipout can will be inserted into a Mark-II Loop Cask and shipped to ANL/E (MSD) for examination.

The Loop Support Operations Facility addition to the TREAT building will provide the following essential functions:

1. Provide storage for two Advanced TREAT loops and two test trains (four pits).
2. Provide the capability to fill Advanced TREAT loops with uncontaminated sodium and to make the final adjustment of sodium level.
3. Provide the capability of checking out loop and test-train instrumentation prior to insertion in the TREAT Reactor (e.g., flowmeter calibration).

4. Remove flux wires from reactor calibration test assemblies.

Since the proposed HFEF Clean Cell would not be available until 3 yrs. after the initiation of testing in TREAT using the Advanced TREAT loop, the following additional operations will have to be carried out in the TREAT Loop Support Operations facility on a time scale consistent with experiment needs:

1. Inserting a test train that contains preirradiated mixed oxide or fresh UO_2 into a loop primary-containment vessel.
2. Inserting the primary containment vessel into the secondary and also removing the primary from the secondary containment.
3. Performing minor repairs on a loop or test train from an aborted test.
4. Removing fuel pins from reactor calibration test assemblies.
5. Cutting loop test sections from test trains using fresh uranium-bearing fuel.

The following functional requirements imposed on the Loop Support Operations facility will permit the essential functions discussed previously to be performed, as well as the additional functions required to support the Advanced TREAT Loop experiment operations prior to the availability of the HFEF clean cell:

1. A filtered exhaust-air system capable of holding the room under a negative pressure.
2. A source of breathing air for "hands on" operation.
3. Storage for two loops and two test trains (for loop receipt and checkout plus storage for aborted tests).
4. Equipment and tanks for loop filling and for uncontaminated sodium discharge.
5. Access to the room for casks containing loops.
6. Elevating devices for lower loops/test trains into their storage pits or raising them out of their storage pits.

7. Facilities for instrumentation, heaters, and ALIP checkout prior to loop insertion into the TREAT reactor.
8. Fixtures for installing test trains into primary containment vessels and for installing primary containment vessels into secondary containment vessels, when the primary and secondary contain ment vessels can be assembled and disassembled from the top.
9. A cutting device for separating a test section containing relocated UO_2 from its primary containment vessel. (The UO_2 was fresh prior to the test in TREAT; and the operation would be comparable to that presently being performed on "R-Series" experiments in an air atmosphere without a fire problem.)

2.1.5.4 Reactor Cooling System

The TREAT reactor is air cooled, and the reactor is maintained at a pressure level during operation that is negative with respect to the TREAT Building. At the present time, there is no plan for a significant change to the TREAT Reactor's cooling system. Modifications to the filter-holder assemblies, the blower, and the emergency power system may be necessary, and will be reviewed during the detailed design phase.

2.1.6 System Alternatives

An investigation was conducted to evaluate the feasibility of utilizing components and systems from the SLSF Project. The generalized results are as follows:

1. The SLSF Annular Linear Induction Pump (ALIP) can be used in the TREAT Upgrade Program with minor additions and modifications.
2. Since the TREAT Program is basically a "transient" type of facility (whereas the SLSF Program is a "steady-state" type of facility), there is no need to utilize the expensive heat exchanger which is incorporated into the SLSF Primary containment vessel. Also, the TREAT Advanced loop has an outer diameter of 16.2 cm (6.360 in.) and an inner diameter of 10.6 cm (4.000 in.) in the test-section area, whereas the SLSF primary containment vessel has an outer

diameter of 11.11 cm (4.375 in.) and an inner diameter of 9.842 cm (3.875 in.) in the test section. It is apparent that there is little incentive to attempt to use the SLSF Primary Containment for TREAT.

3. The SLSF secondary containment vessel has an outer diameter of 13.34 cm (5.250 in.) and an inner diameter of 12.06 cm (4.750 in.). The same incompatibility exists as with the SLSF primary containment when consideration is being given for use in the TREAT Upgrade Program.

4. The maximum outside diameter of the secondary vessel for the TREAT Advanced Loop is 50.165 cm (19.750 in;) and the inside diameter of the SLSF Loop Handling Machine (LHM) is 50.8 cm (20 in.). [The maximum diameter of the SLSF secondary containment vessel is 48.5 cm (19 in.)] When evaluating use of the SLSF-LHM for handling Advanced TREAT Loops, consideration must be given to the requirement that the SLSF-LHM must be available within 24 hr to remove an SLSF loop from the ETR. (The SLSF-LHM weight will be approximately 50 tons when modifications are complete.

5. The new TREAT cask will be designed to be accommodated within a 30-ton limit. It will be physically shorter than the SLSF-LHM. Consequently, this new TREAT cask can be moved between HFEF and TREAT by the SLSF Transporter.

6. To make the study of system alternatives complete, even though a ground rule was established that each facility shall be able to fill loops with sodium, use of the Filling, Storage and Remelt Facility (FS&R) at the ETR was considered. Presently, SLSF loops are in the FS&R from 6 to 9 weeks for each experiment, and the SLSF Project is planning 3 experiments per year. This potential schedular conflict and the additional handling problems (when compared to performing this function in the TREAT Reactor Building), greatly reduces the attractiveness of using the FS&R for filling Advanced TREAT Loops with sodium. Consequently, potential costs for fixtures and FS&R modifications have not been included in the cost summary for the TREAT Upgrade efforts.

7. The HFEF facilities for remote assembly and disassembly of test trains and loops containing preirradiated fuel can be used for

performing comparable functions for advanced TREAT loops. (Reference is directed towards Sect. 2.1.5.3 for the problems of working in an alpha-contaminated cell.) However, relatively minor modifications will be required to grid entry bars, clamp heads, etc., for the test-train assembly equipment designed for the SLSF Project. The exterior dimensions of the Advanced TREAT Loops will be basically consistent with the exterior dimensions of SLSF loops. This will minimize or completely eliminate the need to modify the fixtures and cutting equipment that will be used to disassemble SLSF loops.

8. The power-supply requirements for the ALIP to be used for the reference Advanced TREAT Loop can be met by motor-driven Variacs. Consequently, use of motor generator (MG) sets, comparable to those used for the SLSF Project, will not be required.

The following alternatives to the reference building/crane concept* have been investigated:

1. Figure 2-8 shows a 15-ton cask being carried by the existing 15-ton crane located inside a modified TREAT Reactor Building. The height of the crane rails has been raised to allow the cask to clear the reactor.
2. To eliminate the requirement to raise the crane rails, a new crane was considered (see Fig. 2-9) that would allow a 15-ton cask to protrude upwards between the crane girders.
3. To minimize the effect upon the TREAT Reactor Building and also upon its experimental program, consideration was given to lowering the SLSF-LHM through the roof of the building by means of an external crane. Figure 2-10 shows a Gantry crane having a 50-ton capability lowering the LHM through a hatch in the roof of the TREAT Building. With this concept, the TREAT roof would have to be raised over only 3 of the 7 column spans.
4. Use of an outside traveling bridge crane having a 50-ton capability is shown in Fig. 2-11 lowering the SLSF-LHM

---

* The Loop Support Operations Facility has not been shown in these alternative concepts.

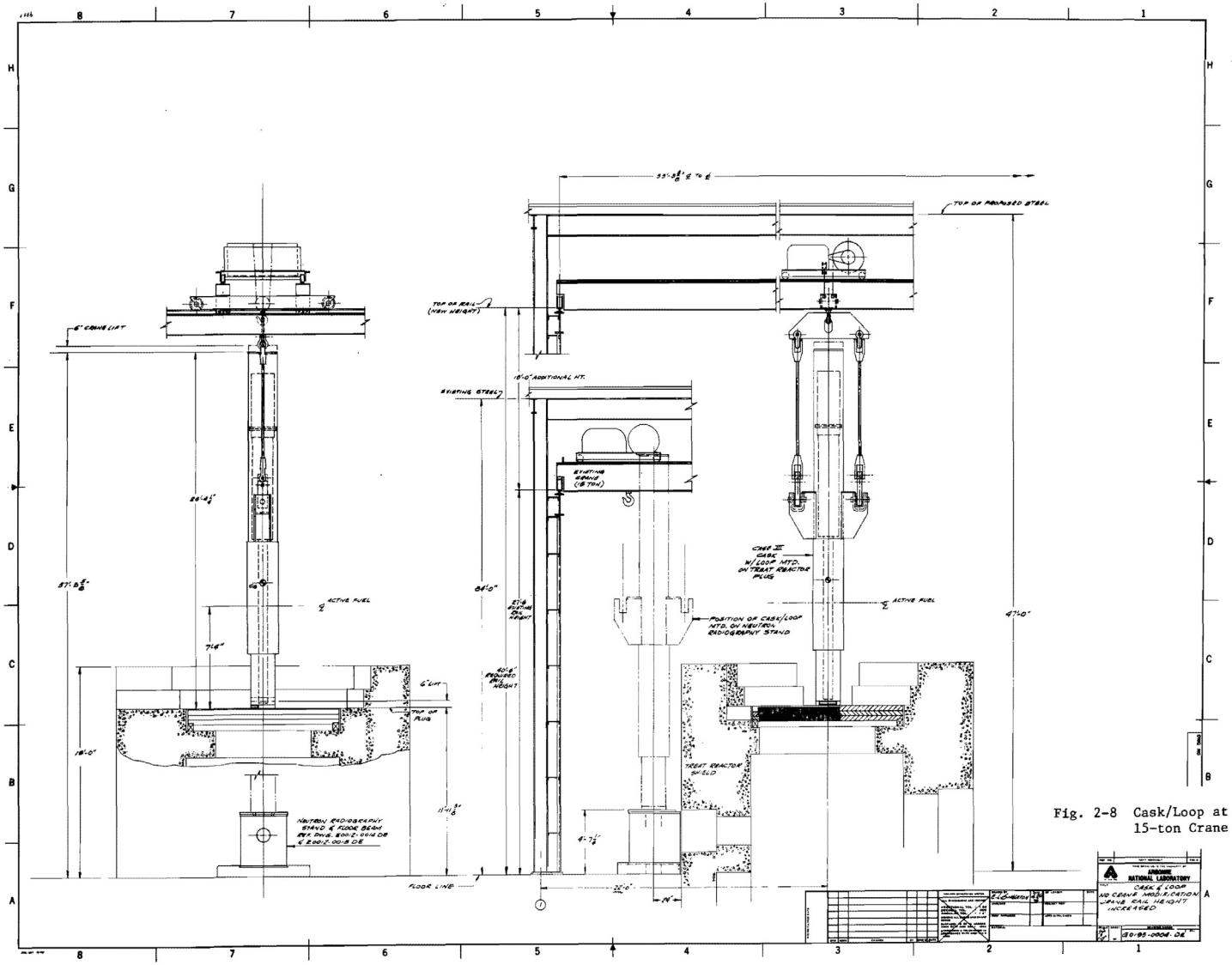

Fig. 2-8 Cask/Loop at TREAT Using Existing 15-ton Crane

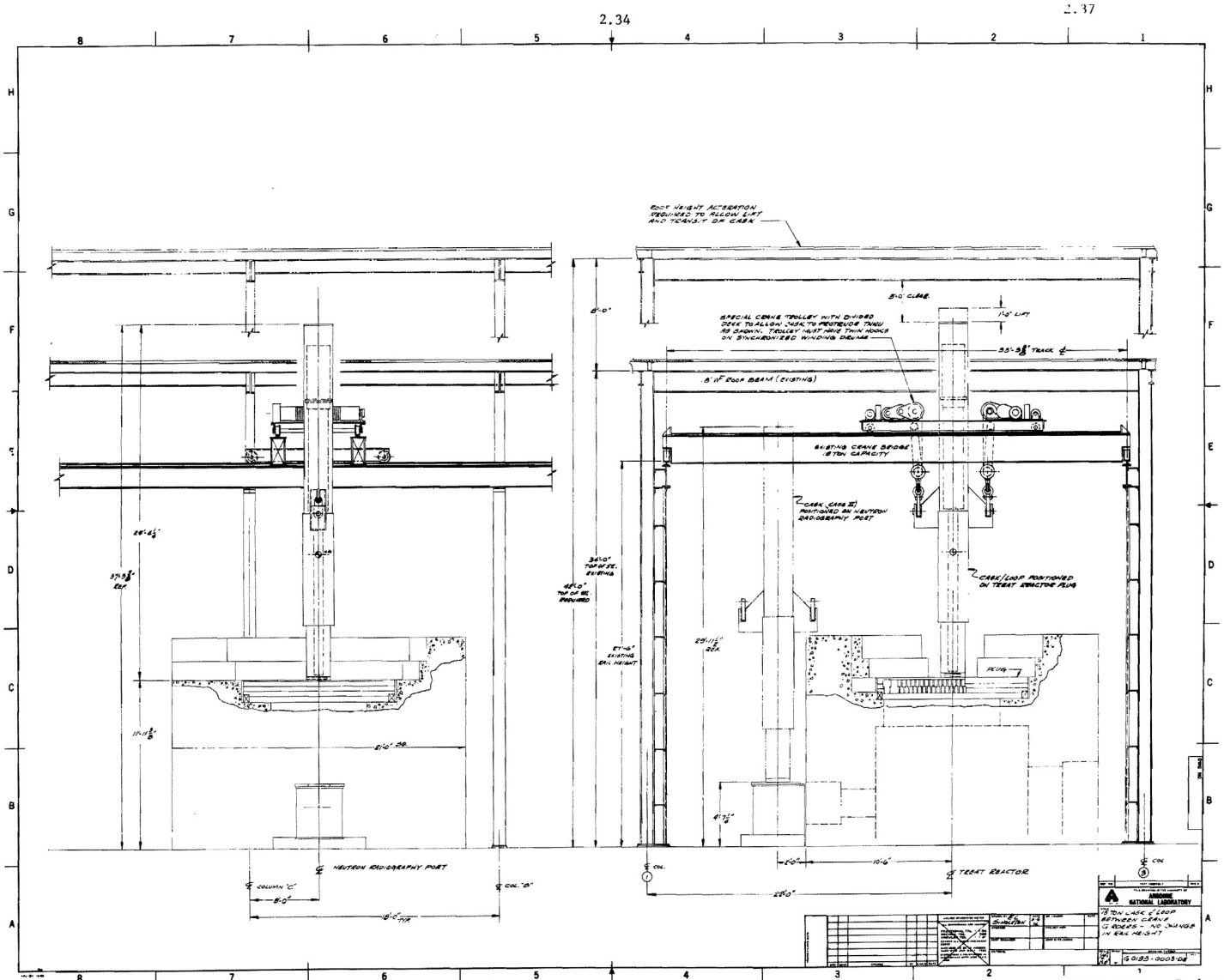

Fig. 2-9 15-ton Cask and Loop between Crane Girders - No Change in Rail Height

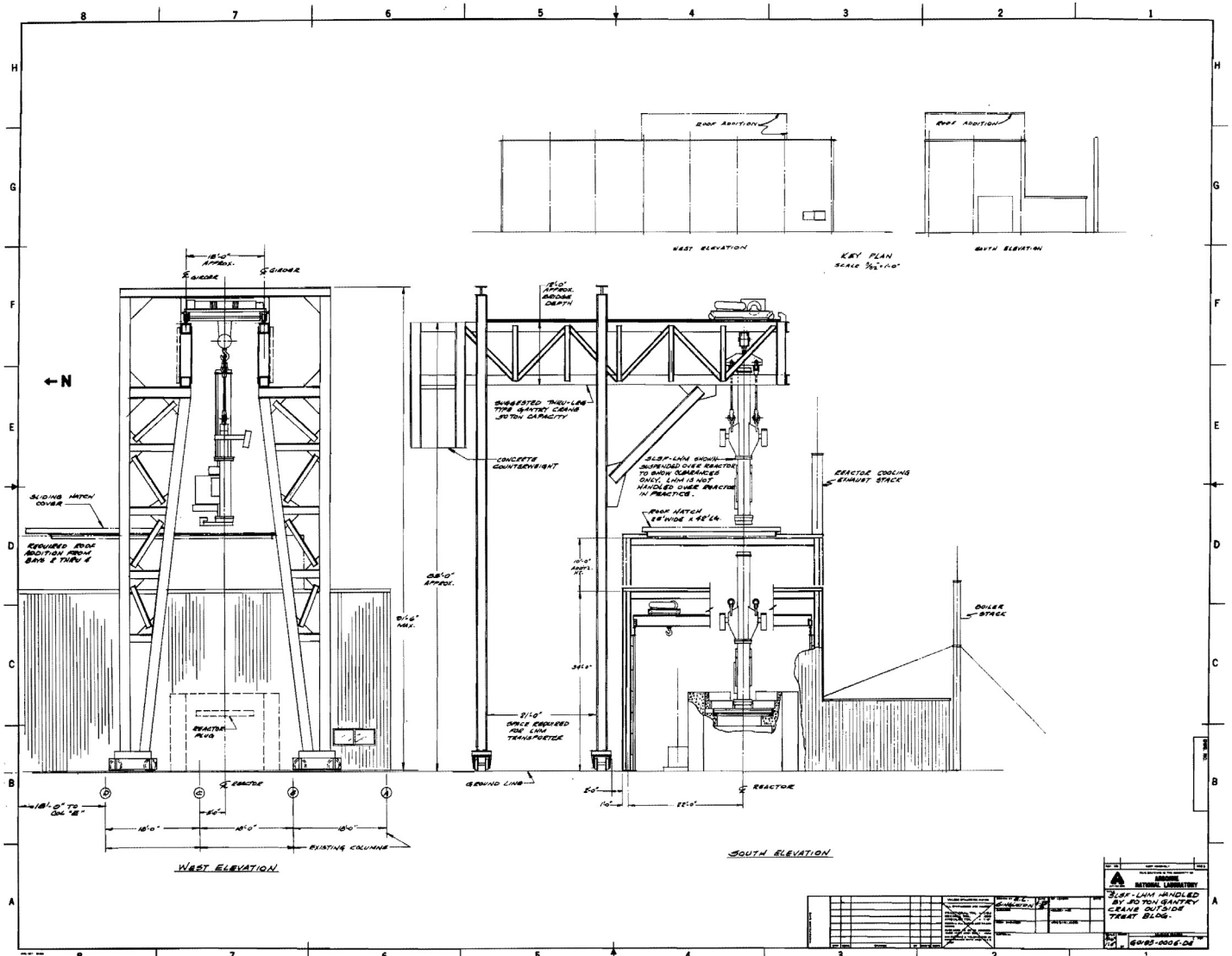

Fig. 2-10 SLSF LHM Handled by 50-ton Gantry Crane outside TREAT Building

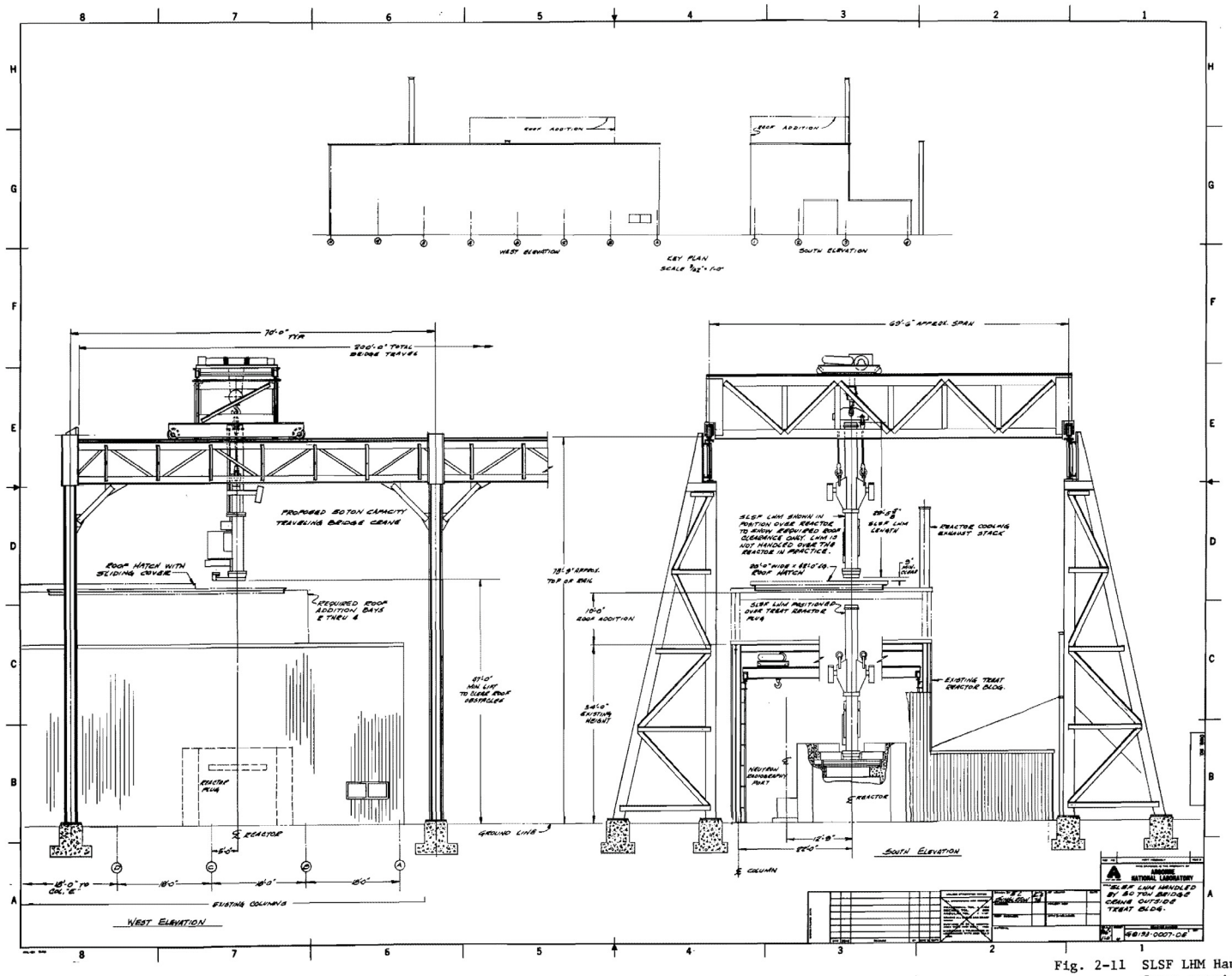

Fig. 2-11 SLSF LHM Handled by 50-ton Bridge Crane outside TREAT Building

through the roof of the TREAT Reactor Building. The building modification is identical to the previous case for the Gantry crane. Fig. 2-12 shows the LHM carried by the SLSF transporter and lifted inside the building, using an external bridge crane.

5. Use of a tower crane having handling characteristics similar to the previous bridge and Gantry crane cases is shown in Fig. 2-13. The building modifications would also be identical to the previously discussed illustrations for the bridge and Gantry cranes.

2.1.7 Summary Statement

The reference design is illustrated in Fig. 2-5. This design will accommodate a 30-ton cask/loop having to open a hoof hatch during moving of the 30-ton cask/loop to and from the reactor. To be able to seriously consider the significant savings that could result from using the SLSF LHM, one must evaluate the programmatic impact of requiring that the LHM must be made available within 24-hr notice to remove an SLSF Loop from the ETR. This requirement led to the choice of a special 30-ton loop-handling cask for handling the TREAT Advanced Loop.

2.2 Advanced TREAT Loop

The principal LMFBR safety-testing need to be met by an advanced test vehicle for TREAT is the determination of fuel-motion behavior in simulated HCDAs. In order to provide the needed data, a number of experiments with preirradiated mixed-oxide fuel are required. Experiments which can be performed with fresh UO_2 also will be required. These can be accommodated within the mixed-oxide capability and will not be discussed further here. Current national capability is limited to the Mark-IIC TREAT Integral Sodium Loop the only test vehicle currently having a record of actual testing with preirradiated mixed-oxide fuels in flowing sodium. The advanced-test-vehicle concept has evolved as an attempt to improve substantially the current capability by providing for both a larger bundle size and an improved thermal-hydraulic simulation with associated coolant-dynamic characteristics. Because of the demonstrated TREAT capability for overpower transients, it must be anticipated that the bulk of the testing program will include overpower-accident simulations conceptually defined as resulting from LMFBR reactivity additions at full flow (TOP accidents) or at degraded flow (as in a LOF-driven overpower accident).

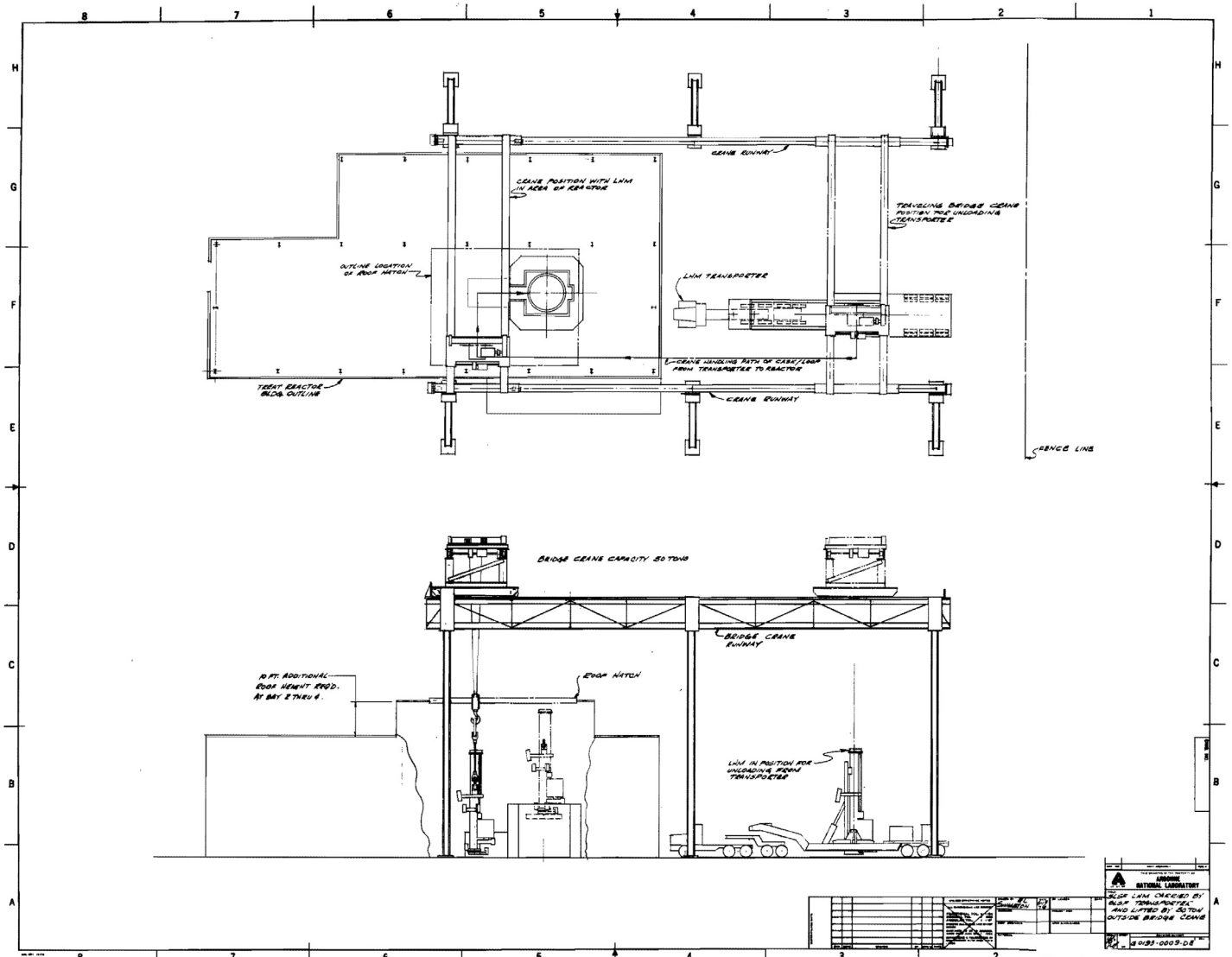

Fig. 2-12. SLSF-LHM Carried by SLSF Transporter and Lifted by 50 Ton Outside Bridge Crane

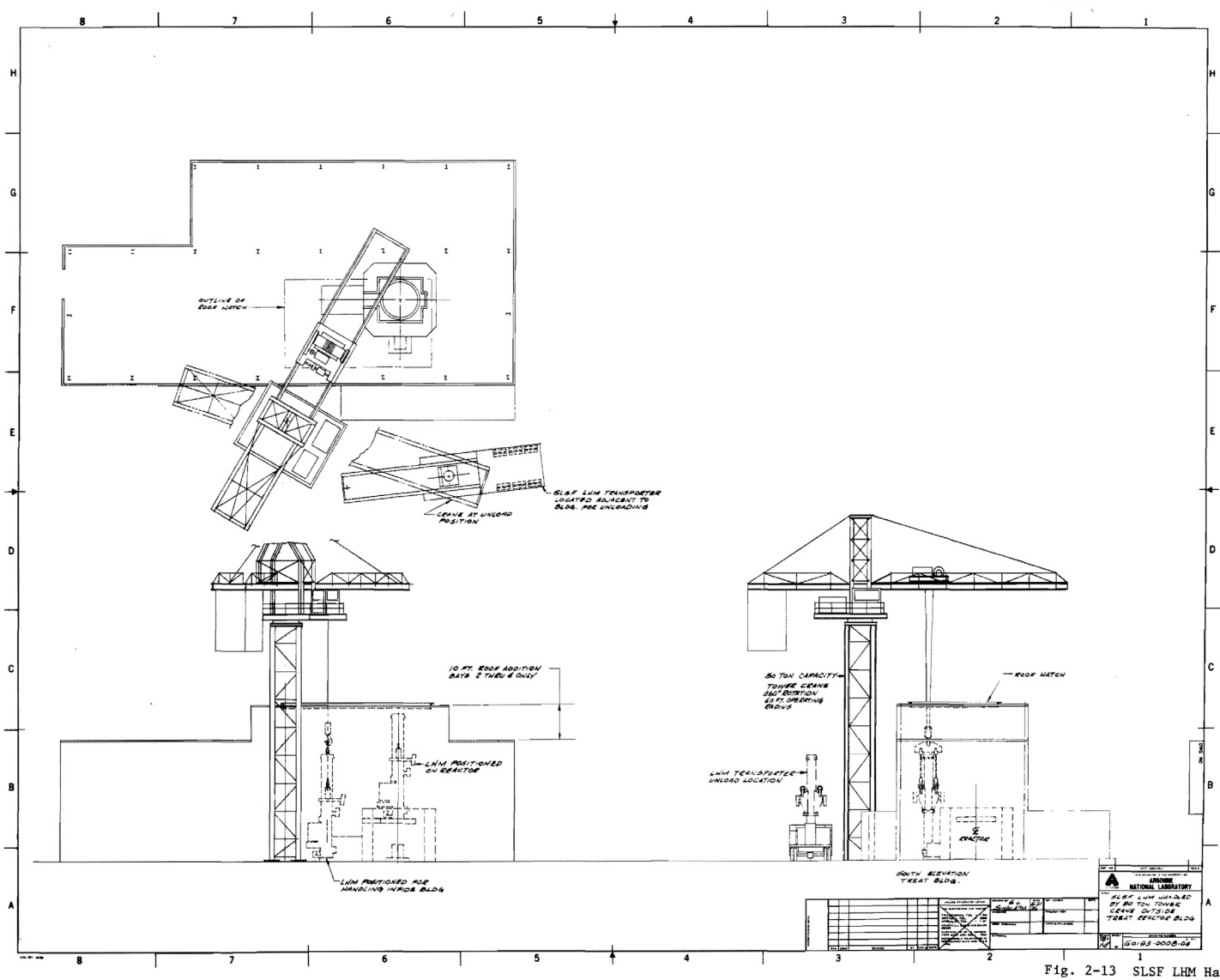

Fig. 2-13 SLSF LHM Handled by 50-ton Tower Crane outside TREAT Reactor Building

In addition to these general testing needs, the advanced test vehicle will have to accommodate fast reactor fuel having an 914-mm-long active fuel column with either an upper or a lower gas plenum. The design bases for fuel were the CRBR and PFR fuel-element designs, the latter a consequence of its potential near-term availability.

2.2.1 Functional Experiment Requirements

2.2.1.1 Summary

Based on the best estimate for the types of experiments needed to establish fuel-motion behavior for simulated LMFBR scenarios, the functional requirements for an advanced test vehicle were established as the basis for the conceptual designs. These functional requirements are listed in Table 2.3. The advanced test vehicle for TREAT will be required to accommodate a variety of bundle sizes and dimensions. The sizing of test-vehicle components might of necessity depend on different cluster characteristics as the basis for design. For example, the basis for most of the thermal hydraulic parameters was a test bundle containing 37 elements having the advanced oxide-fuel dimensions (6.86-mm-dia rods with a maximum wire-wrap diameter of 1.42 mm). However, the radial envelope should be at least large enough to accommodate 61 elements of the current CRBR design (5.84-mm-dia rods with 1.42-mm-dia wire wraps). The functional requirements are defined in this section so that different test-vehicle concepts may be evaluated on a common basis. This does not mean that such a comparison could be accomplished in a purely technical way. The reference design described in Sect. 2.2.3 does not necessarily meet all the functional requirements without some deviation; however, these deviations are considered to be minor and will not affect the ability of the advanced test vehicle to meet the testing objectives.

2.2.1.2 Test Fuel Requirements

2.2.1.2.1 Fuel Types

Fuel for these experiments will contain mixed uranium-plutonium oxides having the axial dimensional parameters of the CRBR and PFR baseline designs. The elements will have been irradiated in a fast reactor environment to burnups as high as perhaps 5 to 8 a/o. Elements being considered have uranium enrichments in ^{235}U ranging from natural to about 93%. The test vehicle should also consider both advanced-mixed-oxide-fuel radial dimensional characteristics (6.86-mm-dia rods with up to 1.42-mm-dia wire wraps) and other advanced fast reactor fuels. For purposes of engineering

TABLE 2.3 Functional Requirements for an Advanced TREAT Test Vehicle

Parameter	Design Basis or Desired Characteristics	Qualifications or Remarks
FUEL		
Fuel Type	UO_2-PuO_2	Also Advanced Fuels
Condition	Preirradiated	Includes Fresh
Element Length	CRBR & PFR	Includes FFTF
Active Fuel-column Midplane of Element	Centered at TREAT Midplane	±50 mm
Radial Envelope		Also includes:
Number of Elements	61	37 19 19
Rod Dia, mm	5.84	6.86 9.40 7.87
Wire-wrap Dia, mm	1.42	1.42 1.73 1.60
Geometry	Hexcan	Hexcan
THERMAL-HYDRAULIC		
Inlet Sodium Temperature	Up to 400°C	≤220°C Increase for Test
Minimum Flow Duration for Tests	30 s at full flow	Coastdowns Required
Flow Capability at Pretest Steady State	Circulation ≥10%	Equivalent Acceptable
Test-region Thermal Isolation	Mark-II-type Adiabatic Section	
Flow Rate Velocity	7.6-m/s in test region	For 37 elements (5.84- and 6.86-mm-dia rods with 1.42-mm-dia wire wraps)
Total Pressure Drop	Match current CRBR Subassembly	Includes inlet orifice
Inertial Lengths Ref. fuel-column midplane	Match CRBR Subassembly Outlet = 2.23 m Inlet - 2.54 m (±10% allowable)	For 37 elements with 6.86-mm-dia rods; 1.42-mm-dia wires for CRBR & PFR axial element design parameters.

TABLE 2.3 Functional Requirements for an Advanced TREAT Test Vehicle (Contd.)

Slug-ejection Pressurization Dynamics	Inlet or outlet plenum should not pressurize for rapid test-section voiding.	±20% form nominal ΔP (see discussion in text.)
Test-vehicle-system Pressure Control	Adjustable at Operating Conditions.	Up to 2 atm (0.2 MPA)
CONTAINMENT & SAFETY		
Pressure Rating		
Primary Faulted	≥425 atm (>43 MPa) at sodium temp. of 540°C	Critical pressure of sodium
Prooftest	≥200 atm (>20 MPa) at sodium temp. 540°C or its equivalent	Exceeds S-series FCI pressure pulses
Secondary	1 psig (6.9 kPa) for leak checking	
Meltthrough Protection	Passive radial heat capacity protection required	Can be met by primary steel wall with OD/ID = 1.56.
Expansion Volume in Gas Plenum	Equal to Sodium Inventory	
Adjacent TREAT Environment	Consider transient thermal phenomena	Converter elements may reach 1100°C adjacent to test vehicle.
Additional Requirements	Meet TREAT Experimenters Guide where applicable.	
INSTRUMENTATION		
Hodoscope	View Slot will be required	Design for minimum practical optical thickness to target for 1.5-MeV neutrons.

TABLE 2.3 Functional Requirements for an Advanced TREAT Test Vehicle (Contd.)

Pressure Transducers	Gas Plenum	Range 0-8 atm (0-0.8 MPa)
	Inlet & Outlet	Ranges 0-35 atm (10-3.6 MPa) and 0-170 atm (10-176 MPa).
Flow Measurement	Inlet & Outlet	Meter bypass, if present.
Temperature	Inlet & Outlet, & Test Section	In Adiabatic Section.
NEUTRON FILTER		
Test-section Filter	Cadmium, outside primary	Operable up to 1350°
NEUTRON RADIOGRAPHY		
Pretest	Required	At TREAT
Posttest	Required	At TREAT
POSTTEST EXAMINATIONS		
Disassembly	Required	At HFEF
Examinations	Required	By MSD, ANL/E

design studies, the test vehicle should accommodate the current CRBR fuel element length. A nominal sample cooling time of 6 months is assumed. Thus, there is no requirement for decay heat removal from the loop.

2.2.1.2.2 Cluster Size

The number of fuel elements needed to perform a given experiment determines the size of the cluster. However, no firm statement as to the minimum required cluster size in the range of upgraded TREAT capabilities could be established solely on the basis of experiment needs. Undoubtedly, a converter zone could be sized sufficiently large enough that TREAT could accept full LMFBR subassemblies. However, the vehicles for such a capability would far exceed current dimensional, weight, and handling envelopes at the TREAT facility, and exceed the desired implementation schedule. The cluster size identified for design purposes was therefore established to avoid exceeding certain constraining envelopes, such as the 200-mm-dia hole in the concrete support or ACIP capabilities.

It appears that the slot in the rotating plug at TREAT of 200 mm can be readily modified, and should not present a programmatic limitation. Since the PFR fuel extends below the lower TREAT grid plate, the test vehicle must penetrate into a hole in the concrete supports which is 200 mm in diameter. Modifications to enlarge this access hole to a larger diameter appear to be extensive since the core-support loads are carried by the reinforced concrete.

The current hodoscope collimator was recently modified to view larger clusters, but the horizontal field of view was limited to 66 mm. This dimension is just about sufficient to view 61 elements of the 5.84-mm-dia CRBR design. The latter constraint could probably be alleviated, but the cost of doing so might also require a substantial increase in associated electronic systems as well as for the collimator.

For the purposes of the design study, the basis of the desired cluster size for the radial envelope was established as the 61 elements having the current CRBR rod and spacer wire dimensions. However, a 37-element cluster size of the advanced-mixed oxide design (6.86-mm-dia rods with 1.42-mm-dia wire wraps) was established as the basis for meeting thermalhydraulic functional requirements. A mismatch in the capability for bypass flow and the desired value of bypass flow will therefore result for the 61-element cluster size i.e., rapid slug ejections will cause higher inlet plenum pressurization which could exceed the desired limit.

In addition, advanced fuels other than mixed oxides could be accommodated within the envelope defined above. Based on current designs, about 19 advanced fast reactor fuel elements could be tested in the envelope defined by the radial-dimensional constraint for 61 CRBR fuel elements. For the purposes of comparison, Table 2.4 lists the capabilities of a series of radial envelope dimensions including the reference selection.

2.2.1.2.3 Location of Test Fuel Cluster in TREAT

The current hodoscope collimator is focused on the center position in the reactor. The vertical line of focus of the hodoscope corresponds to the vertical centerline of the 200-mm-dia hole in the lower concrete supports. The test fuel must therefore be positioned so that the vertical centerline of the fuel-element cluster coincides with the vertical centerline of the 200-mm-dia hole. A deviation of ±50 mm in line with the hodoscope view slot is permissible. Lateral displacements should be avoided.

The current hodoscope collimator vertical view is 1.2 m. Since the active fuel column of the fuel elements is 914 mm, the midplane of the active fuel column should be located at the midplane of the collimator. The resultant view above the top of the fuel column would be about 150 mm. For some tests, it might be desirable to lower the midplane position of the fuel column to see additional fuel motion above the top of the active fuel. However, the PFR fuel would have to be lowered still further into the region below the grid plate. The resulting increase in overall test-vehicle length and the protrusion below the lower shielding were judged to be undesirable and to be avoided. Upper-plenum fuel, such as CRBR, could nevertheless be lowered somewhat without enlarging the shielding envelope should it prove experimentally advantageous to view fuel motion beyond the 150-mm limit above the top of the fuel column.

2.2.1.3 Test-train Requirements

The primary functions of the test train are to provide the flowpath for the coolant and to hold the fuel in place. In addition, the test train is used to mount instrumentation peculiar to individual experiments.

2.2.1.3.1 Thermal Isolation of Test Region

Current capability of the Mark II or R-Loop test-train designs should be retained. The current capability includes a gas-filled region (adiabatic section) for thermal isolation around the flow tube

TABLE 2,4 Numbers of Elements Which Can be Accommodated in Hexagonal-cluster Geometry within a Range of Envelope Diameters

	MIXED-OXIDE FUELS		ADVANCED FUELS		
Envelope Dia* (mm)	6.86-mm rods 1.42-mm wires	6.86-mm rods 11.11-mm wires	CRBR & FTR-Type	9.40-mm rods 1.73-mm wires	7.87-mm rods 1.60-mm wires
10.08	0	0	1	0	0
10.56	0	1	1	0	0
11.26	1	1	1	0	0
24.72	1	1	7	1	1
26.62	1	7	7	1	1
27.91	7	7	7	1	1
39.34	7	7	19	7	7
42.67	7	19	19	7	7
44.58	19	19	19	7	7
53.98	19	19	37	7	19
58.72	19	37	37	7	19
62.24	37	37	37	19	19
68.61**	37	37	61	19	19
74.78	37	61	61	19	37
77.90	61	61	61	19	37
83.24	61	61	91	37	37
90.83	61	91	91	37	37
94.56	91	91	91	37	37

* The diameter of the circumscribed circle around the inner boundary of the hexcan.

** Reference case, which allows 0.05 mm additional spacing between elements.

containing the test fuel. This region should be capable of being filled with helium or argon gas at 0.5 to 1 atm (0.05 to 0.1 MPa) at room temperature. In some experiments, the pressure in this section needs to be monitored.

2.2.1.3.2 Materials of Construction

Materials of construction should be at the option of the experimenter. Materials available for choice should include stainless steel, Inconel, molybdenum, or niobium.

2.2.1.3.3 Flow-Channel Geometry

The fuel should be surrounded by a hexagonal flow tube for the reference fuel-cluster sizes. The outer shell may be circular or hexagonal as desired.

2.2.1.3.4 Test-train Instrumentation

Test-train instrumentation includes thermocouples in the coolant stream at the outlet and along the test region on the flow tube in the adiabatic section. The ability to add other instrumentation, such as sodium-boiling detectors, should not be precluded. The monitoring of the inlet coolant temperature and flowrate should be accomplished so that a failure of the flow tube will not result in the loss of the inlet-thermocouple or flowmeter-output signals such as by meltthrough of their output cables.

2.2.1.3.5 Safety and Design Considerations

In some experiments, the inner flow tube will reach sodium-boiling temperatures of 1000°C while the outside of the test train remains at the inlet temperature. These different temperatures should be considered in the design since this could result in differences in thermal expansion. At no time should expansions result in the test train putting excessive forces on the test-vehicle containment closures. At this time, no credit shall be taken in the primary containment designs for the containment capability of test-train components in a reactor reactivity accident defined in the TREAT Experimenters Guide.

2.2.1.4 Thermalhydraulic Requirements

2.2.1.4.1 Coolant and Flow

The coolant shall be sodium at inlet temperatures up to 400°C. The inlet temperature during heat-balance calibrations tests should not increase by more than 220°C, since the test vehicle will not have a heat exchanger. The flow rate desired through the 37-element clusters is 7.6 m/s. Since lengths, flow areas, and hydraulic diameters differ

depending on the fuel design, the basis for design should include rod diameters of 5.84 and 6.86 mm with a wire-wrap diameter of 1.42 mm. The basis for length should be the current CRBR length. In addition, an orifice shall be provided at the inlet to permit the match in pressure drop for a CRBR subassembly inlet. In this case, the total ΔP across a CRBR subassembly should fall within the capability of the advanced test vehicle for TREAT.

In some experiments, a controlled flow coastdown will be required. The coastdowns desired will require equipment to function in a controllable manner to reduce flow from 100% to 10% of full flow in from 5 to 20 s. In selection of equipment to accomplish this function, thorough consideration should be given to the high reliability desired for the experiments.

For the purposes of comparing potential concepts, note that a flow duration of 30 s at full flow will meet most of the flow requirements for experiments in TREAT that result in fuel failure. Nevertheless, flow at 10% of full flow, or greater, is desired before the transient to perform test-vehicle checkouts and provide for thermal stability. The desire for pretest operational capability could be accomplished in an alternative manner for a gas-driven system. In addition to the above, note that the various flow paths will require either orifices or other means for adjusting flow. The test vehicle should have provisions for accomplishing such adjustments.

2.2.1.4.2 Inertial Lengths

In experiments for which coolant-slug ejections are an important phenomenon, the behavior of the upper and lower slugs will depend on the inertial length encountered. The larger the inertial length, the lower the initial slug acceleration. For simulations of overpower accidents, the test vehicle should be designed so that these inertial lengths can be simulated. The design implication is that the flow-channel areas above and below the test fuel must be sized so that the inertial length meets the CRBR subassembly parameters.

According to Deitrich,* the inertial length ℓ is equal to:

$$\ell = A_o \Sigma_i \; L_i/A_i,$$

where A_o = flow area in the test section

A_i = flow area in the i^{th} channel

L_i = length of the i^{th} channel

For example, for an outlet of a fixed overall length, an enlargement of the flow area results in a decrease in its inertial length. For the CRBR subassembly, the total inertial length is about 4.77 m, with 2.23 m above the midplane of the active fuel column and 2.54 m below. Since the element itself is 2.845 m long, the inertial length above the top of the element is only about 200 mm and below the bottom of the element about 1.73 m. The outlet flow channel of the test vehicle should therefore be sized to give an inertial length of 200 mm; the inlet (downcomer) to give 1.73 m with a CRBR element as the test element.

For the purposes of meeting this requirement, an allowance no larger than 20% in the total inertial length is considered desirable based on the value computed from the midplane reference. The upper slug inertial length can therefore be increased by 200 mm and the inlet slug inertial length by 208 mm. In this case, the outlet inertial length above the CRBR fuel element can be increased to 400 mm, whereas the inlet could increase by 280 mm to 2 m. Should an FTR element be used, the additional inertial length required to meet the CRBR values could be provided by reducing the flow channel without altering the basic design of the test vehicle.

The use of PFR fuel further complicates the matching process for CRBR. The PFR requires added inertial length above the element since it is shorter than the CRBR. This could be accommodated by adding inertial length again in the form of a reduced flow channel area above the elements. However, the PFR fuel extends 838 mm below the position of the CRBR in the loop relative to the midplane, and this then places a lower limit on the maximum inlet inertial length of 889 mm, or 1.14 m, with the 20% allowance. The result is that the requirement for inertial length must be referenced to the element being considered. Since CRBR, FTR, and PFR are all included, the requirements consider all three. For design purposes, this means that the inlet inertial length for PFR elements must be sized to 889 mm, with 1.14 m being acceptable. The outlet for CRBR elements must be sized to 200 mm, with 400 mm being acceptable.

The implications for design are that both the outlet to the plenum and the inlet from the plenum must be sized based on inertial length, not necessarily only for minimum pressure drop. The result

---

* L. W. Deitrich, Suppression of Sodium Slug Impacts in TREAT Mark-II Loop, Trans. Am. Nucl. Soc., 13, 341 (1970).

will probably be that the requirement for inertial length matching will cause both the outlet and inlet flow areas to be relatively larger than in previous loop designs. Note also that a reactor with bottom-plenum pins might not be simulated since the inlet inertial length may be too large if the advanced test vehicle meets only the criterion for the CRBR inertial length.

2.2.1.4.3 System Dynamic Performance (Bypass-flow Requirements)

For a real subassembly undergoing an HCDA, the pressure drop across the subassembly depends only on the pumping rate of primary cooling system. A disruptive event in a subassembly for the incoherent events postulated in typical reactor-accident scenarios will not cause a pressurization of the inlet plenum. A pressurization will not occur since ample flow paths are available to the free surface through blanket, control, and nonparticipating subassemblies. In effect, the bypass-flow ratio is very large even though 20 to 30% of the subassemblies might be undergoing a simultaneous pressure event in the fuel zone.

Previous test hardware represented by the Mark-IIC loop does not possess this characteristic. Indeed, slugs ejected downward must pass through the pump in the reverse direction. For a pumped system to be made equivalent to the reactor situation, a high capability for bypass flow must be incorporated into the test-vehicle design. For the 37-element cluster, a bypass-flow ratio of 2:1 was selected as a requirement for design (twice the flow bypasses the test region than passes through the test zone). With a pump having this capability, a 5:1 bypass-flow ratio would be available in a 19-pin test. The result would be that any slug ejected downward will not pass through the pump (since the bypass is available) until later in the accident scenario. The back pressure drop of sodium passing backward through a linear induction pump is not well understood, although its effects have been estimated in test analyses, and it obviously has occurred in the previous testing without any apparent consequences.

2.2.1.4.4 System Pressure

The test vehicle should have provisions for adjusting the total system pressure at operating conditions. The pressure range required is 0 to 2 atm (up to 0.2 MPa) gauge.

2.2.1.5 Safety Considerations for Test Vehicle

The advanced vehicle design will be subject to the normal safety requirements identified in the TREAT Experimenters Guide. Those safety requirements having a principal effect on the design parameters are discussed in this section.

2.2.1.5.1 Pressure Ratings and Relief Requirements

Since the test vehicles will contain plutonium, double containment is required. The test-vehicle primary containment should be designed for a pressure rating which corresponds to a faulted condition (abnormal occurrence) of at least 425 atm (43 MPa) at a sodium temperature of 540°C using the criteria established for design of pressure vessels in the ASME Boiler and Pressure Vessel Code. In addition, the proof-test pressure for the test vehicle should exceed 200 atm (about 20 MPa) for a sodium temperature of 540°C or its equivalent. The faulted condition pressure rating of 425 atm (143 MPa) at 540° corresponds to the critical pressure of sodium, a pressure which is not expected nor has been observed in tests thus far conducted in TREAT. The desire to test at 200 atm (120 MPa) or above corresponds to the highest pressure recorded in the S-series experiments in TREAT for oxide fuels reported by Wright. Meeting both criteria will facilitate safety approval of the test vehicle. Note that a vessel undergoing the faulted-condition pressure may deform, but not breach. Therefore, the vessel could not be reused. The current Advanced TREAT vehicle concept exceeds these pressure rating requirements.

The secondary containment should be a leak-tight structure capable of being leak-checked when a pressure of 0.07 atm (7.1 Pa) is present in the containment. Pressure relief in the primary containment should be provided by sizing the gas plenum so that the free gas volume at 400°C is equal to, or greater than, the inventory of sodium present in the test vehicle with a test train containing 37 advanced oxide-fuel elements.

2.2.1.5.2 Meltthrough Protection

In a TREAT reactivity accident, the test fuel will undergo substantial melting. In order to obtain safety approval for

---

* R. W. Wright, J. J. Barghausen, S. M. Zivi, M. Epstein, R. O. Ivins, and R. R. Mouring, "Summary of Atuoclave TREAT Tests on Molten-Fuel-Coolant Interactions," Proceedings of the Fast Reactor Safety Meeting, Beverly Hills, California, CONF-740401-P1, p. 254 (1974).

:rpower and TUC simulations, the practice of requiring the primary containment to be protected against meltthrough without credit for external cooling shall apply. Previous experimental approval has been obtained when the heat-sink material was, in fact, the steel pressure vessel itself. The criterion to maintain the ratio of steel-to-fuel volume per unit length equal to current practice would facilitate safety approval. The current design for the Mark-IIC primary containment, which has received safety approval, requires the outer diameter of the steel pressure vessel to be 1.56 times the inner diameter. The test-vehicle primary containment shall be augmented by the equivalent amount of heat-sink material in the event that the actual test-vehicle wall thickness is decreased to meet the pressure-containment requirement alone.

2.2.1.5.3 In-pile Environmental Considerations

Note that the test vehicle must be compatible with the testing environment in TREAT. In addition to the usual conditions in the TREAT core, the test vehicle may be subjected to high temperatures from adjacent spectral-converting elements of the proposed fuel after the transient. The interaction between the thermal environments should be limited so that a containment breach or mechanical problems will not occur.

2.2.1.5.4 Plutonium Limits

The test vehicle will contain plutonium in excess of the current 150-g limit at TREAT. The plutonium limit therefore needs to be increased so that longer fuel elements and larger cluster sizes can be tested. The plutonium limits acceptable for specific weather conditions are discussed in Sect. 3.4.

2.2.1.5.5 Other Considerations

The test-vehicle design should be reviewed for safety problems associated with, and/or related to, the general hazards of handling liquid sodium and applicable standards or current practice shall apply. The test-vehicle safety evaluations should also consider the problems of sodium-slug impacts and test-vehicle movements during the in-reactor testing.

2.2.1.6 Operations and Data Requirements

2.2.1.6.1 Nondestructive Examinations of Test Fuel

Individual test fuel elements need to be neutron-radioagraphed to determine acceptability for each test. Destructive examinations of sibling test fuel will provide data for pre- and-posttest analysis. Gamma scans of the test fuel are also desirable.

2.2.1.6.2 Neutron Radiography of Test Vehicle

After the test vehicle is loaded, but before each test, a pretest neutron radiograph of the test region is required. A gamma scan is also desirable.

2.2.1.6.3 Instrument Calibrations

Except for thermocouples, the test-vehicle instruments should be calibrated before the test vehicle is installed in the reactor.

2.2.1.6.4 Sample Power Calibrations and Heat-balance Tests

A neutronic mockup of the test vehicle will be needed before a test series to provide for power calibrations of the test sample. Verification of rates of sample energy deposition will be accomplished with the test vehicle and test fuel before each test by performing a heat-balance. The test vehicle should be designed accordingly, since the heat-balance test might introduce a difference in final test-vehicle conditions which would render it unsuitable for the actual test (i.e., thermal cycling leading to failure of all the test region thermocouples).

2.2.1.6.5 Data Acquisition

Table 2.5 summarizes the requirements envelope for data acquisition established for the TREAT Upgrade.

2.2.1.6.6 Posttest-examination Requirements

The posttest phase of the experiment is an important part of the analysis of the experiment and should be considered in the test-vehicle design. It is here that the final disposition of the fuel and clad is determined, and the scenario of the experiment events finalized.

2.2.1.6.7 Neutron Radiography

Neutron radiography of the test vehicle is required after the external outfitting on the test region has been removed. The capability for radiography at 0, 45°, and 90° is desired. Because of the thick pressure walls, removal of the failed test train is desirable in order to improve the radiograph quality.

2.2.1.6.8 Test-vehicle Disassembly

The test region will be shipped for posttest detailed examinations. The test vehicle should be designed so that it will be readily disassembled in HFEF after the test. A sampling method should be available to obtain data on the radioactive gas in the primary containment.

TABLE 2.5 Envelope of Requirements of Data Acquisition for Advanced TREAT Test Vehicle

Instrumentation	No. of Instruments	No. of Analog Tape Channels	Time Resolution Required	Accuracy Desired	No. of CRT Visicorder Channels
I. EXPERIMENT SENSORS					
Thermocouples					
Fast Response	25	25	Continuous	±1% Full Scale (F.S.)	15
Slow Response	15	1 (Multiplexer)	For 1 ms every 15 ms	±1% F.S.	5
Flowmeters	4	8	Continuous	±1% F.S.	8
Pressure Transducers	14	14	Continuous	±1% F.S.	14
Acoustic Microphones	2	6	Continuous	±1% F.S.	4
Fast-Neutron Hodoscope	1	N/A	1 ms	-	N/A
Time	1	1/unit	1-ms-time frame (real time)	Data coherence ±1 ms for all channels, all recorders; Real time ±1%	1/unit
II REACTOR PARAMETERS					
Power	1	2	Continuous	±1% F.S.	2
Integrated Power	1	2	Continuous	±1% F.S.	2
Other Reactor Operating Parameters	15 (max)	1(Multiplexer)	For 1 ms every 15 ms	±1% F.S.	6
III. ENGINEERING PARAMETERS FOR TEST VEHICLE					
Thermocouples, Voltages, Purge-gas Flows	15 (max)	1 (Multiplexer)	For 1 ms every 15 ms	±1% F.S.	4
IV TOTALS					
Sum (Excluding Time)		60	-	-	60
Number of Units		5	-	-	5
Number of Multiplexers		3	-	-	N/A

It would also be desirable to plan for the nondestructive disassembly of aborted tests.

2.2.1.6.9 Postmortem Examinations

The test region of the test vehicle will be shipped for postmortem examinations in an alpha-gamma hot-cell facility. All associated hardware and interfacing must be included in the system design.

2.2.1.6.10 Disposition of the Experiment Components

Re-use of expensive components of the test vehicle should be considered in the design.

2.2.2 Design Concepts

2.2.2.1 Alternative Concepts

The basic choices for a test vehicle for preirradiated fuel are among combinations derived from:

(1) pumped vs. gas-driven for flow generation;

(2) concentric vs. U-tube configuration for the in-pile section;

(3) integral vs. modular assembly.

The current R-series apparatus is a modular system for fresh fuel testing in TREAT. The configuration of the integral (packaged) test vehicle is more desirable for TREAT for preirradiated fuel than a modular design since the latter will require potentially contaminated sodium lines to be broken for disassembly. This will be the case when either a pumped or a gas-driven system is considered. Since TREAT does not have a hot-cell facility, the modular concept offers a potential feasibility question. It was therefore not considered further.

The test objective to obtain coolant-dynamic simulations in the advanced test vehicle tends to favor a gas-expulsion system such as the current R-series apparatus for fresh-fuel tests. For the package system, it would apparently be permissible to incorporate the gas-driver and gas-receiver tanks external to the package so long as steps were taken in the design to assure that the gas lines will not be contaminated during a normal test. The sodium-supply and -receiver tanks would have to be incorporated within the package and withdrawn from the facility through the shield. Since the tankage volume is a major limitation, the running time for an experiment would be limited. For example, the estimated running time at full flow for 37 advanced oxide-fuel elements (6.858-mm-dia fuel rod with 1.42-mm-dia wire wraps) would be about 40 s for the enlarged reference envelope.

A pumped system can be made to achieve the experimental simulation if a high bypass flow were provided. For a sufficiently high bypass-flow ratio, the pump would, in effect, be decoupled from the test section. The inlet-plenum pressure would remain constant when a pressure event caused inlet-flow reversal, thus simulating the events postulated for this type of HCDA. In addition, flow back through the pump itself is to be avoided since this phenomenon is potentially difficult to analyze.

For example, with a bypass-flow ratio of 7:1, the pressure buildup at the inlet for a total test-section blockage (i.e., a pressure event large enough to cut off flow) was estimated to be about 10% of the nominal ΔP. This estimate of pressure increase was based on the characteristic curve for ALIP pumps of current design. In addition, backflow through the pump channel would not occur for some period of time after flow reversal.

For the larger pump selected for the advanced loop, indications are that the pump will have a reduced variation of pressure head with the flow rate relative to an ALIP of current Mark-II design. As a consequence of this reduced pressure-head variation, the need for a high bypass-flow ratio is partially alleviated. The limitations of inlet-plenum pressurization for the accident simulations might therefore be achieved by means of a lower value for the bypass-flowrate ratio. Even so, a potential problem of data interpretation might still remain when flow passes back through the pump when a large pressure event occurs in the test section.

A bypass-flow ratio of 2:1 was established for a 37-element bundle size for a pumped system, although a higher value would be desirable. With the same pump, a bypass-flow ratio of 5:1 could be achieved for a 19-element cluster for about the same flow velocity in the test region.

The tradeoff between a pumped vs. a gas-driven integral system is primarily one related to running time vs. bypass flow required. Of the two, the general conclusion would probably be in favor of gas-driven for dynamic simulations, whereas a pumped system would provide a wider range of capabilities and growth potential related primarily to cluster size.

Ordinarily, there would be little reason to select a "U-tube" in-pile section over a concentric configuration, as illustrated in Fig. 2-14, on an engineering basis alone. A concentric in-pile section is apparently more easily "engineered" and is generally more compatible with the TREAT in-core envelope, its neutron-radiography facility, and an existing pump design.

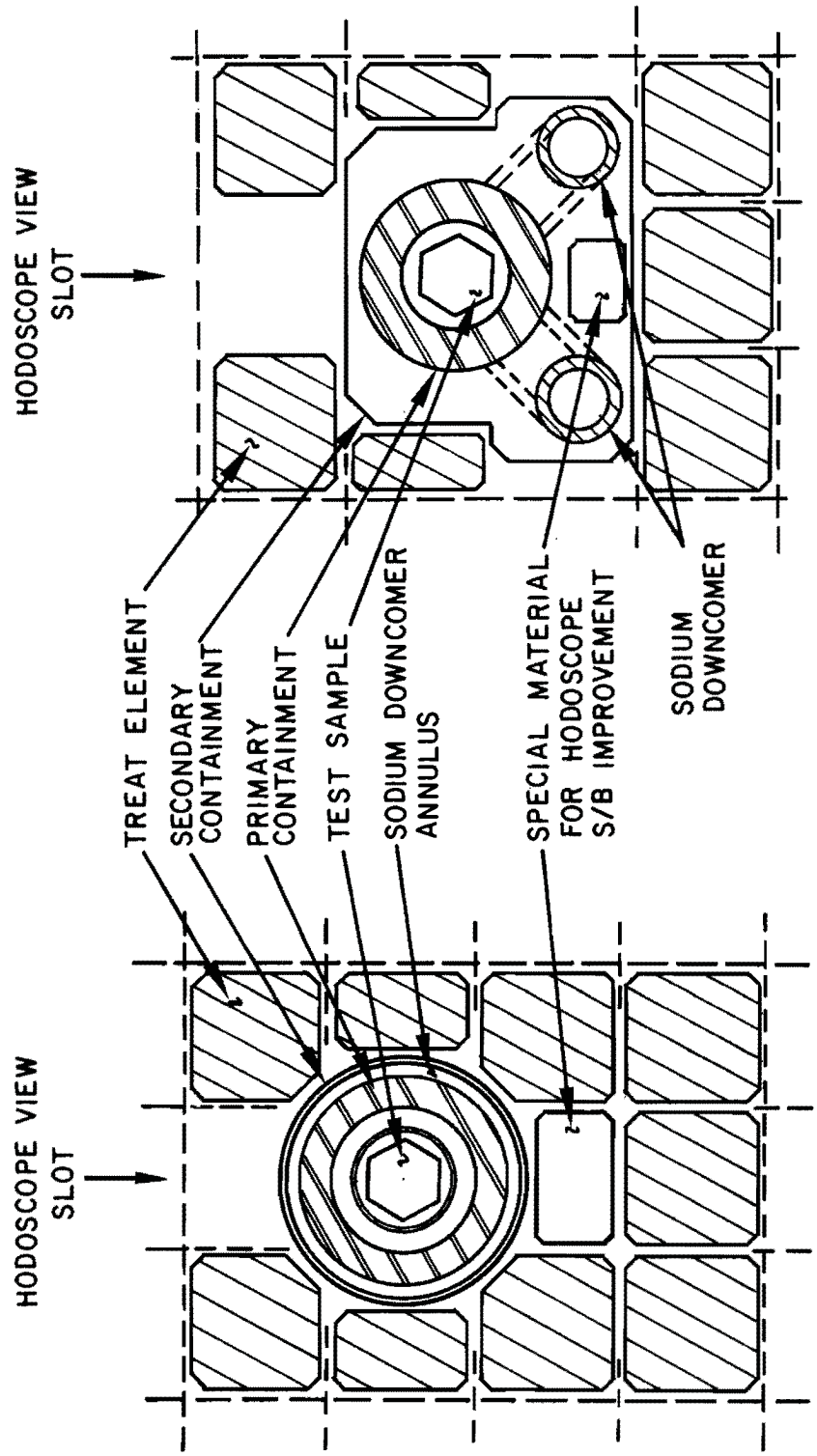

Fig. 2-14 Schematic Representation of Candidate In-pile Configurations for Advanced TREAT Test Vehicle

In addition, no loop or test-vehicle components would add to the asymmetries which are already present in core at TREAT. The concentric design does, however, require a larger diametrical envelope within the primary vessel than for a U-tube configuration. The space is needed to accommodate the downcomer from the pump, with dimensions large enough to meet the requirement for the inlet inertial length.

Since the envelope diameter is now larger, the loop wall thickness must be increased to provide the heat capacity needed for melt-through protection using the same meltthrough criterion. The resultant wall thickness for the concentric design was about 30% greater than for the U-tube configuration. One would therefore degrade the hodoscope performance with the thicker wall. Using current data for hodoscope performance, this degradation was estimated as a reduction of 25% in the signal-to-background ratio.* Since the primary test objective involves the observation of fuel-motion behavior, then the adequacy of the hodoscope performance is of principal experimental concern. Although it is difficult at this time to quantify further the consequences of a selection of one or the other in-pile configuration, the desire still exists to minimize the amount of material in the view of the hodoscope which tends to degrade its performance.

In addition to the above concern, a concentric design may also impose restrictions on the selection and location of other important test-vehicle instrumentation. It is not known at this time what the ultimate consequences for the test objectives would be since viewpoints may differ on the relative capability of the concentric-configuration flowmeters and/or pressure transducers to generate quantitative data. Note also that controlling flow rates in the bypass by orificing its annulus may require more elaborate calibrations than those required for a standard orifice in a circular pipe used in a U-configuration. No further attempt was made to perform evaluations concerning the choice of an in-pile configuration.

2.2.2.2 Concept Selection

On the basis of considerations identified on the previous section, the purely experimental choice for a test-vehicle configuration would be for one having the characteristics of the gas-driven system with a U-tube in-pile section. However, engineering considerations tend to favor a pumped,

---

* The use of the converter may reduce further the signal-to-background ratio.

concentric design, particularly when the PFR fuel elements must be accommodated in the small 200-mm-dia hole in the lower concrete support. In addition, a pumped system would apparently offer a growth potential not inherent in a gas-driven, integral concept because of the limited time for full flow with the latter system concept. The reference design for the advanced test vehicle was therefore based on a pumped system with a concentric in-pile section. The dominating opinion was that this selection possessed advantages which exceeded its disadvantages. In addition, the system selected should also be prototypic to the small-bundle tests in the advanced safety-test facility. Note that these evaluations were not based on detailed tradeoff studies because of the study-time constraints, and the general overall difficulty in reducing experimental goals and objectives into strictly quantitative terms. In no case were special problems discovered which made it obvious that cost itself could be the deciding factor among the primary candidates. The facilities modifications to enlarge the handling envelope would probably be comparable.

2.2.3 Reference Design Description

2.2.3.1 Description of Component Design

The advanced test vehicle consists of four basic subassemblies: (1) test train, (2) primary vessel, (3) pump (ALIP), and (4) secondary containment. Some of the components and features incorporated in the concept are similar to those used in the SLSF vehicle. Figures 2-15, 2-16, and 2-17 illustrate the vehicle concept and its basic subassemblies. The vehicle concept is intended to utilize FTR, CRBR, and PFR pins with a minimum of modifications to the test train. The current concept encompasses combinations of 19-, 37-, 61-, and possibly 91-pin clusters. The concept indicates that a CRBR-pin plenum will penetrate into the pump core area approximately 533 mm (21 in.). The effect of this condition has not been investigated in detail, but it appears to be acceptable. The drawings illustrate a concept of a 37-pin vehicle. Basically, the cross sections for a 37-PFR-pin unit and a 61-CRBR-pin unit are the same except for the pin number and size of the test-train hexagonal pin holder. The 19-pin unit will have a reduced primary diameter and secondary containment for the test section.

Table 2.6 presents the estimated performance capability for the Advanced TREAT Loop.

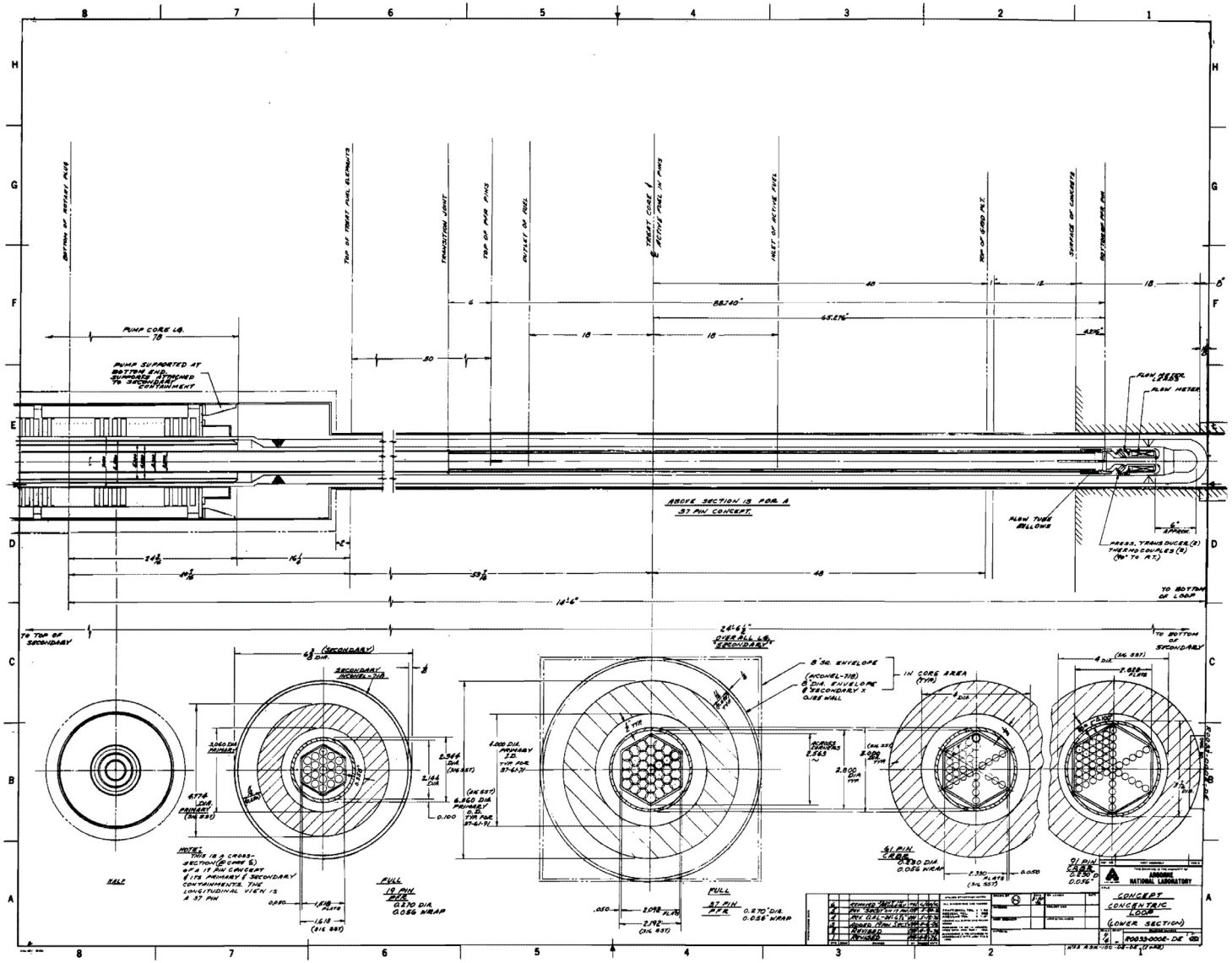

Fig. 2-15 Advanced Test Vehicle - Concentric Loop Concept (Lower Section)

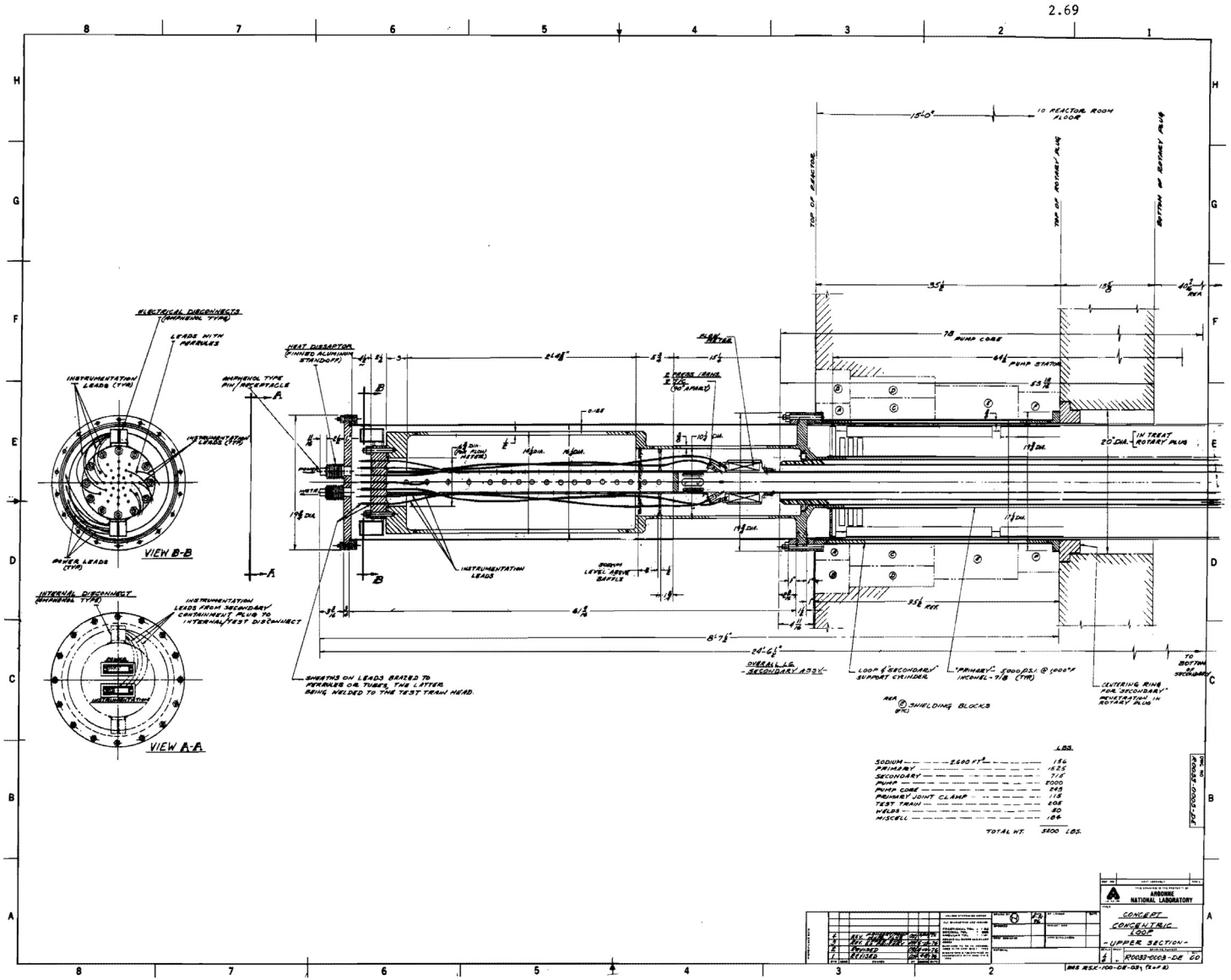

Fig. 2-16 Advanced Test Vehicle - Concentric Loop Concept (Upper Section)

TABLE 2.6 Estimated Performance Capability for the Advanced TREAT Loop

Cluster Size (pins)	Fuel Pin Dia (mm)	Wire-wrap Dia (mm)	Fuel Design	Estimated Bypass Mass Flow Ratio* for Prototypical Flow Velocity	Inlet Inertial Length Relative to CRBR**
19	6.86	1.42	Bottom Plenum Advanced Oxide	5:1	can be matched
37	5.84	1.42	CRBR	3:1	can be matched
37	6.86	1.42	Bottom Plenum Advanced	2:1	28% greater
61	5.84	1.42	CRBR	3:2	15% greater
61	6.86	1.42	Bottom Plenum Advanced Oxide	1:1	40% greater

* Flow rate in bypass divided by flow rate in test section.

** Relative inertial length matches are exceeded on inlet before they are reached on outlet.

Test Train

The test train can be considered to be a series of subassemblies (starting at the bottom and going to the top) assembled in the following order:

(a) Inlet (lower) Instrumentation Head:

This subassembly consists of a permanent-magnet type of flow meter, two pressure transducers, and two thermocouples. The head is attached to the fuel-pin holder by a mechanical joint. The flow meter requires further development work.

(b) Fuel-pin Holder:

This subassembly supports the pins within the hexagonal flow tube and orients the fuel-pin bundle by means of a slot for hodoscope viewing.

(c) Hexagonal Flow Tube:

This subassembly extends from the fuel-pin holder to 152 mm (6 in.) above the top of the fuel pins. The entire length is jacketed with a cylindrical tube referred to as the flow divider. The lower end of the hexagonal tube is attached to flow divider by means of a bellows which compensates for thermal-expansion differentials.

(d) Flow Divider:

The void between the tubes will be filled with an inert gas. The tube will shield 18 thermocouples (3 affixed to each of six flat surfaces of the hexagonal tube) which are attached to the hexagonal tube at predetermined locations. The thermocouple leads pass through a sealed transition ring (approximately 152 mm above the fuel pins) and into the sodium stream of the flow-divider tube.

The thermocouple leads continue upward to the slots located below the flow diverter (approx. 4.57 m above the upper end of the pump core) to the mounting flange head. The leads enter penetrations in the mounting flange head where type 316 stainless steel ferrules are brazed to the thermocouple sheathes. The ferrules are then welded to the mounting flange head forming pressure-tight joints.

(e) Outlet (upper) Instrumentation Head:

This subassembly consists of a permanent-magnet type of flow meter, two pressure transducers, and two thermocouples. The lower end of the head is mechanically attached to the top end of the flow-divider tube.

The upper end of the head is welded to a flow diverter which is welded to a perforated support tube. The support tube is welded to the mounting flange head. The purpose of the perforations is to permit instrumentation access to the center of the mounting head and also to prevent a trapped gas pocket in the support tube within the gas plenum.

The entire length of the test train is approximately 22 ft - 11 in. (6.92 m) and weighs approximately 105 Kg. The test-train weight will vary depending upon type of pin and number of pins.

Primary Vessel

The primary-vessel concept utilizes type 316 stainless steel. The entire vessel will be a single weldment consisting of the in-pile section, pump stator section, lower plenum, upper plenum, and top flange.

The current wall thickness of the pump stator section, 10.15 mm (0.4 in.), appears to be more than adequate to meet the design requirements. Preliminary calculations indicate that it meets the following conditions:

1. 275-atm (27.9-MPa) maximum pressure at 1000°F (538°C);
2. 660-atm (66.0-MPa) pressure under abnormal conditions at 1000°F (538°C);
3. 255-atm (25.8 MPa) test pressure at design temperature of 1000°F (538°C).
4. 313-atm (31.7-MPa) test pressure at room temperature (22.2°C).

The design pressure is 204 atm (20.7 MPa) at 1,000°F (538°C) with a faulted pressure of 425 atm (43.1 MPa) at 1,000°F (538°C). The vessel is designed to permit its removal from the secondary containment without removing the ALIP pump from the secondary containment.

The overall length of the primary vessel is approximately 7.18 M (23 ft - 6 $\frac{11}{16}$ in.). The in-pile section could be a forging which would be turned and gun drilled. The pump-stator section will be fabricated in the same manner. The lower and upper plena can be fabricated from rolled plate and longitudinal welds used at the seam. Seamless pipe or tube is preferred, but availability for the required size could be a problem.

Secondary Containment

The principal function of the secondary containment is to serve as a backup containment in the event a leak develops in the primary vessel. It is not intended to be a secondary high-pressure boundary to the primary vessel. The primary vessel is designed to withstand all pressure conditions in a test;

however, the secondary vessel could withstand a reduced pressure resulting from volume expansion in the event of a primary-wall failure. The current concept is a two-piece containment. The upper section encloses the loop plenum, and the lower section encloses the pump and the in-pile sections of the primary vessel. The lower section would extend to 876 mm below the grid plate of the reactor. The overall length is approximately 7.47 m. The ALIP pump is supported from the bottom by means of a support which is attached to the secondary containment wall.

The in-pile section of the secondary containment is designed to accommodate the optimum TREAT fuel assembly geometry for specific experiments. The current cross section (at reactor-core cross section) is 162 mm in outer diameter for a 19-pin loop and 203 mm in outer diameter for a 37- or 61-pin loop.

The secondary assembly includes the ALIP stator and reusable primary "outfitting" components, such as primary heaters and thermal insulation.

2.2.3.2 Mechanical and Materials

Material selections for the individual subassemblies in a loop are as follows:

1. Test Train

Steel (type 304 or 316) will be used for the hexagonal flow tube, flow divider, instrumentation heads, support tube, and mounting head flange. Further study is planned for the possible use of niobium for the hexagonal tube and possibly for the flow-divider tube. This will require development work in the area of fastening dissimilar metals by other than mechanical means. Techniques such as brazing, explosive bonding, or welding will be considered. A transition section would be another possible technique.

2. Primary Vessel

The material for the primary vessel will be type 316 stainless steel. The existing concept shows a one-piece weldment.

3. Secondary Containment

The materials in this assembly will be Inconel 718 for the lower (in-pile) section and type 316 stainless steel for the upper (out-of-pile) sections. Inconel 718 was selected on the basis of its strength at elevated temperatures. It is conceivable that the surface area of the in-pile section will be exposed to temperatures near 1100°C. The containment is

cylindrical in shape over its entire length, thus permitting a higher pressure internally and lessening distortions at the outer wall surfaces.

2.2.3.3 Generalized Assembly Sequence of the Test-train into the Advanced TREAT Loop

The overall design philosophy of inserting the test-train into the primary containment vessel, and then inserting the primary containment into the secondary containment vessel, appeared to be the optimum approach for assembly and component reuse (see Fig. 2-17). The Annular Linear Induction Pump (ALIP) will be installed into the secondary containment vessel, (SCALIP) so that it will be possible to remove the primary vessel from the SCALIP at TREAT if the loop instrumentation proves that the primary containment vessel has not failed. This approach should substantially reduce handling of ALIPs and secondary containment vessels. A reduction in setup time for an experiment and cost savings are anticipated.

Since the Advanced TREAT Loop will be designed so that all final mechanical and electrical connections can be made from the top, it will be possible to be able to draw only the primary containment vessel (with its test-train) inside of the loop-handling cask. The cask will be designed so that it will be able to accommodate either a primary containment vessel with test-train or the complete loop including the secondary containment vessel.

2.3 Experiment Support Systems

2.3.1 Instrumentation Requirements

2.3.1.1 On-vehicle Sensors

The test zone should be instrumented with pressure transducers, thermocouples, and flow meters at both the inlet and outlet. In addition, the gas-plenum pressure should be monitored during the test. The following desired ranges and/or sensitivity shall apply:

Sensor	Range	Sensitivity
Plenum Pressure	0-8 atm (0-0.81 MPa)	
Inlet and Outlet Pressure	0-170 atm (0-17.2 MPa) 0-35 atm (0-3.5 MPa)	
Inlet and Outlet Flow		0.1 Mv/gpm (1.59 $mV/cm^3/s$)
Thermocouples	0-1370°C	

For system designs containing a bypass, the flow rate in the bypass should be monitored.

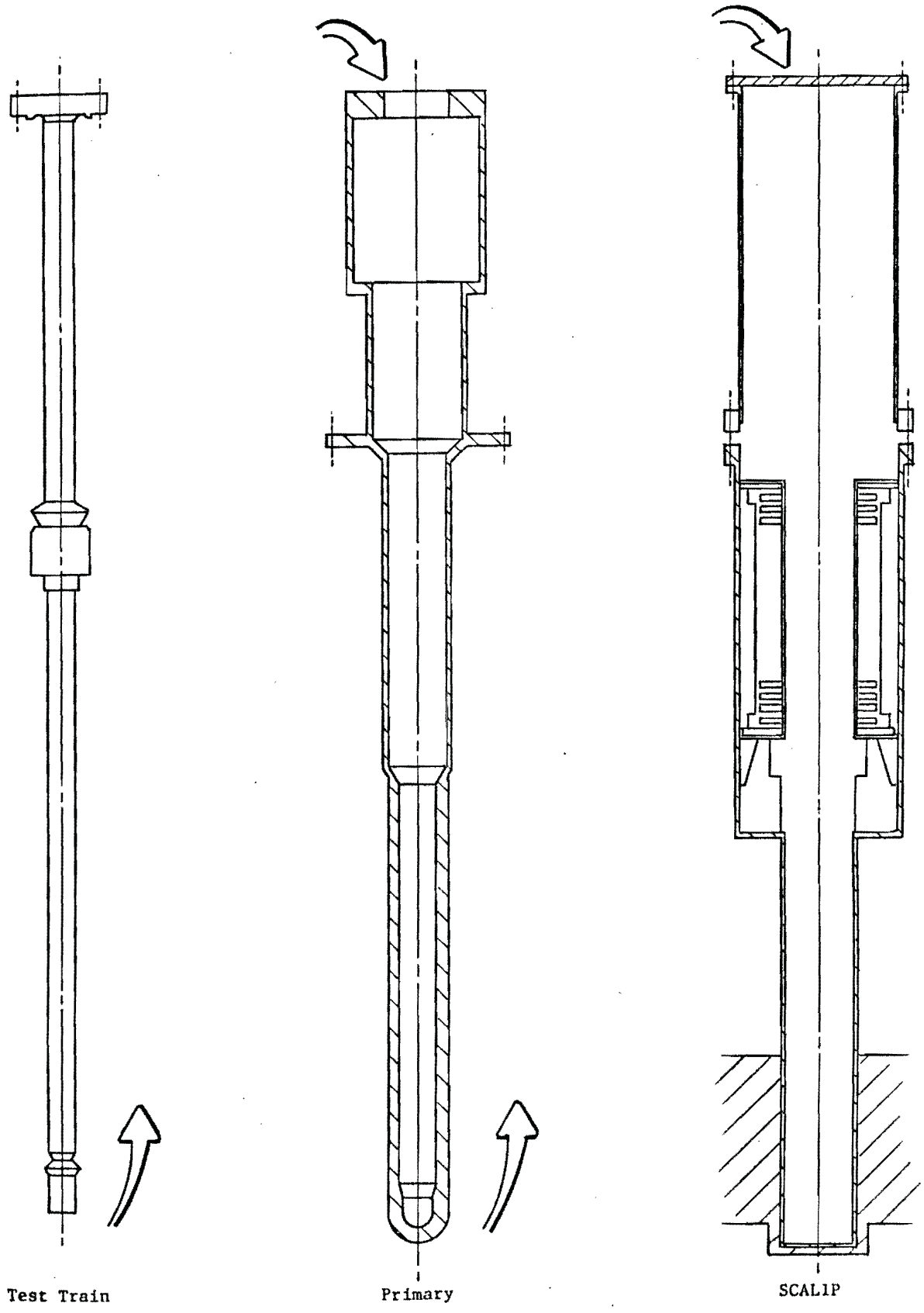

Fig. 2-17 Sequence for Test Train and Loop Assembly

Every attempt will be made so that the related instrumentation will be of a type proven in a TREAT burst environment or that the selection among design alternatives will not preclude their substitution should the original selection prove unacceptable. For tests involving the ejection of sodium slugs, the flow meters should be located as far away from the test zone as possible. In this way, the flowmeter measurements will not be subjected to the uncertainty caused by entrainment of fission gas in the coolant stream.

2.3.1.2 Fuel-motion Detection (Fast-neutron Hodoscope)

Fuel-motion detection will utilize the fast-neutron hodoscope currently installed at TREAT. The present collimator provides a fixed field of view between 66 mm horizontal and 1.219 m vertical. The focus is at the reactor center. Provisions are available to displace the hodoscope collimator laterally within a small range for centering purposes. The test vehicle is to be positioned within the hodoscope field of view using the 100-mm-wide viewing slot containing the slotted TREAT elements. In addition, a small section behind the test assembly will probably be voided of fuel and contain another material in an effort to improve the hodoscope performance.

When selecting materials and configurations, consideration will be given to their effects on the hodoscope performance. In evaluating materials, the signal-to-background ratio for the fuel-motion detection is currently approximately proportional to $\exp[-\Sigma t]$, where Σt is the "optical" thickness to the target through the test vehicle for 1.5-MeV neutrons. Attempts should be made to select materials and configurations which tend to minimize the optical thickness. Note that the requirement for meltthrough protection discussed in Sect. 2.2.1.5 results in values of Σt sufficiently large to cause a major reduction in the signal-to-background ratio. Since the hodoscope is currently the only device having a demonstrated capability for fuel-motion detection, the test-vehicle design should take into account the importance of an optical thickness in meeting the experimental goals.

Hodoscope sensitivity should be high enough so that the gain or loss of fuel in a given row of channels less than or equal to one percent of the fuel in the cluster will be detected. As an example, consider a cluster of 19 CRBR/FTR-type pins, each containing approximately 180 g of fuel, for a total of approximately 3.4 kg. A movement of one percent of the fuel mass into the row of six channels above the original top of the fuel is

equivalent to a gain of approximately 34 g, or 5.7 g/channel. For 61 CRBR/FTR-type pins, with a total of about 11 kg of fuel, a gain of one percent in a row of 10 channels is 110 g, or 11 g/channel.

2.3.1.3 Data-acquisition System

The current data-acquisition system at TREAT is basically adequate for the advanced test-vehicle program. However, additional data-recording channels will be needed to record the data required for the larger-scale experiments. The current system at TREAT is based on analog tape recorders, each able to record up to 14 channels continuously. At present, TREAT has 3 such units available. Each recording channel requires a wide-band amplifier. Currently, TREAT has about 48 Neff amplifiers for this purpose; an additional 16 units will be needed. For signals which need not be recorded continuously, one multiplexer unit is currently available. The multiplexer and tape recorder have the capability to provide continuous data for a time interval of 1 ms e every 15 ms for 15 independent signal inputs. The multiplexer is convenient for recording data related to test-vehicle engineering parameters as well as slow-response sensors in the experiment package. Two additional multiplexers will be required. CRT Visicorders will also be used to record data; 3 additional units are needed.

2.3.2 Instrumentation and Control

The Advanced TREAT loop concept specifies that the primary containment vessel can be separated from the secondary containment by performing a disassembly operation at the top of the loop. Thus, the loop heaters, heater-control thermocouples, and the ALIP will be incorporated into the secondary containment vessel rather than on the primary containment vessel. Loop flowmeters will be located on the test-train. These design features result in a requirement for only two loop instrumentation and control consoles: one in the loop assembly and prooftest facility at ANL/E, and one at TREAT. The TREAT console will be located in the TREAT Reactor Building, and will be so designed that it will be able to control the loop heaters, vehicle/loop instrumentation, and the ALIP when a loop is either in the new "Loop Support Operations" facility or when the loop is in the TREAT Reactor for a test.

2.3.3 Electrical Power Supply

The power supply for a 3-section ALIP, capable of producing 400 gpm (10.025 m^3/s) with a 150-psi (1.03-MPa) head pressure, should deliver approximately 250 KVA of 3-phase 60-Hz power at 420 V. Since there is no

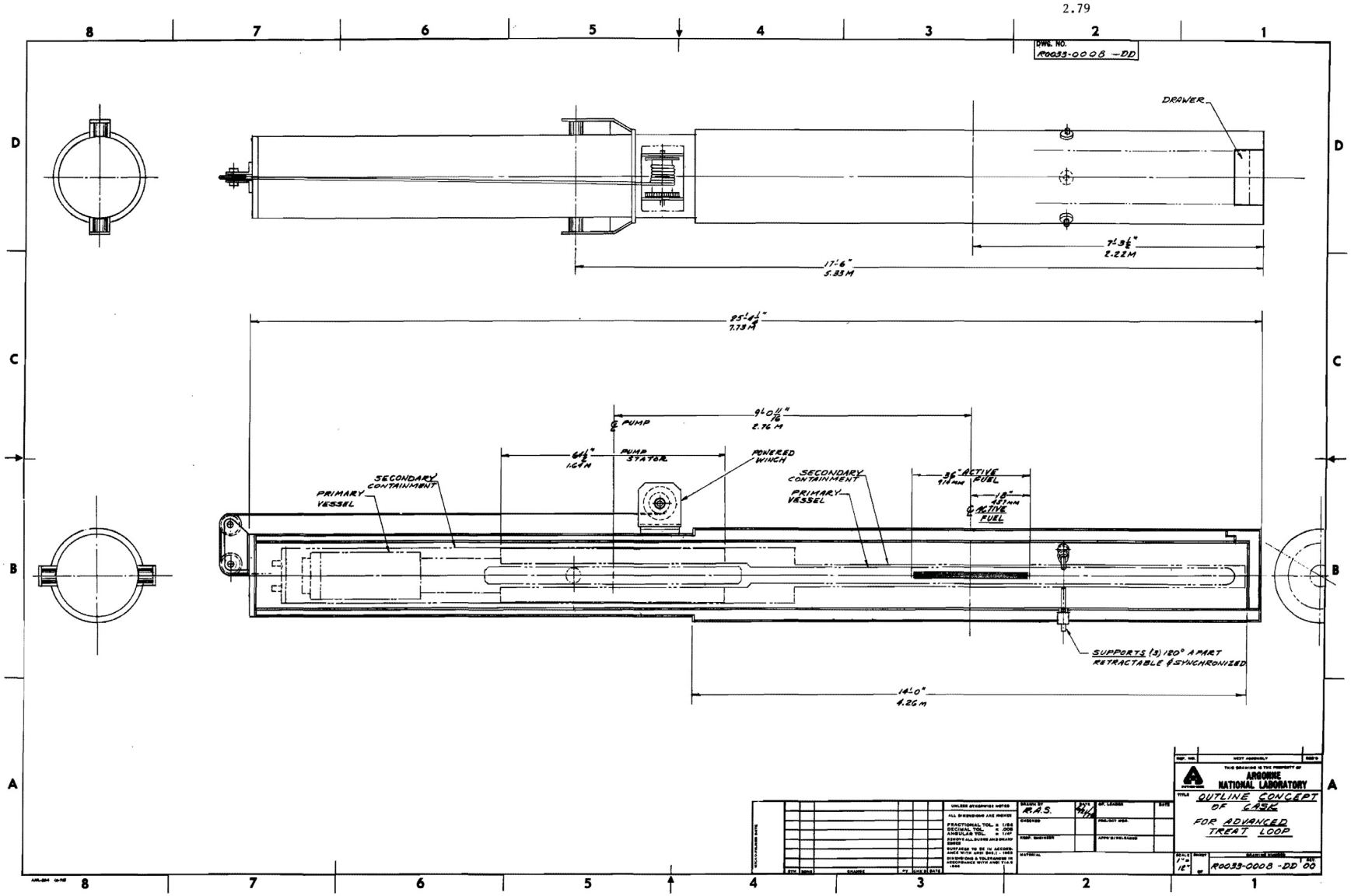

Fig. 2-18 Advanced TREAT Loop Cask

requirement comparable to the SLSF requirement to increase ALIP power from zero to design operating conditions in less than 2 min, the power supply requirements for the reference advanced TREAT loop can be met by motor-driven Variacs. A power-reduction sequence for providing a simulated coastdown condition similar to previous TREAT experiments will be developed by a control system that will be designed so that a smooth power-reduction program will be experienced by the ALIP during simulated coastdown experiments.

2.3.4 Handling Cask

A handling cask will be provided for the Advanced TREAT loop. It will be a bottom-loading cask, with a hoist for raising the loop into the cask or lowering it from the cask. Radial supports will hold the loop during horizontal transport and during the transition from vertical to horizontal. Closures will be provided at top and bottom. The cask will be used only for on-site shipments and handling operations at the INEL.

The nominal test sample heat load is 200 w, corresponding to the activity of 19 pins that were previously irradiated and cooled for six months. Loads up to 400 W may be encountered, however, a heat-rejection system will not be required.

The cask concept is illustrated in Fig. 2-18. The radial shielding is stepped to provide full pretest shielding for intact pins of prototypic fuel dimensions. The stepped sections will also provide additional shielding to accommodate expected fuel relocation resulting from the test plus a margin for contingency, along with partial shielding for the upper loop region. Shielding also will be provided at the bottom of the cask and at the top. The cask will use depleted uranium that is contained within steel inner and outer walls.

The shielding will be designed to accommodate the following two cases: (1) the transient activation of 91 FTR/CRBR pins plus sodium and loop, and (2) the activity of 37 preirradiated pins plus transient activation. The nominal preirradiated samples is expected to be 19 pins, corresponding to the prototypic-enrichment case (see Sect. 3.3). A loaded cask weight of 27,270 kg (approximately 30 tons) has been estimated on this basis.

3.0 FACILITY PERFORMANCE AND SAFETY

3.1 Experiment Requirements

3.1.1 Role of TREAT in Meeting Key Safety Issues

In-pile experimental requirements for resolution of key LMFBR Safety issues are presented in Vol. I. Those requirements cover experiments ranging in size from a single pin to the multisubassembly level, and range in duration from short-period transients to the steady state. In this section, the requirements to be met by the TREAT upgrade will be restated from the standpoint of facility requirements. In order of increasing test size, the requirements to be met by TREAT tests can be summarized as follows:

1. Capsule. Capsule tests, typically of the single-pin size, will be performed to provide data needed to guide development of phenomenological models of fuel response to accident conditions. Such test samples may be run with a liquid-metal bond to a heat sink in order to meet experimental requirements on radial thermal gradients. They may be run in a wet atmosphere; they may be run with heated-wall boundaries or with other special experimental arrangments to tailor the sample exposure conditions. Such tests may be run to the failure threshold to determine margins to failure, and guide failure modelling. Other tests may be carried well past failure and fuel melting to guide model development for postfailure fuel response. Reference oxide fuel and advanced fuels will be studied.

2. Small Bundle (SB) Loop Tests. SB loop tests in the range from 3 to 19 pins will be run to provide data on the "immediate" consequences of failure. The fuel conditions calculated to exist at the time sensor anamolies associated with failure are recorded will be used to assess margins to failure under conditions more prototypic than those of capsule tests. Relative timing of failure-related signals and the onset of fuel motion will be used, along with the sources, velocities, and directions of fuel motion, in order to guide analysis of the LMFBR reactivity changes associated with fuel movement. Coolant voiding associated with the failure events also will be measured and analyzed for use in code development for calculating coolant- voiding reactivity changes in LMFBR accidents. Tests of 19-pin size will provide data on the effects of bundle incoherence of fuel-coolant movements and postexcursion fuel distributions. The latter stages of SB tests will provide data on the extended fuel motion to be expected, leading into a transition phase of fuel movement after

an HCDA. Final distributions and conditions of the sample materials will assist in reconstruction of the accident scenarios and will provide data to be used in assessing any subsequent events in the accident sequence. Prototypic fuel irradiated under prototypic conditions in the Prototypic Fast Reactor or the FTR is needed to ensure adequate cladding response to thermal excursions. Fuel-coolant energetics have been investigated. TREAT data, as extended by model out-of-pile tests and theoretical work, indicate that energetic fuel-coolant interactions will not occur for oxide LMFBR systems. Conditons typical of severe coherent failure have not been simulated. Advanced fuels, which appear to meet the criteria for energetic fuel-coolant interactions, will be tested.

3. Itermediate Bundle (IB) Loop Tests. IB loop tests, in the range from 37 to 61 pins, will provide data on the effects of bundle incoherency on fuel movements and coolant voiding. If carried farther into the accident scenarios, these tests will provide data on recriticality limits during the development of a transition phase and, hence, in the actual boilup and dispersal. For tests emphasizing the later stages, the effects of details of loop hydraulics may be minimal, and test-section designs may effect experimental requirements emphasizing features needed to simulate decay-heat-driven boilup without excessive heat losses to the experiment environment. Typically, these tests emphasize the postfailure fuel behavior and thus will not require irradiated fuel. We plan that they will be done with fresh UO_2 samples. Advanced fuel pins for tests in this size range will also normally be fresh, containing no plutonium. If previously irradiated fuel should prove to be needed for some tests in this size range, the prototypic irradiation conditions for SB tests would not be needed.

3.1.2 Consolidation of Experiment Needs

3.1.2.1 Margins to Failure, Failure Mechanisms and Consequences Energy

TOP tests on margin to failure and failure mechanisms will require pins of prototypic enrichment, irradiated under prototypic conditions. Failure of these pins is expected to require sample enthalpies in regions of high gas retention sufficient to reach the range between solidus and liquidus. Thus, during the preheat stage of the TREAT transient, when thermal gradients are established, this fuel region should be raised to an enthalpy above room temperature of about 200 J/g (corresponding to a preheat temperature of about

1100°C). An additional 950 J/g in enthalpy is adequate to carry the oxide to the solidus and supply half the heat of fusion. (In practice, the preheat and actual transient do not have a sharp boundary, but it is convenient to discuss the transients in this way.)

For relatively rapid excursions with periods less than or of the order of the time constant for radial heat flow, the transient after the preheat will provide nearly adiabatic heating. A preheat of about 150% of design pin power for about 2 s is adequate to establish the large thermal gradients typical of oxide fuels. Then, an excursion with period of about 1 s or less with energy of about 1000 J/g will provide the needed additional enthalpy.

For tests with periods of 1 to 10 s, the situation is somewhat different. The preheat is less important, because these longer periods provide adequate time for development of the thermal gradients as the fuel heats during the actual excursion. In these tests, the preheat is merely a means for minimizing the sample heat losses early in the transient (i.e., to make efficient use of the reactor-energy capabilities). The energy requirement for such a transient will be scoped by assuming that there is no separation between preheat and excursion. This reference case is run by "picking up" the power excursion from an initial level of 300 W/g on a simple exponential transient and proceeding on a 10-s positive period until a sample power level of 480 W/g is reached (30-kW/ft rating for FTR/CRBR fuel). This energy requirement is 1800 J/g. Table 3.1 summarizes TOP energy needs. The division between preheat and burst is arbitrary. It reflects the discussion for the shorter burst periods, $\lesssim$1 s. The total requirement is chosen to provide an energy margin in excess of the value for the case of the 10-s period discussed above.

For TUCOP tests, there is an additional need for a simulation of the flow coastdown. However, energy added during the coastdown reduces the requirements for the preheat. Table 3.1 reflects these changes in showing energy requirements for the TUCOP separately from TOP. These tests are of small-bundle (SB) size. Experiments run short of failure require only realistic thermal environments, which can be provided in single-pin geometry. For experiments run past the failure threshold, however, SB geometry is required in order that immediate postfailure cladding and fuel movements are not unduly impeded by boundary effects, thus causing excessive damage to the sample, which would obscure postmortem reconstruction of the failure. Seven pins provide

Table 3.1 Transient Energy Requirements

1.	Fuel Failure and its Immediate Consequences		
	1.1 TOP		
	Preheat 3 s x 240 W/g	=	720 J/g
	Burst	=	1300
	Subtotal		2020
	Contingency @ 20%	=	400
	Range		2020-2420
	1.2 TUCOP		
	Preheat 1 s x 240 W/g	=	240 J/g
	Coastdown 5 s x 160 W/g	=	800
	Burst*	=	1000
	Subtotal		2040
	Contingency @ 20%	=	410
	Range		2040-2450
2.	Accident Including Development of Transition Phase		
	2.1 TOP + Transition		
	TOP Requirement	=	2020-2420 J/g
	Decay 100 s x 8 W/g	=	800
	Range		2820-3220
	2.2 TUCOP + Transition		
	TUCOP Requirement	=	2040-2450 J/g
	Decay 100 s x 8 W/g	=	800
	Range		2840-3250

*Assumes the cooler, outer fuel near the surface is carried to 500°C beyond the liquidus in a near-adiabatic burst.

the corresponding pin-centered geometry with one interior pin and six interior channels. Three pins provide a channel-centered geometry with channel shielded from structure. Nineteen pins provide a 7-pin internal core.

Power Distributions. Power distributions are shaped axially, if necessary by use of neutron-absorbing shaping collars. Radial power-distribution requirements are based on the following three criteria:

1. The thermal profiles within the test pins. These profiles must be close enough to the actual LMFBR profiles that deviations between them and the test data are small enough that they represent only corrections, that is, the deviations are not large enough to introduce new mechanisms of behavior (such as melting from the outside inward). The thermal gradients should not show edge peaking. Horizontal isotherms should be nearly circular without "lunes" or cusps, and central to edge temperature drops should be within about ±30% of realistic values. The gradients established during the preheat are programmed to compensate for the nonuniform heating during the actual excursion burst. The most severe problems occur for edge pins in a bundle. The above criteria are met for edge pins in a 7-pin bundle with pin-averaged maximum to minimum radial power ratio of 1.44.* For larger clusters with the same ratio, effects of the power depressions become somewhat less.

2. Incoherence between test pins. Different test pins with different powers will attain the same internal conditions at different times. These time differences can be calculated. However, as above, the deviations from the LMFBR case should be small enough that they do not introduce new mechanisms of behavior. Thus, pin-to-pin power variations in a failure-threshold experiment which meet the other two criteria are acceptable for this one, since the first pin fails under realistic conditions. For detection of the initial fuel movements, it is not necessary to have a large core of coherently exposed pins, as long as the hodoscope can "see" a single pin. For the 19-pin SB size, hodoscope sensitivity required under Sect. 2.3.1.2 corresponds to gain or loss of fuel within a single pin of FTR/CRBR type. Experimental edge-to-center pin-power ratios less than typical edge-to-center power skewing in an LMFBR is not necessary, although the capability for "flat power" cluster or central cores within clusters gives increased experimental

---

* A. E. Wright et al., Final Report for the H3 Transient Over-power Failure Threshold Experiment, ANL-75-32, (June 1975).

flexibility. Thus, a target for pin-averaged maximum-to-minimum radial power ratio of 1.2 appears to be appropriate. If special experiments should be needed in which a flatter radial power profile should be required, the use of small sample-enrichment variations is acceptable if these variations would produce only small deviations from the normal, prototypic, irradiation conditions. A maximum-to-minimum ratio for ungraded enrichment of about 1.2 is sufficiently close to unity that this condition would apply.

3. Temperature differences between coolant channels

Test-train designs offer the capability of readily adjusting flow cross-sectional areas compensating for pin-averaged edge-to-center power ratios of 1.6.

On the basis of these three criteria, the desired pin-averaged radial maximum to average power ratio is set at 1.10-1.15.

3.1.2.2 Phenomenology

Energy

Phenomenological tests generally parallel the more direct simulation tests. Thus Table 3.1 covers the needs of the phenomenological test. Since the needs are met in the current TREAT core, there are no specific TREAT upgrade requirements.

Size

Phenomenological tests are typically single-pin tests with special boundary conditions provided in the apparatus design.

Power Distributions Axial power distributions are tailored, if necessary, by use of neutron-absorbing shaping collars. A wide range of radial power distributions may be required within the single-pin test sample. Some tests of this type have been run in TREAT with highly enriched pins and no thermal-neutron filters (i.e., radial maximum-to-minimum ratios $\bar{>}3$). Tests F1 and F2 had moderate filtering (maximum-to-minimum ratio of about 1.6), and the high power EOS tests have extensive filtering (maximum-to-minimum ratio <1.1). Since these requirements are met without loading modified TREAT elements, there is no specific TREAT upgrade requirement.

3.1.2.3 Effects of Bundle Incoherence

IB size tests on phenomena associated with bundle-incoherence effects will generally follow the requirements for Sect. 3.1.2.1 except for size.

3.1.2.4 Transition Phase

Energy. Energy requirements for the initiating accident phase are given for both TOP and TUCOP in Table 3.1. Experiments designed to study the development of the transition phase from the initial postaccident configuration, as well as the subsequent "boil up" of the fully developed transition phase, will require additional energy to mock up the decay heat. Two general areas of Transition Phase tests can be identified: TOP-initiated and TUCOP-initiated. These entries of Table 3.1 were obtained by adding a decay-heat-energy allotment to the TOP and TUCOP energy cases, respectively.

Size. As tests on transition-phase phenomena proceed farther into fuel boilup, larger cluster sizes become more desirable. Nineteen pins (a 7-pin "core" with 12 peripheral pins) are adequate for the initial dispersion and investigation of development of the transition phase, because the initial movements are essentially one-dimensional and the effects of radial structure can be acounted for. As boilup proceeds, mixing and freezing on the peripheral structure become sufficiently large that corrections are no longer small.

Figures 3-1, 3-2, and 3-3 depict the following three cluster-size-related parameters associated with these effects for FTR/CRBR-type fuel pins: (1) ratio of peripheral pins to central pins, (2) ratio of test hexagonal-flow-tube surface area to pin-plenum surface area, and (3) the ratio of test hexagonal-flow-tube surface area to volume. The trends in these three graphs indicate that IB tests in the 37-91-pin range are needed to guide modelling and confirm analytical predictions for the key transition phase regime extending to loss of subassembly structure.

3.1.3 Calibrations

Power calibrations for TREAT tests are obtained by running sample fuel pins in nuclear mockups of the in-core components of test sections. These mockups are loaded and unloaded at TREAT; sample pins, monitor wires, and monitor foils are analyzed at ANL analytical laboratories. This capability needs to be maintained, even though calibration samples for the largest tests to be carried out with the TREAT upgrade will have activity levels greater by an order of magnitude than those of current TREAT calibration runs. The support facilities (Loop Support Operations Facility) to be provided will include provision for disassembly of (uncontaminated) high-activity calibration experiments.

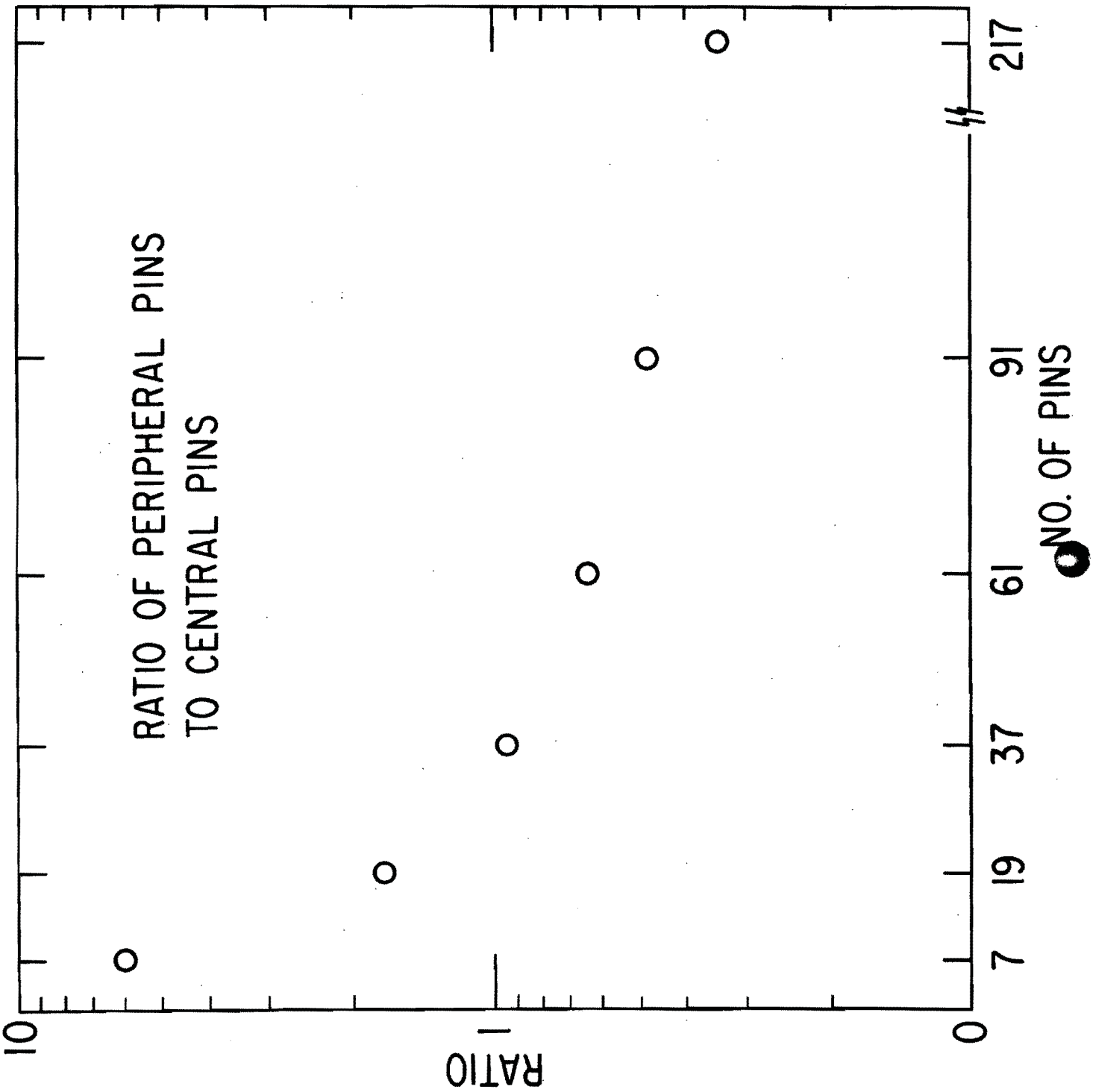

Fig. 3-1 Ratio of Peripheral Pins to Central Pins

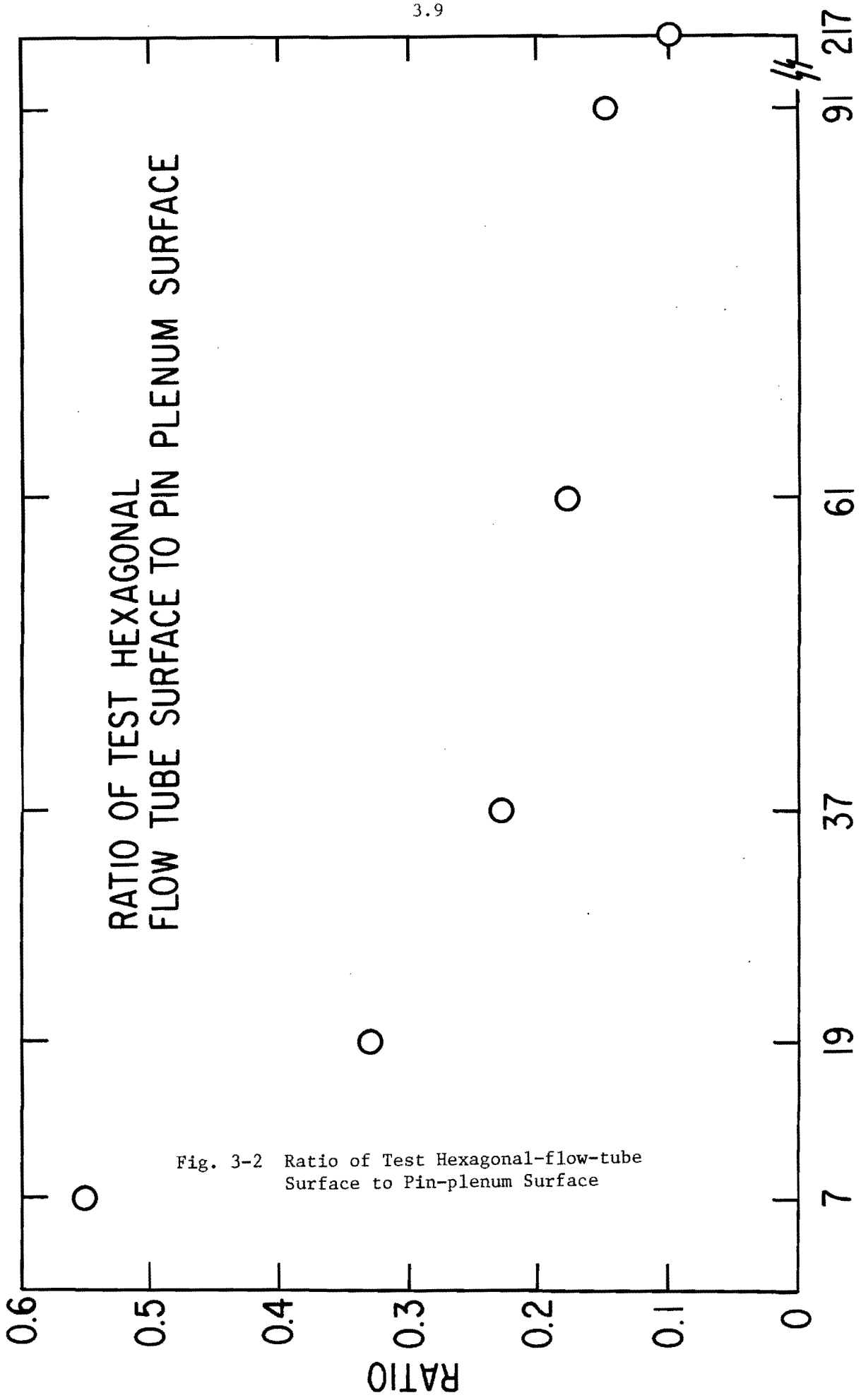

Fig. 3-2 Ratio of Test Hexagonal-flow-tube Surface to Pin-plenum Surface

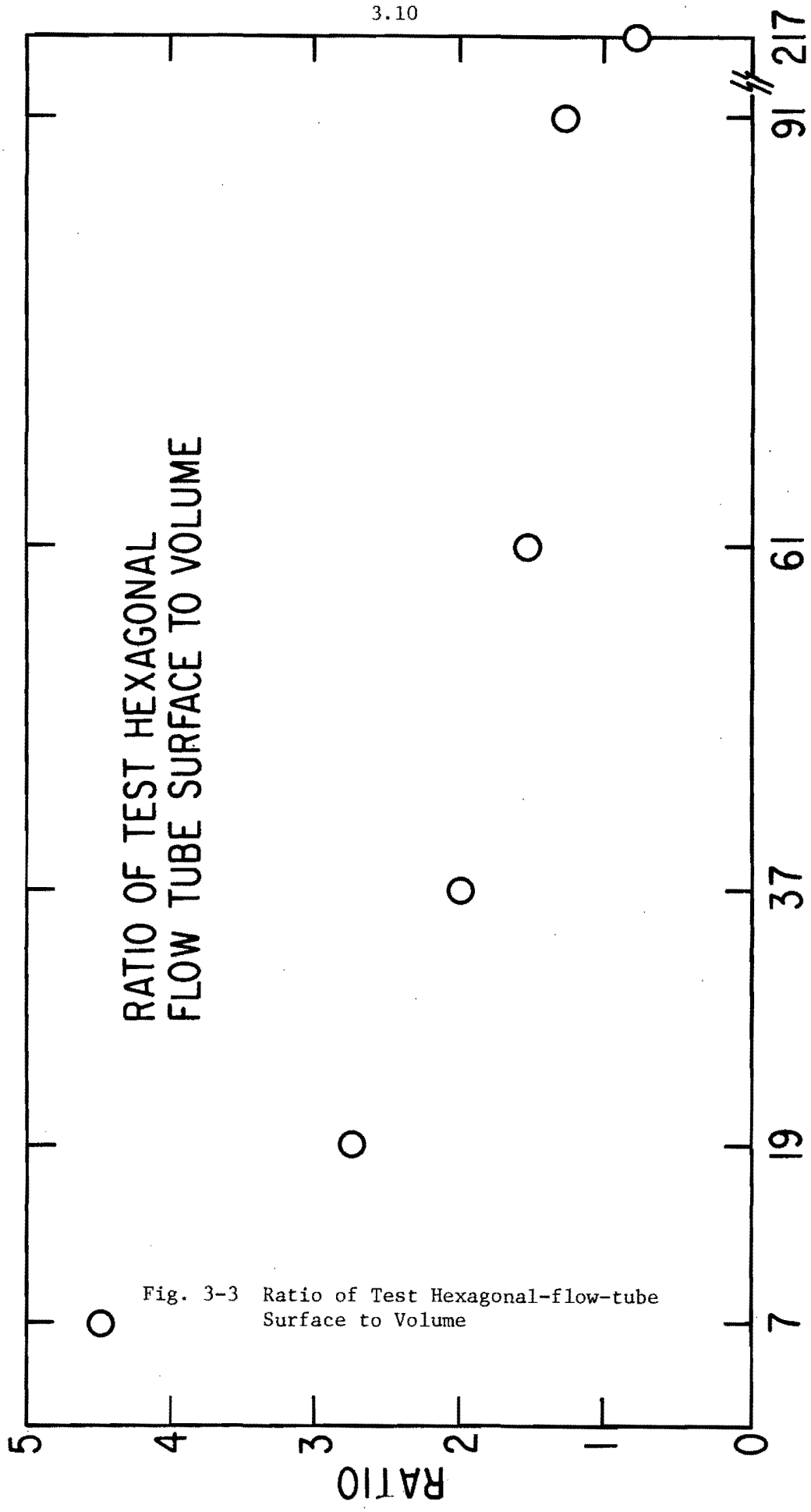

Fig. 3-3 Ratio of Test Hexagonal-flow-tube Surface to Volume

3.2 Current TREAT Capabilities

3.2.1 Current Size Capabilities

One or more TREAT fuel elements can be removed, leaving a test region 10 cm square, or multiples of this. The principal size limitation on samples for the present core is indirect; the sample energy available decreases as the sample size increases. Sample energy also decreases as neutron filters are added to reduce the radial sample power depressions. Thus, experimental requirements effectively limit sample size.

With samples of graded enrichment, 19 pins is the effective limit. Under current TREAT operating limits, such a cluster with a fully enriched central pin is calculated to have capability for up to about 4500 J/g (suitable for a transition-phase type of test). Clusters of uniform enrichment (such as pins irradiated under identical conditions) are filtered to meet TOP or TUCOP requirements; for these tests 7-pin clusters are the limit. Seven-pin clusters are the maximum size for TOP or TUCOP experiments on prototypic-enrichment fuel pins.

For these reasons, the current TREAT loops are 7-pin loops. The fresh UO_2 sample "R" loop has ready stretch capability to 19 pins by changing the test section.

There are current length limitations, as described in Sect. 2.1.1.1. Bottom-plenum pins cannot be run without removing the center section of the TREAT grid plate.

3.2.2 Current Sample-energy Capabilities

Table 3.2 summarizes the current TREAT sample-energy capabilities. Sample energy capabilities are strongly influenced by need for sample filtering. For current TREAT operating limits and current loops, 7 fully enriched, unfiltered, FTR-type pins can be run up to about 7000 J/g in a shaped transient. With filtering to meet TOP and TUCOP requirements, a cluster average of up to 3000 J/g is obtainable (but with a central-pin-energy capability of only about 2200 J/g). With 7 UO_2 pins of graded enrichment, an energy capability of 4500 J/g can be attained with a central enrichment of about 20%, and a peripheral enrichment of about 16%. Higher enrichments require larger enrichment ratios. As noted above, 19 pins with graded UO_2 enrichment can have about 4500 J/g for full enrichment of the central pin.

Table 3.2 Typical Current Energy Capabilities of TREAT

1. With Current Loop Capability	
Graded-enrichment UO_2	Energy capability, cluster-averaged, J/g
7 pins, central 20% enriched	4500
19 pins, central fully enriched	∿4500
Highly enriched mixed oxide (EBR II-irradiated samples)	
7 pins without neutron filter	∿7000
7 pins filtered for TOP/TUCOP	∿3000
2. With Advanced TREAT Loop	
Uniform-enrichment, fully enriched UO_2	
61 pins	∿1800
Prototypic-enrichment mixed oxide	
19 pins	∿1000

Calculations of TREAT performance without core modifications, but with the Advanced TREAT loop, have been made (see Appendix A-4). The results will be repeated here as follows:

1. For 19 prototypic-enrichment advanced mixed-oxide pins in the 19-pin test section, the energy in the central test pin corresponding to full use of the reactor-energy capability (i.e., rod-limited operation) is 1500 J/g.* With current TREAT operating limits, the energy would be about 1000 J/g.

2. For 61 FTR/CRBR-type UO_2 pins of full enrichment, the central-test-pin energy corresponding to the full reactor energy (rod-limited operation) is 2675 J/g.** With current TREAT operating limits, the energy would be about 1700 J/g.

3.2.3 Current Sample Power Distributions

Axial power distributions are tailored as needed by use of neutron-filter shaping collars.

Typical radial power distributions for the unmodified TREAT are given as follows:

1. For current loops, seven highly enriched pins filtered (as in test H3) for TOP and TUCOP tests, the radial pin-averaged maximum to minimum power ratios is about 1.33. The pin-to-pin radial power ratio can be made flat at acceptable enrichment grading for UO_2 pins at a peripheral enrichment of about 16% and a central enrichment of about 20%.

2. For the Advanced TREAT loop, calculations with no filtering*** gave pin-averaged radial maximum-to-average power ratios of about 2.0 and 1.5 for 19 prototypic enrichment advanced mixed-oxide pins and for 61 FTR/CRBR fully enriched UO_2 pins, respectively. Because the 19-pin energy capability is already below requirements for TOP, there is no need to attempt to improve this case with filtering. The improvement of radial power distribution for this 61-pin case is doubtful. The radial power ratio is so large that enrichment grading would be $\sim$2 to 1. Even if the internal fuel temperature gradients in the outer pins could be shown to be acceptable (enrichment grading has only a second-order effect on the internal pin gradients), a cluster with such a

---

* This value was calculated without any neutron filter.

** This value also was calculated without a neutron filter.

*** These are the two cases quoted in Sect. 3.2.2.

large grading would be undesirable for any experiment on the effects of extended fuel motion. It could be used for a test run only to the failure-threshold region. The relatively low energy capability of this case indicates that any improvement in radial power distribution by neutron filtering will be insignificant.

3.2.4 Hodoscope

Currently there are two hodoscope collimators available at the TREAT reactor. The original, located at the south side of the core, views a test region 510 mm high by 57 mm wide, composed of an array of rectangles 22.5 mm high by 3.8 mm wide. The new collimator, located on the north side of the core, views a test region 1.22 m high by 66 mm wide. This test region is divided into a array of rectangles 34.5 mm high by 6.6 mm wide. The new viewing width corresponds to a 61-pin bundle of 5.84-mm-dia FTR/CRBR pins.

Hornyak-button detectors are used to detect sample fuel motion over a wide range of signal levels. Because of nonlinear (supralinearity) response at higher levels, particularly for tests with samples $>\sim$600 w/g, fission counters will be provided. These detectors do not have adequate sensitivity for low power levels, but are used in the range where the supralinearity of the Hornyak-button detector becomes large.

The hodoscope readout can be obtained each 1.5 ms. Longer collection times per cycle can be set as needed.

NaI scintillation detectors can be used to obtain gamma-ray data (for example, to detect formation of stainless steel blockages). These techniques are under development at present.

Pre- and posttest scans can be made of the test section *in situ*, by moving the hodoscope collimator.

For current loops, a sensitivity of about 1 g of fuel per detector is obtained with 7-pin test clusters. Under favorable conditions, single-pin detector data have been unfolded to yield sensitivities of $\sim$0.1 g.

3.3 Upgraded TREAT Performance

3.3.1 Size

The modified TREAT elements described in Sect. 2.1.2 will raise the effective size capability of the reactor by providing higher sample-energy capability on the core centerline, along with flatter radial power distributions (see Sect. 2.1.3.3). The Advanced TREAT loop concept described in Sect. 2.2.3 provides a vehicle capable of utilizing this upgraded reactor capability.

The reference test-train envelope will accommodate either 61 FTR/CRBR-type pins of 5.85-mm diameter or 37 advanced-oxide pins of 6.86-mm diameter. This loop will also accommodate 91 FTR/CRBR pins, and the ALIP will provide adequate flow and pressure drop for these 91 pins (however, it will not be able to provide a bypass flow). Smaller sample sizes can also be accommodated. For advanced oxide pins with unenriched uranium and Pu/Pu+U ratio comparable to that of the outer enrichment zones of FTR or PFR (i.e., prototypic-enrichment pins) up to 19 pins can be accommodated with experimentally useful energy capability.

Either bottom-plenum pins (2.24-m-long PFR pins used as a reference) or 2.92-m-long CRBR type pins can be accommodated. Use of full-length CRBR pins will be dependent upon their availability and the capability of HFEF to transfer irradiated pins to the test-train loading machine.

3.3.2 Energy

The nuclear performance of the upgraded TREAT with modified TREAT fuel and the Advanced TREAT loop has been discussed in Sect. 2.1.3., and is given in detail in Appendix A-3. For 19 prototypic-enrichment advanced mixed-oxide pins with light (i.e., cadmium) neutron filters, the cluster-averaged calculated energy capability is about 2500 J/g. For 61 fully enriched UO_2 FTR/CRBR-type pins, the cluster-averaged energy capability has been calculated to be about 4800 J/g with cadmium filtering.

The sample energy actually available would be degraded, at least for some experiments, if the reactivity available with the modified TREAT were not sufficient to compensate fully for the design temperature swing of the system. An indirect loss in energy capability due to insufficient reactivity margin for TREAT temperature rise is not anticipated. The reference system with a 9 x 9 array in the modified fuel zone is calculated to have an adequate reactivity of 13%.

3.3.3 Power Distribution

The radial power distribution calculated for the 19 advanced-oxide prototypic-enrichment case yields a radial pin-averaged maximum-to-average ratio of about 1.05, with cadmium filter. For the 61 fully enriched UO_2 FTR/CRBR-type pins, this ratio is somewhat higher, about 1.10 (see Appendix A3). It should be emphasized that both these cases use uniform enrichment.

3.3.4 Hodoscope

No change in the hodoscope is planned as part of the TREAT upgrade. Additional detectors will be procured in order to provide full coverage of the available positions.

The new hodoscope collimator has a vertical coverage of about 15 cm above and below full-length FTR/CRBR or PFR fuel stacks. The width corresponds to a 61-pin bundle of FTR/CRBR pins or a 37-pin bundle of advanced oxide pins. If tests are run with somewhat larger samples (i.e., 91 FTR/CRBR pins, or 61 advanced oxide pins), the current hodoscope-collimator capability will provide coverage of all pins except the peripheral pins on the "East" and "West" sides of the test bundle. This appears to be adequate.

Sensitivity of the hodoscope for tests with larger clusters of pins is adequate. For 61 FTR/CRBR-type pins, it is estimated to be 3-6 g. This is well below the minimum requirement of 11 g per channel of Sect. 2.3.1.2. For 19 advanced oxide pins, it is estimated to be about 2 g. This is well below the minimum requirement of 6 g per channel of Sect. 2.3.1.2.

3.4 Operational Safety

3.4.1 Rod-limited Operation

3.4.1.1 Effects of Current Limits

Currently TREAT is operated under the limitation that, should the transient rod system malfunction, the inherent reactor feedback should terminate the excursion with a maximum Zircaloy temperature of 600°C or less.

For transients initiated by essentially a step input of reactivity at low power, this limit means that the maximum pulse energy allowable is about 6% less than that which would raise the core hot spot to a maximum temperature of 600°C.

For shaped transients (this includes pulses with preheats, constant-power transients, and TUCOP simulations), the effect of this limitation depends on the details of the reference shaped transient. However, for typical LMFBR safety-shaped transients the limitation results in a maximum transient energy of about 2/3 of the energy which would produce a maximum core temperature of 600°C.

TREAT with modified elements would have essentially the same performance penalties if this limitation were maintained.

3.4.1.2 Operational Limits Required for Upgrade Capabilities

An analysis has been performed of the capability of the TREAT control system to terminate accidents.* With period scram settings in the 40-60-ms range, the system can safely terminate reactivity accidents without core damage. Since the current transient rod system is capable of reactivity insertion rates up to about 20$/s, ther appears to be an adequate margin to accommodate sample-compaction effects. During the detailed design effort the detailed analysis will be reviewed and modified as needed to reflect the changes in reactor parameters produced by the loading of modified elements.

3.4.2 Reactivity Effects of Sample Compaction

For the purposes of this study, limiting-case calculations were performed on the reactivity effect of compaction of 91 FTR/CRBR fully enriched fuel pins inside the Advanced TREAT loop in TREAT. The maximum reactivity change calculated** with a cadmium filter on the loop (the reference case calls for a "light" cadmium filter) was ∿+0.30%. This provides a limit for the potential reactivity increase expected from possible compaction of the smaller samples, particularly of the prototypic-enrichment samples.

The +0.3% reactivity limit for compaction is small compared with the reactivity swing required to compensate for heating of the reactor, 3.8%. Thus, during a shaped transient run under programmed transient rod control, any such addition would be compensated for by the transient-control-rod system, since the limit for the compaction reactivity addition is small compared with the reactivity of the transient rods. For this reason, in the event of an accident in which the transient rod system were to malfunction, the plant protection system would be adequate.

In this report, the approach taken to accommodate the potential for reactivity addition due to sample compaction has been to derate the reactivity available for a shaped transient from the nominal 3.8% to 3.5%. This decrease corresponds to a decrease in allowable energy of nearly 8%. Accordingly, the calculated sample-energy capabilities given in Sect. 3.2 were obtained by multiplying the actual calculated values corresponding to the full temperature swing by 92%.

---

* W. C. Lipinski, Design Basis for the TREAT Reactor Plant Protection System, ANL/RAS 72-16.

** With ARMCO 18SR cans and heat shields for the modified TREAT elements.

3.4.3 Plutonium Limits

3.4.3.1 Plutonium Limits on TREAT Experiments

At present, TREAT is by its technical specifications limited to running experiments with no more than 150 g of plutonium. In addition, plutonium-bearing samples can only be run under meteorological conditions which will ensure that, following a release from the reactor building of 100% of the plutonium in the experiment facility, the nonoccupational maximum permissible body burden (MPBB) of plutonium will not be exceeded in any receptor at specified locations.

The 150-g plutonium limitation was imposed in 1968, reflecting primarily the experiments planned as of that time, and is stated on p. II-5 of the Operating Instructions for TREAT. The procedure for checking meteorological restrictions has been incorporated in the Operating Instructions as Appendix M.

For the TREAT Upgrade, it is planned to take the following actions:

(1) Remove the 150-g limit, replacing it by a limit established on the basis of calculated doses to receptors at the TREAT control building, the EBR-II complex, and other specified locations downwind.

(2) Evaluate effects on TREAT availability for experimentation if doses to the receptor must be calculated using assumed 100% released values from the building, taking into account INEL meterological data on stability classes, wind speed, and wind direction.

(3) Evaluate the potential for reducing assumed building-release values by taking into account the physical processes which will serve to retain plutonium inside the reactor cavity, ductwork, filters, and building.

(4) Secure approval for a set of release specifications which would provide adequate availability of the reactor for experimentation.

A preliminary study of attenuation of plutonium release from the building has been carried (see Appendix A-5). This indicates that release from the building may be ∿1 percent or less of the amounts assumed released from the loop. An evaluation is given in Sect. B of Appendix A-5 of the meterological conditions under which an assumed 100% release of 1500 g of ^{239}Pu equivalent (representing the plutonium content of 19 mixed-oxide pins) from the TREAT building would lead to acceptable receptor doses at TREAT control, EBR-II, and ARA at INEL. These conditions occur with a probability of ∿90% within the hours of 11 AM and 5 PM averaged over the year.

4.0 COST AND SCHEDULE

4.1 Cost Estimate

The TREAT upgrade cost estimate is an ANL estimate made during the conceptual design phase and is based on the timely availability of funding so that Title I can be initiated in January of FY 1978. Because of the specialized equipment and facilities involved, the cost estimate is based strongly on previous experience with TREAT, TREAT test vehicles such as the Mark IIC, and the cost experience for procurement of SLSF test vehicles and ALIP pumps.

Costs have been obtained for the specific items identified below. Contingencies assigned to the estimates reflect the conceptual status of the design and average 30%. The summary cost estimate is shown in Table 1.2, and costs have be estimated as follows:

1. Test Vehicles

Provision is made for one advanced test vehicle consisting of one loop, an ALIP pump, and associated instrumentation with the unit completely assembled and proof tested, ready for shipment to TREAT. Also included is one model test-train, a calibration test vehicle, and two ALIP cooling modules.

2. Interface Equipment

Provision is made for equipment required for operation of the advanced TREAT test vehicles. No costs are estimated for a loop transporter, since it is assumed that the SLSF transporter will be available. The equipment is as follows:

- One Loop-handling Cask;
- Two Control Consoles (for the test vehicle);
- Two ALIP power supplies
- Additional hodoscope detectors for 61-pin-bundle capability.

3. TREAT Modifications and Support Systems

Provision is made for raising the TREAT building roof and adding a 30-ton-capacity-bridge crane to provide the capability for handling a longer test vehicle and a new loop-handling cask. Provision is also made for a new Loop Support Operations Facility for Loop Filling, Assembly, and Repair. Modifications to the reactor grid support, cooling system and rotating plug shield have also been considered, as well as filling and surfacing work needed to accommodate the SLSF loop transporter. Additions to the TREAT Data Acquisition are also planned.

4. Safety Analysis Report

Analysis and Support is provided for the Preliminary and Final Safety Analysis Reports (SAR) for the upgraded TREAT Facility.

5. Modified TREAT Fuel

Provision is made for the engineering and procurement of about 100 new TREAT fuel assemblies plus some additional special assemblies to be located around the test vehicle in the reactor core. Eighty-two UO_2-graphite and 18 UO_2-stainless steel assemblies are estimated to be required.

Cash flow and obligations for the 36-month TREAT Upgrade project are shown in Table 1.3. The table shows a total estimated cost with contingency and escalation of $12,748,000. The contingency (∿30%) is conservative in order reflect the conceptual level of the design.

4.2 Construction Schedule

The construction schedule for the TREAT upgrade, shown in Fig. 1.2, is based on a facility need date of Jan. 1981. Title I will be completed and Title II started in FY 1978. Procurement of long-lead items may also start in FY 1978. Title III is scheduled to start in FY 1979, and completion of all installation and checkout work by the end of the first quarter of FY 1978. A final SAR for the upgraded TREAT should be completed early enough in FY 1980 so that final review and approval may be received by January 1981. The modifications to TREAT will be scheduled in such detail that the disruption to the facility is minimum. This will minimize disruption to the ongoing experimental program, yet provide the new capability needed for the LMFBR safety program.

APPENDIX A-1

Reactor Physics Characteristics

A-1.1 Purposes and Basis of Reactor-core Modifications

The basis of the proposed local modifications of the reactor core is to replace some of the fuel assemblies near the test vehicle by other fuel assemblies that could be taken to much higher temperature than the present limit of 873K (600°C) for the fuel. The modification would:

(1) harden the neutron-flux spectrum at the outer surface of the test cluster, and reduce the radial gradient of fission power density across the cluster;

(2) at the same time, provide a high-intensity source of neutrons in the reactor core near the test cluster and increase the potential volumetric energy deposition in the test fuel.

This core modification will enhance experiment performance potentials even for small clusters of test fuel pins. The modification is essential to make it possible to perform a range of LMFBR-safety experiments with larger clusters of test fuel pins.

In the present TREAT-facility reactor, the test vehicle induces a large reduction in the fission power density in the core in its immediate vicinity. This depression in power density is highly localized, primarily affecting the first ring of fuel assemblies around the test vehicle. To a much smaller degree it also affects the next ring of fuel assemblies. If the core modification were to be limited to a change in the (uniform) concentration of fully enriched uranium in some fuel assemblies near the test vehicle, retaining the present constraint of a 873K (600°C) peak fuel temperature, only the first ring of fuel assemblies could be changed appreciably. So limited a modification would be of very little value for spectrum hardening and there would be very little increase in the energy-deposition capability - less than 10% according to scoping calculations. A more substantial modification is essential.

The conceptual-design modification of the reactor core utilizes fuel-assembly cans that can be taken to higher temperatures in the coolant air than the current core cans. The design concept is to modify that portion of the reactor core that is included within the central 9 x 9 array of core-assembly locations. The present plan is to relocate the inner ring of eight control-rod

fuel assemblies to unused control-rod locations farther out in the unmodified zone. During the continuing work of more detailed design the need to move rods will be evaluated from the standpoints of: the magnitude of the needed rapid reactivity changes in the modified reactor and the control worths in the new locations; the worths in the present locations; and the implications of having high-temperature modified fuel assemblies nearby if these control-rod fuel assemblies are not relocated. It is likely, also, that a more nearly circular configuration of fuel assemblies will be selected. The reactor physics analyses have modeled the modifications within the square (9 x 9) array as equivalent to modifications within circular rings, preserving areas. This is discussed in Appendix A-2.

One of the principal limitations established to guide the core modification is that there should be no essential development for fuel and for the fuel assemblies in the modified zone. For this reason the selected reference fuel for the modified zone is a graphite-matrix fuel. The conceptual-design reference is a fuel of the type used in the present reactor core, namely, UO_2-graphite. An alternative is UC·ZrC-graphite (composite) with a very low volume fraction ($\sim$1 vol.%) of UC·ZrC.

During detailed design it is planned that additional modified fuel assemblies, with UO_2-stainless steel fuel rods, will be designed. This will provide the option of incoporating an inner modified zone, with UO_2-stainless steel fuel, near the test vehicle in certain safety experiments with enriched test fuel. In the balance of the modified core zone the fuel assemblies with graphite-matrix fuel rods would be retained. The option of a two-zone modification will offer improved flexibility in performance of the broad safety-experiment program, since the two-zone modification will provide even flatter radial distribution of power density as a tradeoff against the potential for volumetric energy deposition in the center of the test cluster.

The Safety Test Facility (STF) Project plans to use a UO_2-stainless steel neutron-spectrum-converter zone around the test vehicle for safety experiments with large clusters of fully enriched test fuel pins. A verification program is planned by the STF Project that will provide verification data also for a UO_2-stainless steel fueled inner modified zone in the upgraded TREAT-facility reactor.

In all of the modified fuel assemblies, the uranium is enriched fully ($\sim$93.5%) in ^{235}U.

Another principal constraint on the modification of the reactor is to use modified fuel assemblies in direct substitution for standard TREAT facility fuel assemblies. Near the test vehicle it is planned to use special partial fuel assemblies. Special slotted assemblies will be used to provide a suitable slot through the modified zone, for hodoscope viewing. The typical full-size fuel assembly will contain a square array of individual fuel rods. The conceptual-design configuration is a 4 x 4 array of square fuel rods [$\sim$23 mm x 23 mm ($\sim$0.9 in. x 0.9 in.)] except for the four corner fuel rods which are chamfered to fit within the chamfered corners of the fuel assembly.

Each fuel rod in the modified fuel assemblies will have a uniform distribution of fully enriched uranium, both laterally and axially. However, within each modified fuel assembly the uranium (UO_2) concentration will be varied from fuel rod to fuel rod to optimize within the temperature limits, the peak concentration for that rod in its location.

Detailed neutronics and thermomechanical considerations that will influence the designation of the UO_2 concentration in a given fuel rod include:

(1) effects of streaming of neutrons in the hodoscope slot for fuel rods in modified fuel assemblies that are adjacent to the slot;

(2) corner locations near the unmodified core zone;

(3) locations near neutron absorbers that induce larger spatial gradients of power density in those fuel rods.

The plan is to specify concentrations for various groups of fuel rods in order to reduce the total number of different concentrations. Nevertheless, a given modified fuel assembly will be loaded in a given core location and with a fixed, preassigned azimuthal orientation.

This procedure of spatially grading the UO_2 concentration from fuel rod to fuel rod in the modified zone will simultaneously optimize:

(1) hardening of the spectrum of neutrons in the core near the test cluster;

(2) the level of production of source neutrons near the test fuel;

(3) the magnitude of available reactivity.

The neutron-flux spectrum is highly thermalized in the present reactor core, and it will remain highly thermalized in the unmodified zone of the core. Since the fuel rods in the modified fuel assembly will be designed for a peak operating temperature much higher than 873K (600°C) which is the operational

limit for the Zircaloy cans of the present core, much higher concentrations of UO_2 will be utilized in those rods. The constraining (optimizing) condition on the UO_2 concentration in a given fuel rod is that under normal conditions of operation the peak adiabatic-heating temperature will not exceed a preassigned value. This procedure of grading from rod to rod progressively hardens the neutron-flux spectrum from the unmodified core zone inward toward the test zone.

Incorporation of a relatively large core-modification zone (9 x 9 array) offers considerable potential for fine-tuning to a range of targets and safety experiments. The conceptual-design approach is to optimize the modified core zone with respect to safety experiments with a 19-pin test cluster where the fuel-pin outer diameter (0.86 mm) is representative of advanced oxide designs, and where the mixed-oxide fuel is prototypical of the outer zones of the FTR and PFR. The optimization will be in the context of a full zone of UO_2-graphite-fueled assemblies, and with a neutron filter surrounding the test fuel radially. The conceptual-design choice of neutron filter is cadmium in the form of a compound with a high melting point that can be used safely in the general vicinity of the test cluster. Cadmium is calculated to be particularly effective as a neutron filter for mixed-oxide (PuO_2-UO_2) test fuel of prototypic enrichment. The neutron-absorption resonance in cadmium at 0.18 eV makes cadmium a highly selective neutron filter for thermal neutrons and for those neutrons that otherwise would be absorbed in the ^{239}Pu in the test fuel in the range of the strong resonance centered at 0.3 eV. In the absence of a neutron filter those neutrons would be absorbed in the outer portions of the test cluster and there would be a steep radial graident of fission density.

For other test clusters and test vehicles, the bulk of the modified zone would remain the same, namely, at least those fuel assemblies that are outside the central (nominal) 3 x 3 array. Possibly there would be a different loading close to the test vehicle, at the least if a larger test vehicle is required. As noted earlier in this subsection, it is planned to design for an option of using fuel assemblies with UO_2-stainless steel fuel rods in the vicinity of the test zone, if the test fuel is fully enriched. Cadmium is calculated to be an effective neutron filter even for larger clusters of fully enriched (UO_2) test pins in conjunction with a full zone of graphite-matrix fuel. The tradeoff features of using an inner zone with UO_2-stainless steel will depend not only upon the constraints on a UO_2-stainless steel fuel

assembly -- primarily the peak normal operating temperature -- but also upon the need for the additional power flattening and upon the adequacy of the available reactivity in the core with a two-zone modification.

The needs for available reactivity in the modified reactor include compensation for:

(1) inclusion of the hodoscope slot, plus possibly a special modified fuel assembly in the core on the side of the test zone opposite the slot (to reduce background signals in the hodoscope detectors);

(2) the temperature increases in the core during the safety experiment;

(3) the range of test-cluster sizes and test-vehicle configurations;

(4) contingency for other operational needs.

In addition, until experiments can be performed to provide direct checks, a conservative approach to design requires assignment of a positive margin of calculated available reactivity to allow for uncertainties in the reactor physics analysis. The basic calculations that have been made in the conceptual-design phase have been in the context of diffusion theory and in the simplifications of a single space dimension. Calculations have been made in two-dimensional diffusion theory to study the special problem of the potential reactivity effects due to conceivable motions (compactions) of test fuel during certain types of safety experiments. However, in these calculations the effects of the hodoscope slot have not been explicitly included.

For the conceptual-design phase, the selected model for reactivity needs is:

Hodoscope Slot	3-4%
Temperature Swing	3-4%
Margin for Uncertainties in Analyses	3%
Operational Needs	1%
Total	∿11% (10% - 12%)

As detailed in Appendix A-3, the conceptual-design reference system is calculated to have an available reactivity of 13%. There is a potential for a further increase in reactivity by increasing the peak normal operating temperature (to 1375K) in the outermost ring of fuel assemblies in the modified zone.

A-1.2 Single-zone vs Two-zone Reactor-core Modifications

In scoping reactor physics calculations that were performed to guide the selection of a conceptual-design reference core modification, three types of modifications were studied:

(1) single-zone, with graphite-matrix fuel, with and without neutron filters around the test cluster;

(2) single-zone, with UO_2-stainless steel fuel;

(3) two-zone, with a UO_2-stainless steel inner zone (near the test vehicle) and a graphite-matrix-fuel outer zone.

The studies included optimization of the modified zone(s) to graded concentrations of fully enriched UO_2 that would project to preassigned peak normal temperatures in the fuel rods in the modified fuel assemblies. The calculations defined relative neutronics and experiment-performance merits of these three types of modifications. The principal focus on experiment performance was on the volumetric energy deposition that could be obtained in the center test pin and on the flatness of the radial distribution of fission power density across the test cluster. The reference test cluster for initial scoping calculations was a 61-pin cluster of advanced-oxide fuel pins of 6.86-mm diameter, where the UO_2 was assumed to be fully enriched. A single, simplified test-vehicle configuration was assumed, although ranges of sizes (7 to 61 pins), test-vehicle wall thicknesses, and fissile-atom concentrations of test clusters were considered. Other parameters considered included: peak temperatures in the fuel(s) of the modified fuel assemblies and sizes of the modified portions of the reactor core.

For the follow-on studies that have led to conceptual-design choices, the focus was enlarged to a major interest in two different test clusters in their correspondingly different test vehicles:

(1) 19 advanced-oxide test fuel pins of prototypic enrichment; the reference is 27% PuO_2 and 73% natural UO_2; the reference outer diameter of the cladding is 6.86 mm.

(2) 61 FTR/CRBR-size fuel pins with fully enriched UO_2 fuel.

The scoping analyses have shown that the experiment-performance potentials for these two reference test clusters would be markedly different in the presence of either a two-zone modification or a UO_2-stainless steel single-zone modification. The differences in potentials are greatly reduced, however, for the case of a graphite-matrix-fuel single-zone modification, as discussed below.

In the presence of a thick UO_2-stainless steel zone near the test cluster (two-zone or UO_2-stainless steel single-zone modification) the volumetric energy deposition in the center of a multipin test cluster is quite insensitive to the number of test pins, at least in the range (7 to 61 pins), and it is almost directly proportional to the total atom concentration of the principal fissile nuclides. Thus, for test fuel of prototypic enrichment, the volumetric energy deposition is approximately one-fourth of the deposition for fully enriched test fuel. By contrast, for a single-zone modification with graphite-matrix fuel, the volumetric energy deposition in the center of the test cluster is a sensitive function of the number of test pins. When the latter modified reactor is optimized to the use of a cadmium neutron filter around the test zone, the volumetric energy deposition that can be obtained in the center of the reference 19-pin target (prototypic enrichment) is much larger than it would be with UO_2-stainless steel fuel nearby but the radial distribution of power density in the 19-pin cluster is somewhat steeper (see Appendices A3 and A-4 for more detail).

In conjunction with a cadmium neutron filter, the graphite-matrix-fuel single-zone modification is calculated to provide a capability for useful energy deposition and power-density flatness also for the reference test cluster of 61 enriched-UO_2 fuel pins. At this stage of design, it appears that the option of an inner zone of UO_2-stainless steel fuel in the modified portion of the core is of interest primarily because of the potential for obtaining very flat radial distributions of power density across test clusters of pins with fully enriched fuel.

For these reasons the conceptual-design reference is a single-zone modification, with graphite-matrix fuel, in conjunction with use of a cadmium neutron filter in the proximity of the test cluster. The reference 9 x 9 array modified zone offers the features of: increased volumetric energy deposition in the center of the test cluster and space for incorporation of a UO_2-stainless steel inner zone. The modified reactor will have the capability for a broad range of safety experiments.

A-1.3 Limitations on Reactor-core Modifications

Important general limitations that have been established for the reactor-core modifications, and that have a major effect on the reactor physics characteristics and experiment performance potentials are:

(1) restriction to a limited portion of the reactor core, in the vicinity of the test vehicle, rather than permit modifications up to the entire maximum 19 x 19 array of fuel assemblies;

(2) retention of the present axial and lateral maximum dimensions of the reactor core;

(3) requirement to replace individual full-size fuel assemblies by corresponding individual modified fuel assemblies; the purposes of this requirement are to limit downtime of the TREAT-facility reactor during the period of upgrading and to provide a capability for rapid reloadings of the reactor core, if desired, between

(4) use of materials with established thermomechanical characteristics at temperatures and in assemblages that will not require essential development.

In the present reactor core there is an important boron impurity in the fuel assemblies. Even replacement of the present fuel assemblies by assemblies that are essentially identical except for reduced neutron-absorbing impurities would increase available reactivity, and this would help to relieve burdens on design of the modified zone. More generally, the option to replace the entire present TREAT-facility reactor core with a new core, possibly with a longer active core, would broaden the possibilities for increasing potentials for experiment performance. However, this option is not within the scope of the effort.

The requirement to replace individual fuel assemblies by individual fuel assemblies leads to a relatively high volume fraction of a strong parasitic neutron absorber for can walls and heat shields, namely, ARMCO 18 SR or an alternative (e.g., a 600-series Inconel). It also leads to reduced volume fractions of fuel in the modified zone. Both the high volume fraction of absorbers and the reduced volume fractions of fuel cause losses in available reactivity. Reduction in fuel volume fraction directly reduces the total volume from which source neutrons are generated, thereby reducing somewhat the volumetric energy deposition in the center of the test cluster. Moreover, if larger aggregates of fuel rods were allowed, conceivably the fuel rods could be taken to much higher temperatures, with suitable thermal insulation. At the higher fuel loadings associated with higher temperatures both available reactivity and experiment-performance potentials would be enhanced.

A-1.4 Reference Modifications of the Reactor from the Viewpoint of Neutronics Considerations

In the context of the discussions in Sections A-1.1, A-1.2, and A-1.3, the reference modifications of the reactor from the viewpoint of neutronics considerations are:

(1) A central array, up to a nominal 9 x 9 array, of fuel assemblies and slotted fuel assemblies in the TREAT-facility reactor core will be modified to include each of two new test vehicles (one corresponding to small-bundle tests and one corresponding to intermediate tests) and associated modified-core zones. The reference concept is a 9 x 9 array.

(2) The reference modified-core zone will feature use of a graphite-matrix (UO_2-graphite) fuel in the form of aggregates of fuel rods within standard-size fuel assemblies that will be used in direct substitution of existing standard fuel assemblies. Special partial fuel assemblies will be used in the immediate vicinity of the test vehicle; the fuel will be UO_2-graphite, in individual fuel rods. The reference full fuel rod has a square-plan cross section, ∿23 mm (∿0.9 in.) on a side. If necessary to improve thermomechanical characteristics, the active fuel rod will be of reduced length, but the total active length of the fuel rods in the modified fuel assembly will be the same (∿1.2 m) as for the present fuel assemblies.

(3) The fuel in the modified zone will be enriched fully (∿93.5%) in ^{235}U. Within each fuel rod the uranium concentration will be uniform, both axially and laterally. The reference concept is that, if shorter fuel rods are used, rods in a given plan location will have the same ^{235}U concentration. The uranium concentration will be graded from fuel rod to fuel rod in order to optimize the hardening of the neutron-flux spectrum near the test cluster and to provide a high-intensity neutron source near that cluster.

(4) The reference material of the fuel-assembly can walls in the modified zone is ARMCO 18 SR. The can-wall thickness is ∿0.51 mm (0.020 in.). The majority of the reactor physics calculations in the conceptual-design study were made with Inconel 600 as the can-wall material. The change to ARMCO 18 SR was primarily due

to the increased available reactivity, by comparison with use of Inconel 600 (also ∿51 mm thick).

(5) A heat shield will be included between the assembly can wall and the fuel rods in each modified fuel assembly, to reduce the rate of flow of heat to the can wall. Most of the reactor physics calculations were made using Inconel 600 as the reference material with an equivalent full thickness of ∿0.24 mm (∿0.009 in.) on each side of the assembly. The present reference choice is ARMCO 18 SR with the same equivalent full thickness, because of the resulting higher avialable reactivity.

(6) In the nominal 7 x 7 central array the fuel in the modified assemblies will be loaded for a peak adiabatic-heating temperature of ∿1375K (∿1100°C). A buffer region, one-fuel-assembly thick, will separate the 1375K region from the Zircaloy-canned fuel assemblies of the unmodified zone. In the buffer region, the loading will be to a peak of ∿1125K (∿850°C). Detailed calculations of transient heat transfer will be required to verify the adequacy of the present reference composite buffering by heat shields and this special buffer region. If feasible, the design peak temperature in these outermost modified fuel assemblies will be raised to 1375K to permit higher ^{235}U loadings; this will be of value primarily in increasing available reactivity and providing correspondingly increased flexibility in design of the core modification.

(7) For all safety experiments utilizing a 9 x 9 modified zone, the same outermost two rings of modified fuel assemblies will be loaded. If there are changes in the modified zone they will be made only by reloading in the inner portion, close to the test vehicle. Such changes are expected between tests using test sections or test vehicles of different sizes, and perhaps when test clusters of greatly differing fissile-atom concentrations are used in successive safety experiments.

(8) The reference uranium loadings in fuel rods in modified assemblies will be based upon safety experiments to be conducted with a 19-pin cluster of prototypic-enrichment mixed-oxide advanced-oxide pins of 6.86-mm diameter, in conjunction with use of a neutron filter around the test zone. The conceptual-design reference

filter material is a cadmium compound of thickness equivalent to 1.0 mm (0.04 in.) of cadmium.

(9) For certain safety experiments with fully enriched test fuel, it is planned to provide an option to use UO_2-stainless steel fuel in the inner portion of the modified zone. The fuel-assembly design would be similar to the design for graphite-matrix fuel. An aggregate of fuel rods, with graded concentration of uranium from rod to rod, would be contained in a fuel assembly with an ARMCO 18 SR can, ∿1.3 mm (0.050 in.) thick. A heat shield of ARMCO 18 SR would be included in each assembly.

(10) For graphite-matrix fuel, graphite top and bottom axial reflectors are planned, each having a nominal total thickness of ∿0.6 m. The reference includes boron-poisoned 0.15-m-thick sections of the axial reflectors, next to active fuel, to limit the fission power density in that fuel at the core-reflector interfaces. The reference axial reflector for UO_2-stainless steel fuel is stainless steel. The present reference is that ARMCO 18 SR cans and heat shields will be continued into the axial reflectors.

(11) Scoping calculations of the time-dependent temperatures in the modified zone and in adjacent TREAT-facility fuel assemblies indicate that it will not be necessary to modify the aluminum extensions of the fuel-assembly cans in the bottom axial reflector for unmodified fuel assemblies that are adjacent to the modified zone. If later, more detailed analysis indicates that modifications are required, the aluminum extensions will be replaced; the present expectation is that Zircaloy extensions would be used in this event.

(12) In the reference normal core loading the full core will be loaded, filling out with regular and slotted fuel assemblies as appropriate.

(13) A single hodoscope slot, of the existing new full height, is included.

(14) The present plan is to move the innermost ring of control-rod fuel assemblies to available control-rod locations farther out in the unmodified zone of the core. A more detailed analysis is needed of the control worths in the modified reactor, at various core locations, and the need for control. It is expected that in their

new locations the transient control rods would satisfy needs for rapid reactivity changes. The detailed evaluations of physics and engineering parameters might indicate that it would be acceptable to leave these control-rod assemblies in their present locations.

APPENDIX A-2
Models for Reactor Physics Analyses

Simplifications and approximations for the reactor physics analyses are described in this appendix. They include:

1. models representing simplifications of the geometrically complex configurations, to permit calculations in one or two space dimensions;
2. models of compositions of local material densities and concentrations;
3. sets of multigroup neutron cross sections;
4. model of idealized reactor state for optimization calculations of uranium concentrations in the fuel rods in the modified fuel assemblies;
5. idealized model of test-fuel compaction, and model for two-dimensional statics calculations of associated reactivity changes.

A-2.1 Models of Gross Geometry Simplifications and Compositions for Calculations in One Space Dimension. Both the present TREAT-facility reactor and the conceptual modified reactor have very complex configurations, geometrically and neutronically. The test fuel cluster and the test vehicle introduce complexities which superficially might seem to be more amenable to simplification, but, in reality, are difficult to represent in one space dimension or even in two space dimensions. The principal difficulty arises in realistic representations of the array of test fuel pins.

The principal gross geometry complexities in the modified reactor outside the test vehicle will be the hodoscope slot, the control-rod fuel assemblies, and the configuration of graded-concentration fuel rods in the modified zone. Calculations of reactivity effects of modeled potential test-fuel compactions during certain types of safety experiments have been performed in a model of two space dimensions. For the other principal reactor physics calculations in the conceptual-design phase, the reactor geometry was simplified to a representation in one space dimension (cylindrical geometry) plus accountings for neutronics effects of the finite height by assignments of effective linear extrapolation distances in the axial direction. The transition between the actual geometry and the representation by concentric circular rings preserved areas. An exception is that the outer radius of the unmodified zone was chosen to represent effects of neutron leakage

rather than preserve area. A core value of r_{core} = 1.065 m was chosen so that the total geometric buckling ($B_x^2 + B_y^2$) in the two-dimensional plan cross section was equal to the buckling in the one-dimensional representation.

For the one-dimensional calculations the test vehicle was represented as a nested set of 10 circular rings, preserving areas of each region. The test cluster was represented as a homogeneous mass whose composition was the volume-averaged composition of a fuel-pin cell. To obtain computer output of averaged fission power density in the various rings of fuel pins, the 19-pin cluster was subdivided into three subregions, and the 61-pin cluster was subdivided into five subregions.

The reference 19-pin test cluster was modeled as 19 fuel-pin cells with advanced-oxide-size fuel pins. The fuel-pin dimensions are: 6.858-mm (0.270-in.) outer diameter 6.096-mm (0.240-in.) inner diameter. Each fuel pin has a spiral wire wrap of 1.42-mm (0.056-in.) outer diameter. The fuel-pin lattice is modeled as having a pitch of 8.38-mm. The fuel is 27% PuO_2-73% UO_2, where the UO_2 is of natural enrichment. The plutonium is modeled as 88% ^{239}Pu and 12% ^{240}Pu in the conceptual-design calculations. In the later, more detailed calculations, finer distinctions will be made, since the actual plutonium composition includes the isotopes ^{239}Pu and ^{241}Pu as principal fissile isotopes, and ^{240}Pu and ^{242}Pu. At ambient temperature, the smear density of the fuel inside the cladding is taken to be 85% of theoretical density. The cladding and the wire wrap are assumed to be Type 316 stainless steel.

The reference 61-pin test cluster is modeled as 61 fuel-pin cells with FTR/CRBR-size fuel pins. The fuel-pin dimensions are: 5.842-mm (0.230-in.) outer diameter and 5.080-mm (0.200-in.) inner diameter. Each fuel pin has a wire wrap of 1.42-mm (0.056-in.) outer diameter. The fuel-pin lattice is modeled as having a pitch of 7.366 mm (0.290 in.). The reference fuel is fresh, unirradiated, fully enriched UO_2 (93.5% ^{235}U). At ambient temperature the smear density of the fuel inside the cladding is assumed to be 85% of theoretical density.

Table A-2.1 summarizes the details of approximations to geometry and composition in the 10 regions that represent the test cluster and the test vehicle.

The modified zone was modeled as starting at the outer surface of the secondary containment of the test vehicle. In reality there will be some

TABLE A-2.1 Models of Geometry and Compositions for Reference Test Clusters and Test Vehicles for Reactor Physics Calculations in One-dimensional Cylindrical Geometry

Region	Outer Radius, cm		Composition
	19-pin Vehicle	61-pin Vehicle	
1-1	0.440	0.387	Fuel-pin cells: for 19-pin
1-2	1.164	1.023	cluster, Volume fraction (fuel = 0.480;
1-3	1.918	1.686	Volume fraction (SS) = 0.153, Volume fraction(sodium) =
1-4	NA	2.352	0.367; for 61-pin cluster,
1-5	NA	3.021	Volume fraction (fuel) = 0.431; Volume fraction (SS) = 0.205 Volume fraction (sodium) = 0.364
2	2.025	3.107	Additional sodium inside hexcan
3	2.158	3.241	Hexcan of Type 316 SS
4	2.723	3.556	Gap
5	2.977	3.810	Flow divider Type 316 SS
6	3.886	5.080	Sodium
7	6.063	8.077	Primary vessel Type 316 SS
8	7.816	9.843	Gap
9	8.133	10.160	Secondary containment vessel (Inconel 718)
10	8.134	10.161	"Gap" (included for flexibility of computations)

gap, but the present plan is that this gap will be small. The first four regions in the modified zone correspond to the total remaining area in the central 3 x 3 array. For the reference 19-pin test vehicle these four regions were assumed to be of equal thickness. For the larger, reference 61-pin test vehicle, the area remaining in the central 3 x 3 array was partitioned into three equal-thickness regions. Purely for convenience of the calculations and accounting, an artificial, very thin fourth region was added.

The next square ring of fuel assemblies, filling out the 5 x 5 array, was represented by five regions, each ∿23 mm (0.9 in.) thick, although the present concept is to use a 4 x 4 loading of individual fuel rods within each modified fuel assembly. Similarly, each of the next two square rings of fuel assemblies was represented by five regions. Therefore, the modified zone, in the central 9 x 9 array, is represented by a total of 19 regions in the one-dimensional calculations. Within each region the concentration of fully enriched uranium is uniform in all directions. The concentration is graded from region to region in optimization calculations. In each region, the assumed volume fractions of fuel, metal (can wall and heat shield), and gap are the averages for a fuel-assembly cell.

Table A-2.2 supplies details of modeled dimensions and compositions for the reactor core and radial reflector.

A-2.2 Multigroup Sets of Neutron Cross Sections for Diffusion-theory Calculations. Two sets of multigroup neutron cross sections have been used in the reactor physics calculations: XSISO48, a 48-group set in the ARC (Argonne Reactor Computations) system; and XSISO18, an 18-group set in the ARC system. These two sets were generated initially for analyses in conceptual design of the STF. Both sets derive from a 119-group cross section set obtained by flux-weighting basic neutron cross sections from the ENDF/B-IV data file.

The 48-group set was obtained by collapsing the 119-group set, with flux weightings based on several different neutron-flux spectra that are representative of the various regions of mixed-spectum reactors of the type of the conceptual STF and this conceptual TREAT-facility modification. Included are representative spectra for the test clusters, the modified zone(s), the present TREAT-facility reactor core, and the permanent graphite radial reflector. The multigroup sets include neutronics effects also of

temperatures above 300 K, e.g., 800 K, 1200 K, and 2000 K, for certain nuclides, in the 48-group set, and 1200 K and 2000 K (and certain other temperatures) in the 18-group set. The principal effects of higher temperature on these cross sections are: scattering of thermal neutrons by graphite; and Doppler broadening of capture resonances and absorption resonances in uranium and plutonium, in the resolved-resonance ranges.

The 18-group set was derived by collapsing the 48-group set over various neutron-flux spectra characteristic of the test cluster and the various reactor zones.

Both sets of cross sections are suitable only for diffusion-theory calculations.

For both sets, scattering of thermal neutrons is represented by transfer matrices that include both downscattering and upscattering of neutrons in energy, as inferred from equilibrium-model thermal-neutron-flux spectra. In actuality, asymptotic neutron-flux spectra are approached only deep in the unmodified zone and in the radial reflector. The 48-group set is less sensitive to the deviations of the actual spatially varying neutron-flux spectra from the representative spectra, but even the 18-group set supplies a reasonable basis for analyses. The 18-group set has been used for the bulk of the one-dimensional calculations and for all of the two-dimensional calculations, but a number of 48-group calculations have been performed to check sets of 18-group calculations.

Throughout the reactor physics analyses of candidate modifications, the ENDF/B-IV $S(\alpha,\beta)$ data representing neutron scattering by graphite has been used.

The energy partitions for the 48-group and 18-group sets are listed in Tables A-2.3 and A-2.4.

A-2.3 Model for Optimization Calculations in One-dimensional Approximation. With a multi-region model of the modified zone, the uranium concentrations in the modified zone are chosen so as to optimize to: attainment of normal peak operating temperatures in all regions of the modified zone and in the unmodified zone at the same time, in a safety experiment that requires maximum performance from the reactor; hardening of the neutron-flux spectrum at the inner edge of the modified zone; maximum available reactivity. These three aspects of optimization are achieved simultaneously.

TABLE A-2.2 Models of Geometry and Composition for Reference Modified Zones and for Unmodified Zones for Reactor Physics Calculations in One-dimensional Cylindrical Geometry

Region	Outer Radius, cm		Composition*	
	19-pin Vehicle	61-pin Vehicle	19-pin Vehicle	61-pin Vehicle
MZ-1	10.400	12.507		
MZ-2	12.666	14.853	VF (fuel) = 0.840	VF (fuel) = 0.810
MZ-3	14.932	17.198	VF (metal) = 0.030*	VF (metal) = 0.033
MZ-4	17.198	17.1981**		
MZ-5	19.490			
MZ-6	21.782		VF (fuel) = 0.860	VF (fuel) = 0.860
MZ-7	24.076	Same	VF (metal) = 0.027	VF (metal) = 0.027
MZ-8	26.366		in MZ-5 to MZ-19	in MZ-5 to MZ-19
MZ-9	28.658			
MZ-10	30.951			
MZ-11	33.244			
MZ-12	35.537	Same	Same	Same
MZ-13	37.830			
MZ-14	40.123			
MZ-15	42.418			
MZ-16	44.711			
MZ-17	47.044	Same	Same	Same
MZ-18	49.297			
MZ-19	51.590			
Unmodified zone	106.6		TREAT-facility fuel-assembly cells	
Liner	106.818***		Aluminum	
Radial Reflector	177.0		TREAT-facility permanent graphite raidal reflector	

* By "metal" is meant the heat shield and the fuel-assembly can wall. The reference material now is ARMCO 18 SR. An earlier reference choice was Inconel 600, and most of the calculations for this Conceptual Design Report were made with Inconel 600. The principal reactor physics difference is that the system optimized to use of ARMCO 18 SR has a higher available reactivity.

** Artificial region, for convenience of computations.

*** In actuality there is a gap, also. This gap has been ignored in the conceptual-design analyses.

NOTE: The geometry model for the first-four regions, MZ-1 to MZ-4 of the modified zone applies to all calculations where the "metal" (fuel-assembly can wall and heat shield) was assumed to be Inconel 600. For the most recent work, with ARMCO 18 SR, a small change was made in the model, namely: for MZ-1 the outer radius was left as 10.400 cm; MZ-2, MZ-3, and MZ-4 were equal-thickness regions. This change has a trivial effect on the reactor physics data reported.

The conceptual-design optimization calculations, for designated sizes and parameters of the modification region, have been performed in the context of the one-dimensional approximation in cylindrical geometry. It was necessary to select a model of an idealized reactor configuration and state for the one-dimensional optimization. The model selected is:

1. The reactor is at ambient temperature.
2. The unmodified zone is clean, without simulation of hodoscope-slot effects and without control rods.
3. The spatial distribution of energy deposition in the reactor fuel is assumed to be the same as the time-averaged spatial distribution of fission power density. Heating is assumed to be locally adiabatic.
4. The time-averaged spatial distribution of fission power density is assumed to be the same as the calculated spatial distribution in the reference idealized cold reactor.
5. The concentration of UO_2 in the modified regions is graded from region to region so that with the resulting distribution of fission power density, and with assumptions nos. 1 to 4, immediately above, the designated peak normal operating temperature is reached in each region, in a maximum normal transient.

The hodoscope slot causes azimuthal flux tilting that will be accounted for in the detailed choices of the uranium loadings in the modified fuel assemblies. Scoping calculations have been made in (r,θ) geometry to provide preliminary information on the nature and approximate magnitudes of azimuthal variations in the radial distribution of fission power density across the reactor core. An idealized and conservative model was chosen to represent the hodoscope slot in the unmodified zone. The calculational model and results are described in Appendix A-3. The indications are that the hodoscope slot will cause some flux tilting in the direction of increasing the relative power density in a sector of the unmodified zone. Flux tilting is expected in the modified zone, but to a lesser extent.

The current optimization model does not take specific account of this effect of gross flux tilting. Nor does it take into account radial flux tilts in the opposite direction, caused by neutron poisoning of the unmodified zone and by heating of the unmodified zone during the safety experiment. The best present estimate is that these opposing effects of flux tilting largely cancel, and that the present optimization model

TABLE A-2.3 Partitions of the Neutron Energy Range from 10 MeV Down through* Thermal Energies: 119-Group Set and 48-group Set of Neutron Cross Sections

Group	Lower Bound of Neutron Energy E_{min}, eV	Lethargy ΔU	119-group set, Groups	Group	Lower Bound of Neutron Energy E_{min}, eV	Lethargy ΔU	119-group set, Groups
1	5.48812+6**	0.6	1-6	25	1.37096+1	0.5	80-81
2	3.01194+6	0.6	7-12	26	8.31529	0.5	82-83
3	1.65299+6	0.6	13-18	27	5.04348	0.5	84-85
4	9.07180+5	0.6	19-24	28	3.05902	0.5	86-87
5	4.97871+5	0.6	25-30	29	2.38237	0.25	88
6	2.73237+5	0.6	31-36	30	1.85540	0.25	89
7	1.49956+5	0.6	37-42	31	1.43154		90-92
8	8.65170+4	0.55	43-46	32	1.13373		93-94
9	4.08677+4	0.75	47-49	33	8.81034-1		95-96
10	2.47875+4	0.5	50-51	34	6.55216-1		97-98
11	1.50344+4	0.5	52-53	35	4.48545-1		99-100
12	9.11882+3	0.5	54-55	36	3.61440-1		101
13	5.53085+3	0.5	56-57	37	2.49346-1		102-103
14	3.35463+3	0.5	58-59	38	2.07066-1		104
15	2.03468+3	0.5	60-61	39	1.59830-1		105-106
16	1.23410+3	0.5	62-63	40	1.19782-1		107-108
17	7.48519+2	0.5	64-65	41	9.97376-2		109
18	4.53999+2	0.5	66-67	42	8.23109-2		110
19	2.75365+2	0.5	68-69	43	5.98906-2		111-112
20	1.67017+2	0.5	70-71	44	4.98691-2		113
21	1.01301+2	0.5	72-73	45	3.98366-2		114
22	6.14421+1	0.5	74-75	46	2.97804-2		115
23	3.72665+1	0.5	76-77	47	1.48907-2		116-117
24	2.26033+1	0.5	78-79	48	4.74190-3		118-119

* Cut-off in the thermal-neutron energy range at ∿4.742 meV.

** The format "+6" means "times 10^6."

TABLE A-2.4 Partitions of the Neutron Energy Range from 10 MeV Down through* Thermal Energies: 18-group Set Plus Comparison with 48-group Set

Group	Lower Bound of Neutron Energy, E_{min})eV	Corresponding Groups of 48-group Set
1	1.653+6	1-3
2	4.979+5	4-5
3	1.500+5	6-7
4	4.087+4	8-9
5	1.503+4	10-11
6	5.531+3	12-13
7	2.035+3	14-15
8	7.485+2	16-17
9	2.754+2	18-19
10	1.013+2	20-21
11	3.727+1	22-23
12	1.371+1	24-25
13	5.043	26-27
14	1.855	28-30
15	4.485-1	31-35
16	1.198-1	36-40
17	4.987-2	41-44
18	4.742-3	45-48

* Cut-off at ∿4.742 meV.

reasonably accounts for the net effects. In the later, more detailed design work the present optimization model will be refined.

A-2.4 Models of Geometry and Reactor State for Calculations of Reactivity Effects of Test-fuel Compaction

There is further discussion of compaction calculations in Appendicies A-3 and A-4. For the sake of completeness of the present summary, some of this information is presented here.

The model of test-fuel compaction that has been chosen for this stage of design is that fuel and other materials initially would mix uniformly within the radial confines of the primary vessel, and then UO_2 would slump or be pushed toward a cylindrical zone that is centered at axial midheight of the initially uncompacted fuel rods. The UO_2 would displace materials that then move to the space left by the UO_2 compaction. At "zero compaction," the test fuel cluster is assumed to be mixed with the other materials within the volume spread over a vertical distance defined by the original top and bottom of the fuel rods, and bounded diametrally by the primary vessel. Because of the horizontal mixing and movement of fuel from the original "uncompacted" case, this model therefore imposes a discontinuity between "uncompacted" test fuel and test fuel that has begun to compact.

The model assumes that, at full compaction, a cylinder of volume V_o is filled with molten UO_2. Let V_1 be the volume remaining of the original volume that is bounded by the inner diameter of the primary vessel, diametrally, and the top and bottom of the initially uncompacted fuel, axially. The "percentage compaction" is defined as the percent of the UO_2 initially in volume V_1 that is assumed to have moved into volume V_o. The volumes of all materials initially in the total volume V_o plus V_1 are assumed to be conserved.

This model of geometry of compaction is the same as the model currently used in the STF studies. Other models of compaction could be conceived, and further evaluation will be needed later.

For the present two-dimensional (r,z) calculations of the reactivity effect of test-fuel compaction, the reactor physics model selected is that the reactor is in state that emphasizes the relative importance of the test cluster. The reactor is assumed to be hot, with the thickness of the unmodified zone reduced to yield a k_{eff} of 1.05 to increase the relative importance of the test cluster.

Two-dimensional calculations for the modified states of compaction were compared with a two-dimensional calculation for the initial state to provide a direct calculation of the reactivity effect of test-fuel compaction. All compaction calculations were made with a test cluster of fuel pins of fully enriched UO_2. The choice of 91 pins was made for purposes of conservatism.

Other compaction calculations were made for a two-zone system where the UO_2 stainless steel inner zone extended to the outer boundaries of the central 5 x 5 array. The principal two-zone study was of a system where Inconel 600 was used for the fuel-assembly can walls and heat shields throughout the modified zone. For that study the thickness of the unmodified zone used for the single, graphite-matrix case was retained. Consequently the two-dimensional, two-zone k_{eff} was even lower, $\sim$0.98, and thus the relative importance of the test cluster was emphasized even more than in the single zone case. This analysis is believed to be highly conservative.

One check calculation was made for a two-zone system utilizing ARMCO 18SR substituted for the Inconel 600. The starting point for this calculation was a new choice of the thickness of the unmodified zone so that k_{eff} was 1.05 in the modeled initial hot system.

APPENDIX A-3
Neutronics Data for Reference Modified Reactor

A-3.1 Introductory Discussion and Statics Data

Appendix A-1 presents background discussions and a summary of the bases for specific choices in the core modification, including type of fuel, operating normal peak temperatures, and size of the modified zone. Appendix A-2 describes the geometrical models selected for calculations, multigroup neutron cross sections, the basis for optimization of the uranium loadings in the fuel rods in the modified zone, and the bases for analysis of reactivity effects of modeled test-fuel compactions. Appendix A-3 presents results of reactor physics calculations for the reference system. The primary data presented are: available reactivity; changes in reactivity corresponding to changes in the reference test fuel cluster and test vehicle, or changes in temperature; kinetics parameters; and experiment-performance potentials, namely, energy deposition and flatness of radial distributions of fission power density across the test cluster. Results are given for the radial variation in the neutron-flux spectrum across the reactor, and the radial distribution of fission power density in the reactor core at core midheight. Calculated reactivity effects of test-fuel compactions are discussed for an idealized compaction model.

It has been decided to make ARMCO 18 SR the reference material for the fuel assembly can walls and heat shields in the modified zone. The earlier choice was Inconel 600, and the bulk of the basic information presented in Appendix A-3 was obtained from an extensive series of calculations for system utilizing Inconel 600. The new choice, ARMCO 18 SR, was made to assure a margin of available excess reactivity to meet the anticipated needs. Optimization to a single-zone graphite-matrix modification within the central 9 x 9 array of fuel-assembly locations yields a calculated reactity of 13.2% for the cold clean system without a hodoscope slot, with ARMCO 18 SR. With Inconel 600, the corresponding reactivity calculated is 10.6%. The present target for calculated reactivity is 11%.

A number of new optimization calculations have been completed for the new reference system with ARMCO 18 SR. The results confirm the expectation that the basic reactor physics characteristics of the modified reactor are the same whether Inconel 600 or ARMCO 18 SR is used, except for the difference in

reactivity. If upon more detailed evaluation it is determined that there would be a considerable margin of available reactivity in the present conceptual modified reactor, this will provide increased flexibility in detailed design and a potential for somewhat improved performance.

The summaries of calculated reactor physics data are clearly labled to indicate whether they pertain to use of ARMCO 18 SR or Inconel 600. Comparisons are included for selected checkpoints.

The principal results of reactor physics calculations for alternative reactor modifications are presented in Appendix A-4. The present Appendix, however, includes results for other test clusters and for effects of removing the reference neutron filter.

Table A-3.1 summarizes the basis model for the dimensions and compositions of a 19-region partition of the reference modified zone. As noted in Appendix A-2, the one-dimensional simplification preserves areas of successive rings of fuel assemblies in that zone. Within each full-size fuel assembly there is a partition into five regions, representing smeared fuel rods, can, heat shield, and gaps. The transition from the actual square rings to circular rings does not preserve thickness of the ring. Also, the inclusion of the can, heat shield, and gaps increased the total area of each circular ring. For this reason there is a difference between 4 x 4 array of individual fuel rods in the reference modified fuel assembly and the selection of a partition into 5 regions. These differences do not have an important effect on the results. Indeed, scoping calculations have indicated that the use of larger fuel rods in most of the volume of the modified zone would introduce relatively small perturbations in neutronics data and in experiment-performance potentials.

It is planned that special partial fuel assemblies will be used in the immediate vicinity of the test vehicle and sized to fit the particular test section that is inserted. This special portion of the modified zone has been represented as four circular regions in the reactor physics calculations. The model of the dimensions of these first four regions depends upon which of the two reference test sections is inserted: the test section for the reference 19-advanced-oxide-pin test cluster, or the test section for the reference cluster of 61 FTR/CRBR-size fuel pins. For the reference 61-pin test section, this first portion of the modified zone was partitioned into three regions of equal thickness; for convenience of computer input, a thin fourth "region" was included, as shown in Table A-3.1. These first four regions extend to the

TABLE A-3.1 Model of Dimensions, Smeared Compositions, and Peak Fuel Temperatures in Regions of Reference Modified (9x9) Zone (UO_2-Graphite Fuel)

Central Array	Modified-zone Region Number	Outer Radius, cm	Composition		Peak Fuel Temperature, K
			VF (fuel)	VF (metal)	
3 x 3	1	10.400	0.840	0.030	1375
	2	12.676	↕	↕	↕
	3	14.932	↕	↕	↕
	4	17.198	0.840	0.030	↕
5 x 5	5	19.490	0.860	0.027	↕
	6	21.782	↕	↕	↕
	7	24.076	↕	↕	↕
	8	26.366	↕	↕	↕
	9	28.658	↕	↕	↕
7 x 7	10	30.951	↕	↕	↕
	11	33.244	↕	↕	↕
	12	35.537	↕	↕	↕
	13	37.830	↕	↕	↕
	14	40.123	↕	↕	~1375
9 x 9	15	42.418	↕	↕	~1125
	16	44.711	↕	↕	↕
	17	47.004	↕	↕	↕
	18	49.297	↕	↕	↕
	19	51.590	0.860	0.027	~1125

*By "metal" is meant the fuel-assembly can wall and heat shield.

TABLE A-3.1 (Cont'd) Inner Four Regions of Modified Zone for the Reference 61-Pin Test Section

Modified-Zone Region Number	Outer Radius, 10^{-2} m	Composition		Peak Fuel Temperature, °K
		VF (Fuel)	VF (Metal)	
1	12.507	0.81	0.033	1375
2	14.853	↑	↑	↑
3	17.198	↓	↓	↓
4*	17.1981	0.81	0.033	1375

*The fourth region was included only for convenience of computer inputs. These radii were modified slightly in calculations performed more recently, with ARMCO 18 SR. The basic idea of a partiition into three regions of equal thickness plus a fourth, then region was retained.

outer boundary of the central 3 x 3 array of fuel-assembly locations in the present TREAT-facility reactor. Beyond this all region dimensions are independent of the test vehicle.

Table A-3.2 summarizes the concentrations of ^{235}U in the 19 modified regions, optimized for the reference 19-advanced-oxide-pin test cluster and test section, in conjunction with use of a neutron filter in the gap between the primary vessel and the secondary containment. As discussed in Appendix A-2, the optimization was done with a one-dimensional calculation for a cold, unpoisoned, fully loaded reactor. Comparisons are made between Inconel 600 and ARMCO 18 SR can walls and heat shields.

This same basic optimization model (with Inconel 600) has been applied to a calculation of a local reoptimization of a modified zone in the context of the reference 61-pin test section, and a 61-pin test pin cluster with fully enriched UO_2 (no plutonia), and a cadmium filter. The reoptimization is for the first four regions of the modified zone. Table A-3.3 compares the two different locally optimized gradings of ^{235}U atom concentrations across these first four regions. The differences are small. It appears that it is the difference in test-section size that will primarily influence the details of the particular partial fuel assemblies that are used, rather than the higher relative volumetric power density in the 61-pin test cluster. This is confirmed by a calculation in which the 61-pin cluster and test section, plus cadmium filter, was substituted for the 19-pin cluster and test section. In this calculation the first region of the modified zone was thinned to allow space for the substitution. The result was a difference of $\sim$0.05 in reactivity, a 0.4% change in the volumetric energy deposition in the center of the 61-pin test cluster, and a similarly very small change in the radial distribution of fission power density across the test cluster. The trends and general magitudes noted for these systems utilizing Inconel 600 also apply to the new reference systems with ARMCO 18 SR can walls and heat shields.

Table A-3.4 summarizes the experiment-performance characterstics for the 19-pin test cluster of prototypic-enrichment PuO_2-UO_2 fuel pins for each of three optimized modified reactor cases: ARMCO 18-SR with cadmium, and Inconel with and without cadmium. Clearly the neutron filtering by cadmium is very effective in flattening the radial distribution of fission power density across this test cluster. The basic reason for this dramatic reduction in the power spike is that cadmium has a neutron-capture resonance close to the

TABLE A-3.2 Calculated* Grading of ^{235}U Atom Concentrations Across Optimized Modified (9 x 9) Zone

(Reference: 19-pin Test Cluster and Test Section with Cadmium Neutron Filter)

Modified-zone Region-number	^{235}U Atom Concentration, 10^{26} atoms/m^3 Fuel		C/^{235}U Atom Ratio	
	INCONEL 600	ARMCO 18 SR	INCONEL 600	ARMCO 18 SR
1	1.635	1.381	517	613
2	1.385	1.147	611	739
3	1.228	1.001	690	847
4	1.117	0.899	759	944
5	1.032	0.821	822	1034
6	0.964	0.758	880	1120
7	0.905	0.705	938	1205
8	0.850	0.657	999	1293
9	0.797	0.613	1065	1386
10	0.744	0.570	1141	1491
11	0.688	0.528	1235	1610
12	0.629	0.485	1351	1753
13	0.567	0.442	1499	1924
14	0.505	0.400	1684	2127
15	0.325	0.263	2619	3237
16	0.289	0.239	2945	3563
17	0.256	0.218	3325	3906
18	0.225	0.198	3784	4301
19	0.197	0.179	4322	4758

*Based on one-dimensional diffusion-theory calculations using 18-group set (XSISO 18) of neutron cross sections for cold reactor.

TABLE A-3.3 Comparison of Calculated* Locally Optimized Gradings of ^{235}U Atom Concentrations in the First Four Regions of the Modified Zone: 19-pin vs 61-pin Test Cluster and Test Section

(INCONEL 600 CAN AND HEAT SHIELD)

Modified-zone Region Number	^{235}U Atom Concentration, 10^{26} atoms/m^3 Fuel	
	19-pin Optimization (Advanced Oxide)	61-pin Optimization (FTR/CRBR)
1	1.635	1.734
2	1.385	1.437
3	1.228	1.246
4**	1.117	1.246**

* XSISIO 18 multigroup cross sections.

** Note that region No. 4 is an artificial, very thin region for the 61 pin case.

TABLE A-3.4 Experiment Performance Potentials for Test Cluster of 19 Prototypical-enrichment Advanced-oxide Fuel Pins*:

	Inconel-600 Can Walls and Heat Shields		ARMCO 18 SR Can Walls and Heat Shields
	No Filter	Cadmium Filter	Cadmium Filter
Fission Energy Generated in Center of Test Fuel Pin, kJ/kg fuel	2535	2360	2415
Nodal Max/Min Across Test Fuel Pins**	2.26	1.26	1.27
Ratios of Pin-averaged Fission Power Density			
outermost/center	1.44	1.17	1.18
1st ring/center	1.05	1.05	1.05
Max/Avg of Fission Power Density in Outermost Test Fuel Pins	1.57	1.07	1.07

* In each case the modified zone was optimized toward a peak adiabatic-heating fuel temperature of 1125K in the outermost ring of fuel assemblies and 1375K in the balance of that zone. The 18-group set of cross sections was used.

** Twelve nodes were used in the outermost ring of test fuel pins, where the power-density spike is steepest.

neutron-fission resonance of the ^{239}Pu at 0.3 eV. Actually, the model used ^{239}Pu in place of the sum of the ^{239}Pu and ^{241}Pu concentrations that would be in the plutonium, and so the improvement by the cadmium filter might be somewhat overstated.

For the earlier reference system, with Inconel 600, calculations were made to determine experiment-performance potentials for the test cluster of 61 FTR/CRBR-size test fuel pins (no PuO_2; UO_2 fully enriched) in the 61-pin reference test vehicle. Table A-3.5 summarizes results. Results would exhibit the same trends for ARMCO 18 SR can walls and heat shields. Variations studied were: cadmium filter or no filter, and nature of optimization of modified reactor zone. Comparing with data in Table A-3.4 it may be observed that, when no cadmium filter is included, the radial distribution of fission power density across the reference 61-pin cluster is much flatter than the unfiltered distribution across the reference mixed-oxide 19-pin cluster. The ^{239}Pu fission resonance at 0.3 eV introduces a power spike that overrides the effects of target size and concentration of fissile atoms. When a cadmium filter is included in both cases, the distribution is flatter across the 19-pin cluster than across the 61-pin cluster. Nevertheless, even for the 61-pin cluster a cadmium filter is helpful in flattening power distributions at the cost of a small percentage reduction in energy deposition in the center pin.

In Table A-3.5 for the two cases identified by "modification optimized for 19-pin case," the 61-pin test was substituted for the 19-pin test, and the first modified-zone region was thinned to accommodate to the larger 61-pin test section. There was no other change in the modified zone. The principal reason for the larger value of the fission energy generated in the center pin when the cadmium filter is removed is that the relative power density in the modified zone is increased. A reoptimization of the modified zone for the case where there is no cadmium filter would largely cancel the increased energy generation in the center test pin.

A-3.2 Comparison of 18-group and 48-group Calculations

Comparison calculations have been made to determine the nature and magnitudes of differences in calculated neutronics and experiment-performance characteristics between results of 18-group (XSIS018) and 48-group (XSIS048) calculations. The 18-group set used has been obtained by collapsing the 48-group parameters with respect to neutron-flux spectra characteristic of various degrees of spectrum hardness (see Appendix A-2). Nevertheless, the generic

TABLE A-3.5 Calculated Experiment Performance Potential for Test Cluster of 61 FTR/CRBR-size Fuel Pins of Fully Enriched UO_2 in Reference 61-pin Test Section* (Inconel-600 Can Walls and Heat Shields)

	Modification Optimized for 19-advanced-oxide-pin Case		Reoptimized First Four Regions of 19 Advanced-oxide-pin Modification
	Cd Filter	No Filter	Cd Filter
Fission Energy Generated in Center Test Fuel Pin, kJ/kg	4480	4950	4500
Nodal Max/Min Across 61 Test Fuel Pins**	1.34	1.56	1.33
Ratios of Pin-averaged Fission Power Density			
outermost/center	1.27	1.38	1.26
3rd ring/center	1.14	1.17	1.14
2nd ring/center	1.06	1.07	1.06
1st ring/center	1.02	1.02	1.02
Nodal Max/Avg of Fission Power Density in Outermost Test Fuel Pins	1.05	1.13	1.05

* XSISO 18 multigroup cross sections; single-zone modification with graphite-matrix fuel.

** Twelve nodes in outermost ring of test fuel pins.

spectra used for this collapsing are only approximate representations of spectra that will arise in the modified TREAT-facility reactor, and direct comparison calculations are useful as checks. Table A-3.6 summarizes results of scoping calculations with regard to an earlier, 7 x 7, candidate modification. The reactor modification was for a uniform peak temperature of 1375K throughout the entire modified zone and for Inconel 600. The 18-group optimization was for the reference 19-pin test cluster and test vehicle, but without a cadmium filter. The 48-group calculation then was a k_{eff} calculation for that optimized system; the reactor was not reoptimized. Differences were found to be small except that the 48-group calculation predicted a 0.9% reduction in available reactivity.

Comparison calculations of this type were made also during the early scoping phase of the conceptual design work for a range of core modifications. In each case, the calculated available reactivity for the 48-group case was found to be smaller by $\sim$0.5% to $\sim$1%. Differences in calculated experiment-performance potential (i.e., energy capability and radial power distribution) were small, and the differences in the fission energy generated in the center test fuel pin were largely attributable to a need for a 48-group reoptimization of the uranium concentrations in the modified zone.

A-3.3 Diffusion Theory vs Transport Theory

During the present phase of reactor physics analyses only diffusion-theory calculations have been made. The reference two sets of multigroup cross sections must be modified for transport-theory calculations. In the course of earlier calculations for potential modifications of the TREAT-facility reactor core, and for candidate multizone reactors for a Safety Test Facility, calculations comparing diffusion theory and transport theory indicated that the transport-theory calculations implied: slightly larger available reactivity; somewhat flatter radial distributions of fission power density across the test fuel clusters; and slightly higher magnitudes of fission-energy generation in the center test fuel pin. It is expected that this trend will apply also to the present reference modification of the TREAT-facility reactor core.

A-3.4 Calculated Effects of Heating Reactor Core and Test Fuel

Heating of the reactor core in the course of a safety experiment causes a reactivity loss. The principal contributor to this reactivity loss is the net increased leakage of thermal-energy neutrons from the unmodified zone.

TABLE A-3.6 Comparison of Results of 18-group and 48-group Calculations of 7 x 7 Modification

[Optimized toward 1375K through Modification Zone; 19-pin Test Cluster and Test Section without Cadmium Filter Inconel-600 Can Walls and Heat Shields]

	XSISO 18*	XSISO 48**
Fission Energy Generated in Center of Center Test Fuel Pin, kJ/kg	2600	2660
Nodal Max/Min Across 19 Test Fuel Pins	2.32	2.35
Ratios of Pin-averaged Fission-Power Density		
outermost/center	1.45	1.51
1st ring/center	1.05	1.07
Nodal Max/Avg of Fission Power Density in Outermost Test Fuel Pins	1.59	1.55

* Optimization calculation.

** Direct k_{eff} calculation, using results of XSISO 18 optimization calculation.

The time behavior of the spatial distribution of power density across the reactor will be governed by the preassigned time dependence of the power density in the test fuel cluster and by the detailed reactivity-control distribution in the unmodified zone. To a first approximation the reactivity loss due to heating is the same as the reactivity loss," i.e., initial reactivity control, by those control rods in the unmodified zone that are withdrawn during the course of the safety experiment. Correspondingly, to a first approximation the gross spatial distribution of power density is affected in the same way by the control rods and by the heating. The gross effect is to tilt the power density toward the modified zone of the core and toward the test cluster.

Both of these reactivity-control effects are unaccompanied by local spatial variations in power density. Only two of the control rods are used at any one time for transient control. Heating is non uniform locally, both radially and azimuthally (and axially). The hodoscope slot causes a depression of power density in its general vicinity and a gross tilting of the power density toward the general portion of the reactor that is opposite the slot (see Appendix A-4 for further discussion about effects of the hodoscope slot on the spatial distribution of power density).

Later studies will determine the detailed behavior of the spatial distribution of power density as a function of time during a safety experiment and the associated adjustments in the loadings of uranium in the fuel rods in the modified zone. A first approximation to the spatial redistribution of power density caused by heating was obtained by calculating the cold and hot reactors in an idealized one-dimensional model, without neutron poisoning and without a hodoscope slot. For a system similar to the reference conceptual modified reactor, the largest increase in the power density in the unmodified zone; the plots are for a system utilizing Inconel 600, but the distribution will be quite similar for the system utilizing ARMCO 18 SR.

Correspondingly, there is an increase in the calculated relative fission-energy generation in the test cluster. In reality, for test clusters of the reference sizes and compositions the energy generation in the test cluster is determined predominantly by the fission power densities and the total energy generation in the modified-zone regions, with the largest contribution from the portions of the modified zone that are closer to the test cluster. With this optimization model, optimization to the cold reactor implies that the peak temperatures in the modified zone actually would be reached before the

fuel temperature in the unmodified zone reached its preassigned maximum value. On the other hand, in this model, optimization of the modified zone for conditions of the corresponding hot reactor would result in the peak temperature in the unmodified zone being reached before the modified zone generated its maximum potential energy. Furthermore, optimizing to the hot reactor would require a reduction in the ^{235}U concentrations in the modified zone. This reduction would cost reactivity, and it also would reduce the hardness of the neutron-flux spectrum at the edge of the test cluster.

Continuing, more detailed design studies will be required to investigate the adequacy of the optimization model and to determine an appropriate balance of satisfaction of needs for: reactivity; energy depositions in the center of the test clusters; flatness of the radial distributions of fission power density across the test clusters; the relative (reactivity) importances of the test clusters in regard to potential reactivity increases of test-fuel motions; and the relative reactivity importance of the unmodified zone and needs for negative reactivity feedback upon heating of that zone. These more detailed studies are of the nature of fine tuning.

Heating of the test cluster during a safety experiment will tend to increase the neutronics shielding of the center test fuel pin because a significant fraction of the fissions there will be caused by neutrons in the energy range where there are fission resonances. More of the neutrons in that energy range will be absorbed in the hot test fuel pins surrounding the center pin, because of Doppler broadening of the fission resonances and the ^{238}U capture resonances.

For the reference 19-pin prototypic-enrichment test cluster, preliminary calculations indicate that the heating of the test fuel will cause a reduction of the order of 25% in the relative fission power density in the center test pin at a mean temperature of 2000K in the test cluster (at midheight). In an actual safety experiment the net average reduction will depend upon the variation of temperatures in the test fuel in the surrounding rings during the experiment.

In the presence of a thick UO_2-stainless steel inner zone in the modified reactor, this effect of heating of the test fuel would be smaller. Nevertheless, for prototypic-enrichment test fuel pins the calculations indicate that the potential energy deposition in the center test fuel pin will be much greater if there is a full graphite-matrix modified zone, plus a cadmium

filter, rather than a full UO_2-stainless steel modified zone or a two-zone modification.

For a 61-pin test cluster of fully enriched UO_2 it is expected that there might be a significant but smaller reduction in the calculated potential energy deposition in the center test pin when these effects of heating of the test fuel are included. The use of a UO_2-stainless steel inner zone in the reactor would diminish this percentage reduction. The detailed design studies of reactor modification must take this effect into consideration in evaluating the relative merits of a full graphite-matrix zone and the merits of a two-zone system for safety experiments with fully enriched test fuels.

A-3.5 Spectra of Multigroup Neutron Flux in Test Fuel Clusters

As discussed in Appendix A-1, the purpose of hardening the neutron spectrum at the outer edge of the test fuel clusters is to reduce the radial spike in the distribution of fission power density in the test fuel cluster. Use of a high-temperature UO_2-stainless steel inner zone, in a two-zone modification, or use of a full UO_2-stainless steel modified zone, will flatten the radial distribution of power density to an overall max/min of 1.05 or less. Even for a peak normal operating temperature of 1375K in the modified fuel, and even for a 9 x 9 modified zone, the core modification with a full graphite-matrix zone will not harden the neutron flux sufficiently to yield very flat distributions across the test cluster. A cadmium filter is very effective in providing additional flattening at a small net cost in reducing the fission-energy generation in the center pin of a cluster of 19 prototypic-enrichment test fuel pins. For test pins without plutonium, the radial distributions of power density are much flatter even without a cadmium filter. The cadmium filter is of value in flattening further, but to obtain even flatter distributions other filters would be needed that would cause large reductions also in the power density in the center test fuel pin.

The effectiveness of the cadmium in filtering neutrons entering the 19-pin PuO_2-UO_2 test cluster lies in its removal of neutrons with energies in the vicinity of 0.3 eV, which is the peak energy for a very important fission resonance of ^{239}Pu. There is a sufficiently high flux of neutrons in the modified zone, in that neutron-energy range, to cause a large power spike in the outer rings of test fuel pins if no filter is used. For the 61-pin cluster of test fuel pins containing only fully enriched UO_2 (no plutonium), the spectrum in the modified zone is hardened enough to reduce the magnitude of

the power spike arising from very soft neutrons in the unmodified reactor. There remains a large band of neutron energies where the fission resonances in the ^{235}U are the cause of a persisting radial gradient in fission power density across the test cluster. To provide more detailed background information on these effects, a breakdown of the spectral distributions of fission events is given in Table A-3.7. The cases summarized are: 19 prototypical-enrichment advanced-oxide test pins, with and without a cadmium filter, in a reactor optimized for a 19-pin cluster plus the cadmium filter; and 61 enriched-UO_2 FTR/CRBR-size test pins, with and without a cadmium filter in that reactor, with a thinning of the first region of the modified zone to provide space for the 61-pin test vehicle. As a reference point, approximately 95% of the fission events at the position of peak power density in the unmodified zone occur in neutron energy groups 15 through 18.

Most of the data in Table A-3.7 was obtained for the earlier reference calculations, utilizing Inconel 600. Comparison data are included for the new reference modification, utilizing ARMCO 18 SR.

A-3.6 Calculated Experiment Performance Potentials for Smaller Clusters of Fully Enriched UO_2 Test Fuel Pins in 61-pin Test Section

For a system with Inconel 600, calculations were made for 19- and 37-pin clusters of FTR/CRBR-size, fully enriched UO_2 test fuel pins. The model of approximation is that only the test cluster is reduced in size and that sodium fills the space left by removal of test fuel pins. This model is acceptable for a scoping study if the gross 61-pin test section is used without reduction in the thickness of the primary vessel.

Table A-3.8 summarizes the calculated experiment-performance potential for these smaller test clusters and, for convenience of reference, also the potential for the 61-pin cluster. In each case, a cadmium filter was included.

A-3.7 Optimizations for Smaller Modification Zones and for Higher Peak Temperature in the Outermost Ring of Modified Fuel Assemblies (Single Zone; Graphite-Matrix Fuel)

For a system with Inconel 600, studies were made of the effects on available reactivity and on experiment-performance potentials if smaller modified zones were chosen. The reference test configuration was the 19-pin cluster (prototypic-enrichment fuel) in the 19-pin test section, plus a cadmium filter. In one study the modification zone was reduced to the central 7 x 7 array; the outermost ring of modified fuel assemblies was optimized to

TABLE A-3.7 Normalized Spectral Distributions of Fission Density in Reference Test Fuel Clusters*

		INCONEL 600								ARMCO 18 SR	
		Normalized Spectrum in 19-pin Cluster				Normalized Spectrum in 61-pin Cluster				Normalized Spectrum in 19-pin Cluster	
Neutron Energy Group	Lower Bound of Energy, eV	Outermost Node		Central Node		Outermost Node		Central Node		Outermost Node	Central Node
		Filter	No Filter	Filter	No Filter	Filter	No Filter	Filter	No Filter	Filter	Filter
1	1.653×10^6	0.0389	0.0236	0.0519	0.0533	0.0327	0.0285	0.0515	0.0522	0.0372	0.0500
2	4.979×10^5	0.0507	0.0303	0.0658	0.0664	0.0692	0.0595	0.1009	0.1013	0.0483	0.0631
3	1.500×10^5	0.0378	0.0223	0.0486	0.0485	0.0700	0.0595	0.0976	0.0969	0.0360	0.0465
4	4.087×10^4	0.0365	0.0213	0.0463	0.0456	0.0753	0.0632	0.1006	0.0987	0.0348	0.0444
5	1.503×10^4	0.0193	0.0112	0.0244	0.0239	0.0437	0.0365	0.0569	0.0555	0.0200	0.0254
6	5.531×10^3	0.0233	0.0134	0.0289	0.0281	0.0523	0.0434	0.0630	0.0610	0.0230	0.0287
7	2.035×10^3	0.0185	0.0106	0.0216	0.0210	0.0357	0.0295	0.0352	0.0339	0.0181	0.0212
8	7.485×10^2	0.0621	0.0355	0.0760	0.0736	0.1219	0.1003	0.1252	0.1203	0.0602	0.0741
9	2.754×10^2	0.0637	0.0363	0.0755	0.0728	0.1042	0.0854	0.0857	0.0820	0.0619	0.0737
10	1.013×10^2	0.1116	0.0635	0.1117	0.1075	0.1230	0.1005	0.0743	0.0708	0.1093	0.1100
11	3.727×10^1	0.2113	0.1200	0.1798	0.1727	0.0836	0.0681	0.0605	0.0576	0.2100	0.1794
12	1.371×10^1	0.1220	0.0691	0.0852	0.0817	0.720	0.0586	0.0576	0.0546	0.1242	0.0872
13	5.043	0.1272	0.0720	0.1132	0.1083	0.0355	0.0288	0.0309	0.0293	0.1336	0.1194
14	1.855	0.0419	0.0237	0.0508	0.0485	0.0352	0.0285	0.0354	0.0334	0.0446	0.0544
15	0.4485	0.0317	0.0454	0.0203	0.0469	0.0445	0.0866	0.0248	0.0521	0.0348	0.0224
16	0.1198	0.0035	0.3669	0.0001	0.0003	0.0010	0.0975	-	0.0004	0.0039	0.0001
17	0.04987	-	0.0291	-	0.0007	-	0.0210	-	-	-	-
18	0.004742	-	0.0057	-	-	-	0.0048	-	-	-	-
Total**		0.9998	0.9999	1.0001	0.9998	0.9998	1.0002	1.0001	1.0000	0.9999	1.0000

* Cold (300K) reactor and test cluster; midheight of fuel rod. The entry for a given energy group and for a given space location is the fraction of fission density at that location that is due to fissions by neutrons in that neutron energy group.

** Rounded off, group by group.

TABLE A-3.8 Calculated Experiment Performance Potentials for Test Clusters of 19 to 61 Pins of Fully Enriched UO_2 in Reference 61-pin Test Section* (Calculations Performed with Inconel 600)

	19 Pins	37 Pins	61 Pins
Fission Energy Generated in Center of Center Test Fuel Pin, kJ/kg	6410	5280	4480
Nodal Max/Min Across Test Cluster**	1.14	1.24	1.34
Ratios of Pin-averaged Fission Power Density			
4th ring/center	N/A	N/A	1.27
3rd ring/center	N/A	1.18	1.14
2nd ring/center	1.09	1.08	1.06
1st ring/center	1.03	1.02	1.02
Nodal Max/Avg of Fission Power Density in Outermost Test Fuel Pins	1.04	1.05	1.05

* XSIS018 multigroup cross sections; single-zone modification with graphite-matrix fuel, plus cadmium filter.

** Twelve nodes in outermost ring of test fuel pins.

TABLE A-3.9 Effects on Performance of using Smaller Modified Zones

Size of Modified Zone	Change in Available Reactivity in Cold Reactor	Change in Fission-energy Generation in Center Test Fuel Pin
9 x 9 (reference)	0	0
7 x 7	+ 1.1%	-13%
5 x 5	+ 1.5%	-24%

1125K and the balance of the assemblies to 1375K.

By comparison with the corresponding 9 x 9 modification:

1. The calculated reactivity is higher in the 7 x 7 array, by 1.4%.
2. The calculated fission-energy generation in the center test pin is ∿15% smaller, with the 7 x 7 array.
3. The flatness characteristics of the radial distribution of fission power density across the 19-pin test cluster are almost identical, for the 9 x 9 or 7 x 7 array.

Other scoping studies were made for a modified zone with Inconel 600, optimized throughout to 1375K and without a cadmium filter. In these cases there were somewhat larger changes in the flatness characteristics of the radial distribution of fission power density across the 19-pin test cluster, but it is expected that these changes would be diminished by inclusion of a cadmium filter. The principal remaining effects would be on reactivity and relative reactivity importance of the unmodified zone (larger for smaller modified zones), and on the energy generation in the center test fuel pin.

Some results are summarized in Table A-3.9.

Optimization of a 9 x 9 modification zone with or without a cadmium filter yielded the same calculated available reactivity (to within 0.1%). Optimization of a 9 x 9 modification zone to ∿1375K (1100°C) throughout was calculated to increase reactivity by 1.9%, in comparison with an optimization to a reduced peak temperature of ∿1125K (850°C) in the outer ring of modified fuel assemblies; this reactivity change would be approximately the same for the new reference system with ARMCO 18 SR.

The changes in calculated flatness characteristics across the test cluster are small, and there is only a 2% increase in the potential energy generation in the center test pin, with the increased peak temperature in the outer fuel assemblies.

A-3.8 Data of Neutron Kinetics with Graphite-matrix 9 x 9 Modification

Starting with the clean, cold system in an idealized configuration where there is no hodoscope slot and no control rods are inserted, the reactivity effect of heating the reactor was calculated using ARMCO 18 SR. A 19-pin test cluster was included. The available multigroup cross sections are limited at temperatures above 300K. The calculational choices were: a uniform temperature of 800K (527°C) in the unmodified zone, and a uniform temperature of 1200K (927°C) in the modified zone. The assumption of 800K uniformly in

the unmodified zone is believed to be a good representation, in reactivity change, of an actual nonuniform temperature with a peak of 873K (600°C). The understatement of the temperature change in the modified zone has a small effect on the calculated reactivity loss of 3.8% upon heating. (The value was 3.4%, for Inconel 600.) This compares with a calculated reactivity loss of 5.9% upon a uniform heating of the unmodified fully loaded reactor, with a 19-pin test cluster, to 800K.

The mean prompt-neutron generation time, Λ, was calculated for the reference modified reactor, using the technique of adding an α/v absorber uniformly in all regions of the modified reactor, determining the reactivity change ($\Delta\rho$), and using the formula $\Lambda \sim -\Delta\rho/\alpha$. The result: $\Lambda \sim 4.6 \times 10^{-4}$ s. (This value was $\sim 4.2 \times 10^{-4}$ s for Inconel 600.)

Both the reactivity effect of heating and the value of Λ were calculated a for the same idealized reactor state. For that state, and assuming that approximately one-half of the total reactivity change in heating can be added, above prompt criticality, to initiate a pure burst, the inferred value of the initial asymptotic reactor period is 4.6×10^{-4} s/(1/2 x 0.038), or about 24 ms. A similar analysis for the fully loaded unmodified reactor, with a 19-pin test cluster, yielded: $\Lambda \sim 6.8 \times 10^{-4}$ s and an initial asymptotic reactor period of 6.8×10^{-4} s/(1/2 x 0.059) or $\sim$23.0 ms.

This comparison indicates that the kinetics characteristics for pure bursts in the modified reactor will be quite similar to the corresponding kinetics characteristics of the unmodified reactor.

A-3.9 Estimated Needs and Supply of Available Excess Reactivity

Appendix A-1 includes a brief discussion of estimated needs for available excess reactivity in the cold reactor. The estimated total is 11%. Of this, 3 to 4% is needed for the hodoscope slot, based on an estimated reactivity loss of 3 to 4% for the new full-height single slot in the present, unmodified reactor. It is expected that the slot in the modified reactor will cause a smaller net loss in reactivity, but a margin is included for possible local adjustments to minimize possible power spikes due to streaming of thermal neutrons in the slot.

A reactivity loss of 3.8% was calculated in heating the unmodified zone uniformly to 800K (527°C) and heating the modified zone. The one-dimensional calculation was for a clean fully loaded reactor without control rods. This is the present reference estimate for the maximum reactivity required to

compensate for heating during safety experiments, excluding effects of spatial redistributions of test materials.

A total of ∿4% is allowed for uncertainties in the conceptual design analyses and for an operating margin. Comparison calculations of the original minimum-critical loading of the TREAT-facility reactor indicated that the XSIS018 multigroup cross sections, plus one-dimensional diffusion theory, overestimated available reactivity by 3%. A portion of this difference may be due to uncertainties in the detailed composition of the reactor core and the radial reflector that influence the critical loading. A number of thermocouple-instrumented fuel assemblies were included in the reactor core. Their effect on reactivity is not accurately known. It is expected, however, that these assemblies will also be used in the upgraded core. This type of uncertainty applies also to analyses of the available reactivity of recent reactor loadings.

Other uncertainties in the calculation of the reactivity of the modified reactor arise from the present modeling of the geometrically and neutronically complex configuration of the modified fuel assembly as equivalent to a volume-averaged ("smeared") composition. Conceivably this total reactivity allowance of 11% might be insufficient. There is a reactivity margin of 2% in the reference modified single-zone reactor, since the calculated reactivity is 13%. Use of a UO_2-stainless steel inner modified zone in some safety experiments with enriched-fuel test clusters is calculated to reduce reactivity (by ∿2.5%, if the central 5 x 5 array is reloaded with UO_2-stainless steel fuel). Candidate means for increasing the available reactivity are: to design for a temperature higher than 1125K (∿850°C) in the outermost ring of fuel assemblies in the modified zone; and/or to design to a smaller modified zone, at a cost of some reduction in energy generation in the center test fuel pin, and with a loss in flexibility for potential two-zone loadings. Smaller reactivity gains could be realized by loading more heavily loaded driver fuel assemblies into the cooler peripheral regions of the unmodified zone as "spike" assemblies.

Restating, the reference modification is a 9 x 9 array, single zone of graphite-matrix fuel optimized to a 19-pin reference test cluster and test vehicle with a cadmium filter. In the 7 x 7 center the peak modified fuel temperature is 1375K; in the outermost ring of the modified fuel assembly, it is 1125K. The calculated available reactivity of this configuration, with a

fully loaded core, at ambient temperature is 13%, with ARMCO 18 SR cans and heat shields. Replacing the 19-pin reference with a 61-pin vehicle reduced reactivity slightly (0.3%) in spite of the use of 61 pins of fully enriched UO_2, because of the effects of fuel displacement in the modified zone and increased volume of steel in the 61-pin vehicle. A reduction of the size of the test cluster to 19 fully enriched UO_2 test pins in the 61-pin vehicle would cost an additional 0.4% in reactivity, with this idealized model of a clean unpoisoned reactor.

A-3.10 Reactivity Effects of Modeled Compactions of Test Fuel Cluster of 91 FTR/CRBR-size Pins of Fully Enriched UO_2

In safety experiments with test clusters of high total fissile mass, there is a potential for nontrivial reactivity changes during the experiment arising from spatial redistributions of test materials. The overall spatial redistribution usually encountered is a dispersal, i.e., the removal of fuel to locations of lower average reactivity worth, thereby causing a loss in reactivity. A restoration of this anticipated loss in reactivity must be considered to be one of the needs for available reactivity in the reactor in order to continue the planned safety experiment to its designated completion. On the other hand, if at the same time during the safety experiment there were to be a redistribution of test fuel to locations of increased average reactivity worth, i.e., a "compaction" of the test fuel, then there must be mechanisms for compensating for this reactivity increase. One mechanism is the inherent net negative reactivity feedback upon heating of the reactor, especially the unmodified zone. Another mechanism is the response of servo-controlled control rods. To obtain an initial perspective on the possible severity of effects of test-fuel compaction, calculations were performed in the model by means of two-dimensional (r,z) diffusion theory.

The compaction model adopted is similar to the model used in the corresponding analysis for STF. Compaction is viewed as occurring in two steps. First, all of the materials in the test cluster (fuel, cladding, wire wrap, and sodium) are smeared with all other materials in the volume (V) defined by the inner diameter of the primary vessel, radially, and by the original active height of the uncompacted configuration, axially. The top and bottom axial reflectors/ blankets of the test cluster are assumed to be unaltered, including sodium there initially. (Thus, for "zero" compaction there is this first step of smearing out of all materials radially; in this

procedure there is a distinction between uncompacted and "zero" compaction.) For 100% compaction, it is modeled that the UO_2 fills a cylinder of volume V_o with mass equal to the total mass of UO_2 in the test cluster and with density equal to 79% of the theoretical density of the UO_2. "Fifty-%" compaction is defined to be the movement of 50% of that UO_2 in the Volume $V_i \equiv V - V_o$ into the volume V_o, and the corresponding displacement of non-UO_2 materials from V_o to V_1. Other percentages of compaction are defined analogously.

In these calculations it has been assumed as a limiting case that a test cluster as large as 91 FTR/CRBR-size pins, with fully enriched UO_2 fuel, is being utilized in a safety experiment involving gross fuel redistributions. The reactor state is modeled as a configuration of a 9 x 9 reference array of modified fuel assemblies, with graphite-matrix fuel, at high temperature. Within the limitations of the geometry models it was not feasible to include effects of the hodoscope slot. Therefore, to assign a reasonable relative importance to the test cluster, a one-dimensional calculation was made to determine a reduced thickness of the unmodified zone for which the calculated k_{eff} would be reduced to 1.05. This same thickness was used in the two-dimensional calculations, which indicated a slightly lower value of k_{eff}. To permit use of the 18-group set of neutron cross sections in the two-dimensional calculations it was necessary to compromise on the models of temperatures in the various zones. The temperature in the unmodified zone was modeled as 1200K uniformly, the closest to 800K that was available. A correspondingly high temperature of 2000K was chosen for the modified zone. Note that if the preferred models of lower temperatures could have been followed, then the selected value of the reduced thickness of the unmodified zone would have been larger to obtain $k_{eff} = 1.05$, with the net result that the calculated reactivities of test-fuel compactions would have been almost the same.

For the reference single-zone modification, two sets of calculations were made. In one set, a cadmium filter was not included in the test vehicle. In the other set of calculations, a cadmium filter was assumed to be present. The reactivity changes as a function of percentage compaction are listed in Table A-3.10 as calculated for the modified system utilizing Inconel 600. These reactivity effects would be approximately the same for a system utilizing ARMCO 18 SR.

Appendix A-4 includes results of compaction calculations for the case of a candidate two-zone modification of the reactor core with a UO_2-stainless steel inner zone.

TABLE A-3.10 Reactivity Effect of Modeled Compactions of 91-Pin Test Fuel Cluster of Fully Enriched UO_2 (Calculations Performed with Inconel 600)

Percentage Compaction	Reactivity Change, % Cadmium Filter Present	No Cadmium Filter
Uncompacted	0 (Reference)	0 (Reference)
0	0.13	0.23
25	0.19	0.32
50	0.20	0.35
75	0.16	0.30
100	0	0.04

A-3.11 Radial Distribution of Fission Power Density Across the Reactor at Axial Midheight

In the present unmodified reactor, the insertion of the test vehicle and test cluster causes a local depression in the fission power density in surrounding fuel assemblies. This depression essentially damps out within the first ∿0.2 m in the cold reactor. When a graphite-matrix modified zone is introduced, there is little depression in the power density in the unmodified zone at the interface with the modified zone. Grading the uranium concentration in the modified zone from fuel rod to fuel rod, each ∿23 mm thick, introduces gradients of fission power density across fuel rods that are of the order of 10% except in fuel rods near stronger discontinuties, such as the unmodified zone and the cadmium filter. In the vicinity of the unmodified zone a 15% gradient across the rod is calculated. In the first region of the modified zone, near the cadmium filter, the calculated gradient is ∿30% in 23 mm. Figures A-3.1 and A-3.2 illustrate the radial distribution of fission power density in the modified zone and in the driver zone, respectively, per unit volume of fuel, normalized to unit peak density in the cold clean unmodified zone; the plots are for a system utilizing Inconel 600, but the distribution will be quite similar for the system utilizing ARMCO 18 SR.

The actual corresponding radial distribution of absorbed-energy density will be somewhat different. Some of the gammas produced in fission will be absorbed by structural material rather than fuel. In addition, capture gammas have different spatial distributions of production and subsequent absorption. Some of the energy is generated in slowing down of neutrons, and

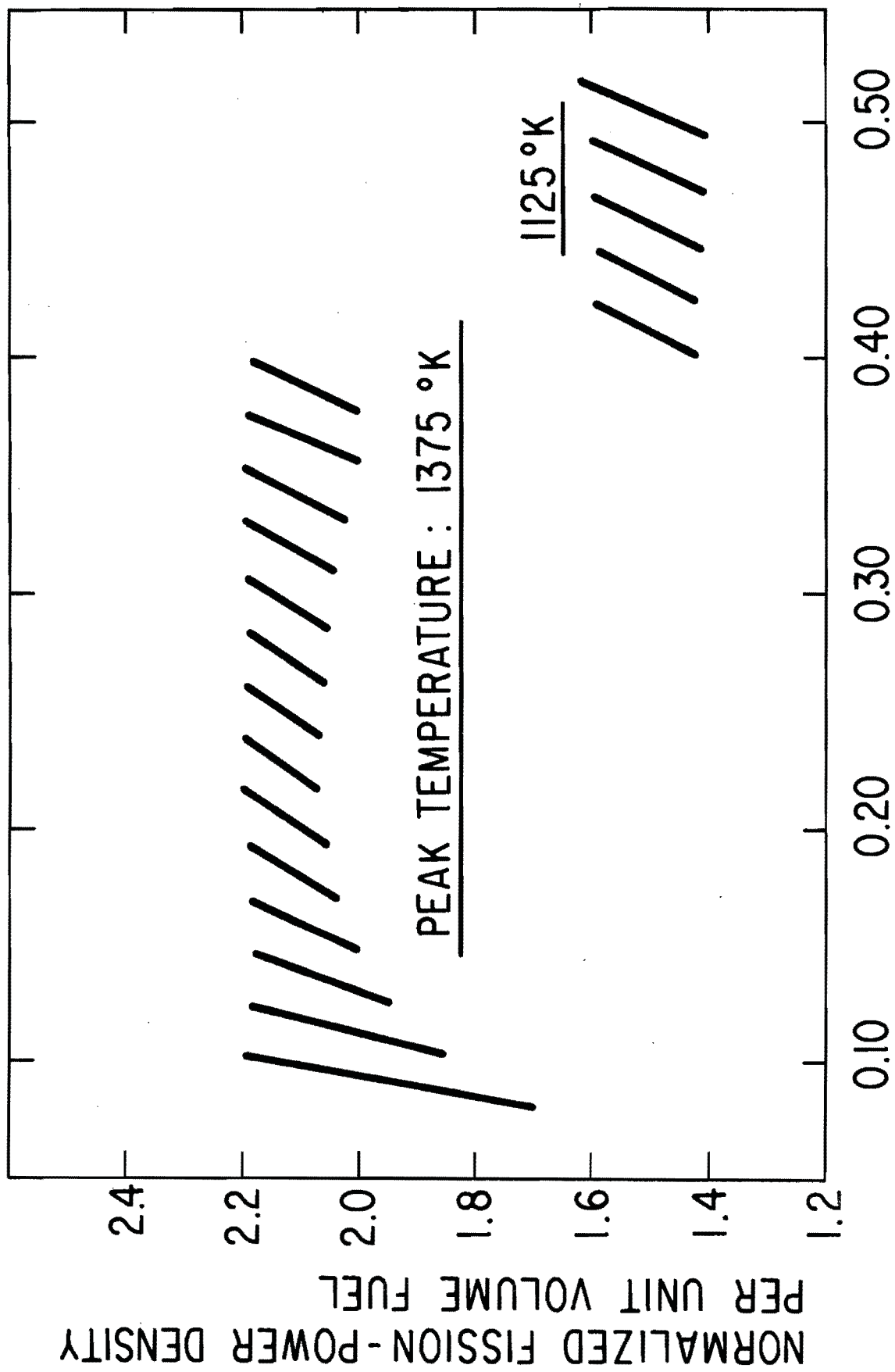

A-3-1 Normalized Radial Distribution of Fission Power Density Per Unit Volume of Fuel in Modified Zone of Reactor

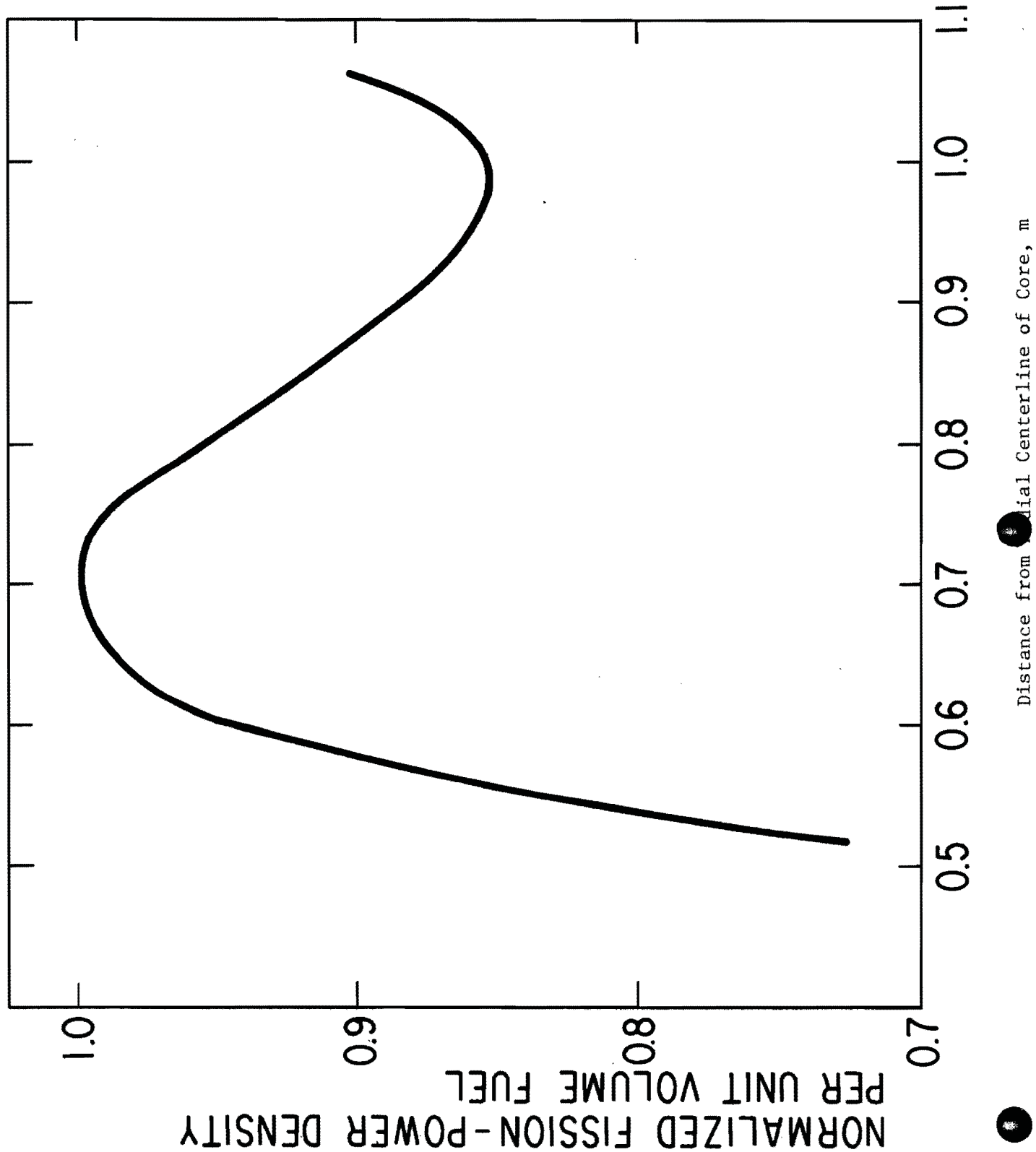

A-3-2 Normalized Radial Distribution of Fission Power Density Per Unit Volume of Fuel in Unmodified Zone of Reactor

neutrons and gammas typically travel considerable distances before such events occur. Approximately, however, the distribution of absorbed-energy density is proportional to the distribution of time-integrated fission power density. If it is assumed further that the distribution of time-integrated fission power density is proportional to this calculated distribution of fission power density, and that heating is adiabatic, then all preassigned peak temperatures in the reactor fuel are reached simultaneously in a maximum transient. If the fuel in the unmodified zone is taken to a peak of ∿875K (600°C), then the peak temperatures in the modified zone are ∿1125K (∿850°C) in the outermost ring of fuel assemblies, and ∿1375K (∿1100°C) in the rest of the modified fuel assemblies. This is the optimization model for the modification. In the more detailed design this model will be revised to reflect the realities of neutron and gamma transport and capture-gamma production and transport.

APPENDIX A-4
Additional Scoping Calculations

This Appendix has four general areas of discussion and data:

1. Candidate alternative design options for the modification of the reactor, including:
   a. optimization of the modified zone for a reference 19-pin test without a neutron filter, instead of with a cadmium filter;
   b. use of a boron filter, instead of cadmium;
   c. two-zone modification, with a UO_2-stainless steel inner zone and the same reference graphite-matrix fuel assemblies in the outer zone,
   d. three-zone modification, with graphite-matrix innermost and outermost zones and a UO_2-stainless steel middle zone.
2. Azimuthal tilting of power density due to the hodoscope slot.
3. Comparisons between the reference (single-zone) modified reactor and the present unmodified TREAT-facility reactor, including:
   a. results of highly simplified calculations comparing reactivity-control effectiveness;
   b. experiment-performance characteristics.
4. Results of earlier calculations for a different test cluster and vehicle, and for a different modified fuel assembly, illustrating effects of variations in neutronics models and multigroup parameters.

A-4.1 Optimization without Neutron Filter

The reference optimization includes the use of a cadmium neutron filter near the 19-pin test cluster. The cadmium filter affects the neutron-flux spectrum and causes a localized relative depression in power density in nearby regions in the modified zone when it is present. The optimization restores the power density by increasing the region-by-region concentrations of fully enriched uranium. If, then, a safety experiment were to be conducted without a cadmium filter, it is expected that the potential energy generation in the center of the test cluster would be limited by the increases in the relative power density in the first few regions of the modified zone.

On the other hand, if the modified zone were to be optimized to a test without a neutron filter and then a filter was included, the modified fuel near the test cluster would not reach its peak acceptable fuel temperature in

a maximum transient, and there would be some reduction in the potential energy generation in the center of the test cluster. The relative magnitudes of the fission energy generated in the center test fuel pin in these two types of optimizations have been examined in a limited study of a system utilizing Inconel 600. An optimization was made for a modification without a filter, and then a cadmium filter was introduced. The results for these two cases were compared with the reference optimization in which filter was included. The comparison indicates that:

1. The neutron-flux spectrum at the inner edge of the modified zone is sufficiently hardened, and also there is sufficient shielding of the center test fuel pin by the outer two rings of fuel pins in the 19-pin cluster, so that there is only a 2% net loss in the fission-energy generation in the center pin, by comparison with optimization including the filter.

2. The calculated gross radial nodal max/min ratio across the cluster, of fission power densities with a cadmium filter is slightly higher (1.27 vs. 1.26) when the initial optimization is to a system without a filter.

In the more detailed design the optimization basis will be reevaluated, with tradeoff studies of the relative merits of optimizing to various test clusters and to various test-vehicle configurations.

A-4.2 Optimization with a Boron Neutron Filter Instead of Cadmium

Optimization calculations were made with boron filters rather than with a cadmium filter. In these calculations the boron was modeled as uniformly distributed within the (instrumentation) gap between the primary vessel and the secondary vessel of the test vehicle. This corresponds to the model of the cadmium filter. Diffusion-theory calculations were run with the standard XSISO 18 multigroup set of neutron cross sections. In this application, optimization with transport theory rather than diffusion theory is not expected to have a large effect on the comparative results of relative energy generation in the center test pin.

Table A-4.1 summarizes comparison results for optimization studies with: (a) no filter; (b) cadmium filter; (c) boron filter for various concentrations of boron. In each case the reference 19-pin cluster and test vehicle were included; the modified zone was the reference 9 x 9 array; the optimization was a full optimization of the modified zone. The calculated available reactivity of the modified system was very nearly constant, regardless of the concentration of boron, the use of cadmium, or the complete absence of a neutron

TABLE A-4.1 Calculated Experiment-performance Characteristics for 19-pin Test Cluster as Functions of Neutron Filter in Associated Optimized Modified Reactors* (Inconel-600 Can Walls and Heat Shields)

	No Filter	Cadmium Filter	Boron Filter, Concentration: 10^{30} atoms/m^2** 3.0×10^{-3}	5.0×10^{-3}	7.0×10^{-3}
Fission Energy Generated in Center of Center Test Fuel Pin, kJ/kg	2535	2360	1990	1805	1670
Nodal Max/Min Across 19 Test Fuel Pins***	2.26	1.26	1.42	1.31	1.25
Ratios of Pin-averaged Fission Power Density					
outermost/center	1.44	1.17	1.20	1.17	1.14
1st ring/center	1.05	1.05	1.04	1.04	1.04
Max/Avg. of Fission Power Density in Outermost Test Fuel Pins	1.57	1.07	1.18	1.12	1.09

* In each case the optimization was for 9 x 9 modified zone: 1125K in outermost ring of modified fuel assemblies; 1375K in the balance of the modified zone. XSISP18, diffusion-theory calculations of cold clean system. The modified zone is fueled with graphite-matrix fuel rods throughout.

** The "concentration" is the smeared boron atom concentration, in the instrumentation gap, times the thickness of the gap.

*** Twelve spatial nodes in the outermost test fuel pins.

filter. The systems studied utilized Inconel-600 can wall and heat shields for the modified fuel assemblies.

A-4.3 Two-zone Modification with UO_2-stainless Steel Inner Zone

The reference 9 x 9 modified zone provides enough space for possible substitution of assemblies with UO_2-stainless steel fuel rods in place of graphite-matrix-fuel modified assemblies in a central portion. Full UO_2-stainless steel modified fuel assemblies would replace full graphite-matrix modified fuel assemblies. Special partial fuel assemblies would be used to minimize the gap outside the secondary containment of the test vehicle. Similar to the graphite-matrix-fuel modified fuel assemblies, each UO_2-stainless steel assembly would contain an aggregate of individual fuel rods, with grading of the concentration of fully enriched UO_2 from fuel rod to fuel rod as appropriate to their locations in the reactor core. With UO_2-stainless steel modified fuel elements inside the central 5 x 5 array, a very hard neutron-flux spectrum is approached at the inner edge of the UO_2-stainless steel zone. The reference concept now is to replace only the graphite-matrix fuel assemblies in the inner portion of the full graphite-matrix modified zone, rather than reload the entire 9 x 9 central array with modified fuel assemblies optimized fully to the inclusion of the UO_2-stainless steel inner zone.

Calculations have been made for two-zone systems with Inconel 600 cans and heat shields, based on a central 5 x 5 zone with UO_2-stainless steel, and with the outer two rings of modified graphite-matrix fuel assemblies unchanged from the single-zone specification. Additional calculations have been run with ARMCO 18 SR cans and heat shields, both for a choice of returning the modified graphite-matrix assemblies and also for a new, fully optimized two-zone modification.

Table A-4.2 presents calculated results for cases where only the UO_2-stainless steel is reoptimized rather than the entire two-zone system. The central 5 x 5 array is filled with the UO_2-stainless steel assemblies around the test vehicle. A comparison is included of reactivity and experiment-performance characteristics in the 61-pin reference test cluster of enriched UO_2, for a full graphite-matrix modified zone. The assumed peak temperature of the UO_2-stainless steel fuel is 1375K ($\sim$1100°C). As noted, there was an increase in calculated available reactivity of 1.5%, to 10.5%, when ARMCO 18 SR is used for can walls and heat shields through the modified zone.

Table A-4.2 Comparison of Reference Modification with Two-zone Modification (UO_2-stainless steel Inner Zone)* (61-pin Test Cluster of Fully Enriched UO_2)

	Inconel 600		ARMCO 18 SR
	Reference Single-zone (9 x 9) Modification	Two-zone (9 x 9) Modification**	Two-zone (9 x 9) Modification**
Calculated Available Reactivity, %	10.6	9.0	10.5
Fission Energy Generated in Center Test Fuel Pin, kJ/kg	4500	2880	2815
Nodal Max/Min*** Across 61-pin Cluster	1.33	1.05	1.05
Ratios of Pin-averaged Fission Power Density			
4th ring/center	1.26	1.04	1.04
3rd ring/center	1.14	1.02	1.02
2nd ring/center	1.06	1.01	1.01
1st ring/center	1.02	1.00	1.00
Max/Avg of Fission Power Density in Outermost Test Fuel Pins	1.05	1.01	1.01

* XSIS018; only the inner, UO_2-stainless steel zone, is optimized for the two-zone system.

** UO_2-stainless steel inner modified zone extending to outer boundary of central 5 x 5 array.

*** Twelve spatial nodes in the outermost test fuel pins.

The available reactivity is increased if also the graphite-matrix outer zone is modified in a two-zone modification. For the two-zone modification with a 5 x 5 inner zone and with ARMCO 18 SR cans and heat shields, the calculated reactivity was increased by 1.8%, to 12.3%. This reoptimized system was calculated to have a potential energy deposition of 3035 kJ/kg in the center of the test cluster, an increase of almost 8% over the value (2815 J/g) reported in Table A-4.2, for a system where only the UO_2-stainless steel inner zone was optimized.

The predominant potential interest in using a UO_2-stainless steel inner zone is to attain much flatter radial distributions of fission power density across test clusters with fully enriched test fuel pins. Earlier, scoping calculations on modifications to a full UO_2-stainless steel single zone, or to a two-zone modification with a UO_2-stainless steel inner zone, have shown that the neutron-flux spectrum in the test cluster is so hardened that, to a good approximation, the fission-energy generation is directly proportional to the total concentration (atoms/m^3 fuel) of fissile nuclides. In this environment, therefore, there would be very low energy generation in a prototypical-enrichment test cluster.

Calculations have been made (two-dimensional r,z) to obtain estimates of reactivity effects of modeled compactions of a test cluster of 91 UO_2 fuel pins. The UO_2 is enriched fully in ^{235}U. In an earlier evaluation of compaction, a two-zone system utilizing Inconel-600 can walls and heat shields was calculated. The model of compaction within the test vehicle is discussed in Appendicies A-2 and A-3. For that two-zone system, however, the thickness of the unmodified zone was kept the same as for the study of compaction with a graphite-matrix single-zone modification. Consequently, the worth of the test cluster was considerably overstated. Nevertheless, the maximum calculated reactivity effect was only 0.6% at 100% compaction. For smaller percentages of compaction the reactivity increase was smaller. The calculated reactivity increase was a monotonically increasing, almost linear function of the modeled percentage compaction.

New calculations of compaction effects have been made for a two-zone system with ARMCO 18 SR instead of Inconel 600. In the new calculations, the model of the effective reactor state that was used for compaction calculations with a full graphite-matrix modified zone was followed. Specifically, the reactor was assumed to be at high temperatures, and the thickness of the

unmodified zone was chosen so as to make k_{eff} = 1.05 (one-dimensional calculation). The selected thickness was the same as the standard thickness in this case, i.e. the outer radius of the core was 1.065 m in the one-dimensional calculation. For this model, 100% compaction was calculated to increase reactivity by only 0.3%. Again, the reactivity change calculated was almost linear with the percentage compaction.

For comparison with compaction calculations for a single-zone, graphite-matrix modification see Table A-3.10.

A-4.4 Three-zone Modifications

A brief study has been made of the reactor physics and experiment-performance features of three-zone modifications. The stimulus for this study was to increase the potential for energy deposition in enriched test clusters by comparison with a two-zone modification. The tradeoff is a radial distribution of power density across the test fuel cluster that is not quite so flat. An alternative would be to use a thinner UO_2-stainless steel zone in a two-zone modification.

The three-zone system features an outermost zone of graphite-matrix fuel, a middle zone with UO_2-stainless steel fuel, and an innermost zone of graphite-matrix fuel. The outermost zone buffers the reactor from the large reactivity loss that would occur if the UO_2-stainless steel zone extended to the unmodified zone. It provides also an initial hardening of the neutron-flux spectrum. The UO_2-stainless steel middle zone hardens the spectrum very substantially. The innermost zone acts to remove a lingering component of low-intermediate-energy neutrons that traverse the UO_2-stainless steel from the outer portions of the reactor, thereby reducing the power density in the outer rings of test fuel pins. It also softens somewhat the very high energy portion of the flux spectrum, thereby increasing the probability for fission in the center test fuel pin.

Comparison calculations have been made for two-zone systems, varying the thickness of the UO_2-stainless steel inner zone and keeping the modification boundary at the 9 x 9 boundary. In each of the two-zone and three-zone calculations, the entire modification zone was optimized. ARMCO 18 SR can walls and heat shields were utilized. The results are:

(1) For a given flatness of the radial distribution of power density across the reference test cluster of 61 pins of fully enriched UO_2, the three zone system offers a higher potential for energy deposition in the center pin

than the two-zone system. The calculated percentage increase is ∿15% for nodal max/min in the range 1.1 to 1.2 in the test cluster.

(2) The calculated reactivity of the three-zone system reaches its maximum at the limit of a zero-thickness innermost zone, i.e., at the limit of a two-zone system, if the inner two zones extend to the outer boundary of the 5 x 5 central array. As the thickness of the innermost zone increases, the flatness across the test cluster decreases. At a nodal max/min of ∿1.20 across the test cluster, the calculated reactivity is 11.7% (vs 12.3% for the fully optimized two-zone system).

(3) As the thickness of the UO_2-stainless steel zone in the two-zone system is reduced, reactivity, energy deposition, and nodal max/min increase. The calculated reactivity of the two-zone system is 12.3% when the UO_2-stainless steel inner zone extends to the 5 x 5 boundary. This compares with 13.1% for the full graphite-matrix modification

A-4.5 Azimuthal Tilting of Power Density Due to the Hodoscope Slot

The presence of the single hodoscope slot will induce azimuthal variations of power density in the reactor. Power tilting has been observed in the present TREAT-facility reactor. To obtain a gross estimate of the magnitude of such a tilt, a highly simplified model of the slot was adopted, representing it as a thin medium, at $\theta = o$, that is "black" to neutrons of all energies. Only that portion of the slot outside the modified zone was represented in this way. The extension of the slot into the modified zone was not included. Then a two-dimensional (r, θ), 18-group diffusion-theory calculation was made of the cold clean system to obtain power densities for comparison with power densities in the absence of the slot.

There results a gross tilting of power density toward the side of the reactor ∿180° away from the slot. The volumetric power densities are increased 20% at the peak in the unmodified zone, and 7% in the middle of the (graphite-matrix) modified zone, relative to the power density at the center of the test cluster. There is a large azimuthal sector near $\theta = 180°$ where the radial distribution of power density is almost asymplotic. Near the slot there are very large depressions of power density, because of the highly conservative model for the slot.

In optimization calculations, azimuthal tilts of this magnitude are, to large measure, counteracted by effects of heating in the reactor that induces tilts toward the test cluster. Detailed studies will be made with realistic modeling of the slot.

A-4.6 Relative Reactivity-control Effectiveness: Modified Reactor vs Unmodified Reactor

The conceptual-design plan is to move the present inner ring of 8 control-rod fuel assemblies to core locations farther from core center, well into the unmodified zone. As discussed in Appendicies A-1 and A-2, this shift is expected to provide adequate reactivity control in the various functions of the control system. To provide additional background data, highly simplified scoping calculations have been run to compare reactivity-control effectiveness of the modified and unmodified reactors. This represents the beginning of the calculational effort that will be required to delineate fully the capabilities of each type of control rod in the modified reactor.

The comparison starts with cold, clean reactors. Then natural boron is added uniformly in the radial ring from ∿0.516 m to 1.065 m that composes the unmodified zone in the upgraded reactor. The inner boundary of this ring is the outer boundary of the area-equivalent modified zone. The relative changes in reactivity for modified vs. unmodified reactors give a gross indication of the realtive effectiveness of the totality of control rods in these two reactors. Results are summarized in Table A-4.3. The calculations were made for a modification utilizing Inconel 600.

TABLE A-4.3 Relative Reactivity-control Effectiveness: Modified Reactor vs. Unmodified Reactor (In Region from 0.516 m to 1.065 m) [Inconel-600 Can Walls and Heat Shields]

Change in Reactivity in Unmodified Reactor, %	Ratio of Reactivity Changes: Modified/Unmodified
- 6.1	0.78
-11.8	0.75
-14.9	0.69

A-4.6 Relative Experiment-performance Characteristics: Reference Modified Reactor vs. Unmodified Reactor

Diffusion-theory calculations have been performed for the reference 19-pin and 61-pin cases in the cold clean fully loaded TREAT-facility reactor without a modified zone to afford gross comparisons with corresponding calculations for the reference modified reactor. Application of diffusion theory to such heavily absorbing test vehicles and test clusters is less accurate

for the unmodified reactor. As yet, transport-theory calculations are not avialable. There are, however, clues as to the trend of differences between diffusion theory and transport theory, and as to general magnitudes of the differences, from still earlier calculations with a 37-pin target of FTR/CRBR-size fuel pins of PuO_2-UO_2 with fully enriched UO_2. No filter was included. The calculations were 16-group calculations, with two groups of thermal neutron energies. The calculated nodal max/min across the test cluster in diffusion theory was ∿15% higher than in transport theory. The calculated energy generation in the center of the test cluster of ∿20% lower in diffusion theory than in transport theory..

When a cadmium filter is included, with effects simulated by use of black-boundary conditions on the neutron flux in the appropriate energy groups where the cadmium is "black," the accuracy of the comparisons of diffusion-theory results is improved. In the perspective of these cautionary notes, the results of the diffusion-theory calculations are summarized in Table A-4.4. Included are calculations with and without a cadmium filter, and for the 19-pin and 61-pin test. The majority of the calculated results for the modified reactor were obtained in calculations in which Inconel 600 was utilized for the can walls and heat shields. Some data are included also for a 19-pin cluster in a system utilizing ARMCO 18 SR in place of Inconel 600. There are small changes in calculated experiment performance if ARMCO 18 SR is used.

In brief summary, with a cadmium filter the principal difference in experiment-performance potential between the modified and unmodified reactors lies in the potential magnitudes of the fission-energy generation in the center of the test cluster. This applies both to the reference 19-pin cluster of prototypic-enrichment advanced-oxide test pins, and the reference 61-pin cluster of FTR/CRBR-size test fuel pins with fully enriched UO_2 (no plutonium). As may be observed in Table A-4.4 there are also somewhat improved characteristics of flatness of the radial distributions of fission power density across the test clusters.

A-4.7 Early Scoping Calculations: Effects of Variations in Neutronics Models and in Multigroup Parameters

In the first phase of the conceptual-design work, the focus was on a 61-pin test cluster of Advanced-oxide-size fuel pins with 27% PuO_2 and 73% fully enriched UO_2. The preliminary test-vehicle configuration selected was smaller diametrally than the present reference 19-pin test vehicle. Also, in

TABLE A-4.4 Comparison Diffusion-theory Calculations* of Potential Experiment Performance: Modified Reactor vs. Unmodified TREAT-Facility Reactor (Inconel Can Walls and Heat Shields)

	19 Advanced-oxide Pins of Prototypic Enrichment				61 FTR/CRBR-size Pins of Fully Enriched UO_2			
	Unmodified Reactor		Modified Reactor		Unmodified Reactor		Modified Reactor	
	No Filter	Cadmium	No Filter	Cadmium	No Filter	Cadmium	No Filter	Cadmium (Reoptimized Reactor
Fission Energy Generated in Center of Center Test Fuel Pin, kJ/kg	1500	1350	2535 (2415)**	2360	2675	2215	4950	4500
Nodal Max/Min Across Test Cluster***	7.3	1.36	2.26 (I.27)**	1.26	3.14	1.40	1.56	1.33
Ratios of Pin-averaged Fission Power Density								
4th ring/center	NA	NA	NA	NA	2.07	1.31	1.38	1.26
3rd ring/center	NA	NA	NA	NA	1.27	1.16	1.17	1.14
2nd ring/center	2.94	1.23	1.44	1.17	1.09	1.07	1.07	1.06
1st ring/center	1.12	1.06	1.05	1.05	1.02	1.02	1.02	1.02
Max/Avg. of Fission Power Density in Outermost Test Fuel Pins	2.45	1.10	1.57	1.07	1.51	1.06	1.13	1.05

* XSISO 18

** Data for a system with ARMCO 18 SR can walls and heat shields.

*** Twelve spatial nodes in the outermost fuel pins.

those early, scoping calculations, the concept of the modified fuel assembly involved a larger volume fraction of fuel and a smaller volume fraction of Inconel 600. Nevertheless, the trends and approximate magnitudes of effects of variations in some of the multigroup parameters and neutronics model are of interest also for the conceptual-design reference modification.

Two variations of particular interest are: the effects of the magnitude of the axial reflector savings on reactivity and on other neutronics characteristics and the choice of the model of scattering of thermal neutrons by the graphite in the graphite-matrix fuel and in the graphite reflector. In all of the calculations discussed in Appendix A-3 for the reference modifications, a reflector-savings value of 0.15 m was used for each of the axial reflectors of the modified zone. This is believed to be a reasonable, conservative estimate. It includes effects of the extended heat shield and can of the modified fuel assembly, and also effects of whatever neutron poisoning might be needed in a portion of the axial reflectors to limit power spikes in the modified fuel assemblies. Among the earlier calculations were studies of the effects of uncertainties in the axial reflector savings. Over a total range from 0.15 to 0.25 m, the maximum reactivity change was $\sim$0.8%. The reactivity change is the principal neutronics effect.

For an earlier reference single-zone, 7 x 7 modification without a neutron filter, comparison calculations were made to investigate the effects of choice of the model for scattering of thermal neutrons by graphite. The ENDF/B-IV $S(\alpha,\beta)$ scattering representations have been used consistently for the calculations for the conceptual-design reference systems. This is believed to be the best present information for the graphite scattering parameters. Nevertheless, for comparison purposes, and to explore the sensitivity of the neutronics characterization to the choice of this model, calculations were performed also for a free-gas model of thermal-neutron scattering for that earlier reference modification,. For each of these two scattering models the full 7 x 7 modified zone was optimized to a peak temperature of 1375K throughout. With the $S(\alpha,\beta)$ scattering model the reactivity was 0.9% smaller; the calculated potential fission-energy generation in the center test pin was $\sim$4% larger; the calculated nodal max/min of fission power density across that 61-pin cluster was higher (2.37 vs. 2.23; and the optimized uranium concentrations in the various regions of the modified zone were within 4% of the corresponding concentrations for the free-gas model.

APPENDIX A-5

Plutonium-release Considerations

A. Factors Limiting Release from Facility

We will examine factors which will cause release from the building to be less than 100% of the test inventory in an actual release event.

To this end we hypothesize a 100% fuel release from the experiment vehicle to the reactor cavity, and a scenario resulting in partial release to the reactor room and eventually from the reactor building. At this time no fallout, agglomoration, or plate-out is credited, either in the reactor cavity, the reactor room, or externally on the way to the receptor.

This study examines the mechanisms required to move the fuel from the reactor cavity out into the reactor room and from there out of the building. If the TREAT cooling is operating, release will be into the reactor cavity, then into the ducts, and finally to the filters. This case will not be considered further.

The only mechanism available for the first movement (assuming reactor coolant system is not operating) is to use the heat in the fuel and from burning sodium to heat the air in the reactor cavity, increasing the gas-aerosol volume of the cavity at constant pressure. The fractional change in volume (f_{v_c}) required to maintain the pressure at ambient is the fraction of the gas-aerosol mixture which leaves the cavity and enters the reactor room.

The mechanism for effecting the second movement (out of the building) is to use the incremental enthalpy (above room ambient temperature) of the gas-aerosol mixture leaving the reactor cavity plus the heat provided by burning the remaining sodium aerosol which leaves the cavity to heat the gas-aerosol mixture in the reactor room. As in the cavity, a volume change is effected (at constant pressure) which must leave the building to maintain ambient pressure. This fractional change (f_{v_r}) is the fraction of gas-aerosol mixture in the reactor room which will leave the building.

Determination of f_{v_c} and f_{v_r} solves the problem of determining an upper limit on the amount of plutonium leaving the building, $(w_{Pu})_{out}$, since:

$$(w_{Pu})_{out} = (w_f)\ (f_{v_c})\ (f_{v_r})\ (\text{w/o of } PuO_2)\ (239/271);$$

w_f = weight of fuel in experiment facility. The basic scenario for plutonium escape from the reactor building used in the calculation is as follows:

1. The experiment contains w_f grams of UO_2-PuO_2 fuel, w_{Na} grams of sodium, and w_{ss} grams of stainless steel inside the pressure vessel over the active fuel length. 1000 cal has been added to each gram of fuel (total = 1000 w_f cal).
2. The above defined fuel, sodium, and stainless steel (originally at an ambient temp = 873K) are assumed to form a vapor-aerosol mixture which escapes from the experiment to the reactor cavity, which contains a 361-element-array core.
3. Heat is transferred from the vapor-aerosol mixture to the air in the reactor cavity and to the Zircaloy-plus-aluminum-sheet clad encasing the four sides of the core and the coolant holes.
4. At the same time the sodium and the oxygen of the cavity air interact to form Na_2O, releasing 1600 cal/g of Na_2 formed and depleting the oxygen from 20% to 5% (threshold). (Some stainless steel burns also, but very little is in vapor form on entering the cavity. Also, the heat release on burning ss is ∿780 cal/g of oxides formed.)
5. The energy imparted (heat of formation) goes to heat further the gas-aerosol mixture plus the zirconium and aluminum.
6. The cavity is assumed to be leaky, so that sufficient gas-aerosol mixture leaves the cavity for the reactor room (originally at an ambient temp of 300K) to maintain the pressure at ambient.
7. The remaining sodium interacts with the oxygen in the reactor room air, releasing the heat of formation of 1600 cal/g of Na_2O.
8. This burning heat plus the heat content above the room ambient of the gas-aerosol mixture heats the room air. The resulting gas aerosol-mixture volume change leaks out of the assumed leaky reactor building. Results are given in Table A-5.1.

The fraction leaking out defines the maximum amount of plutonium which can escape to the environment from the reactor building. Calculations for maximum plutonium release were performed using the following basic data and assumptions:

1. It was estimated that there are ∿730 cubic feet (20.7 m^3) of air in the reactor cavity @ 600°C, composed of 1.7 kg of O_2 and 6.4 kg N_2. The 1.7 kg of O_2 available for burning sodium and stainless steel.

TABLE A-5.1 Plutonium Released

No. of Pins	w_f (weight of fuel), g	w_{Na} (weight of sodium), g	w_{ss} (weight of stainless steel), g	ΔT_c, K	f_{v_c}	ΔT_R, K	f_{v_R}	Pu out, g
217	44000	16100	31800	734	0.320	16.7	0.0526	163
169	34300	12600	24800	636	0.272	9.3	0.0302	62.0
127	25800	9470	18700	541	0.221	5.0	0.0163	20.4
91	18500	6790	13400	452	0.167	2.1	0.00702	4.91
61	12400	4550	8970	364	0.107	0.62	0.00206	0.603
37	7500	2750	5420	257	0.022	0.08	0.000272	0.0097
19	3900	1430	2820	177	-0.103*	θ	0	0
7	1420	520	1030	66	-0.128*	θ	0	0

*Inleakage from O_2 depl.

Assumptions: 8.1 kg of air in reactor cavity
3750 kg of air in reactor room
228 kg of Zircaloy in cavity
122 kg of aluminum in cavity
PuO_2 is 25 w/o of fuel
Pu is β^9Pu

Fission heat input to fuel = 1000 cal/g of fuel

In forming the sodium oxide (Na_2O), the Na/O consumption ratio is 2.875, and 2157 cal/g of sodium are released. In forming the stainless steel oxides (Fe_3O_4, CrO_3, and NiO), the oxygen-to-metal mass-consumption ratio is 2.107, and 1155 cal/g of stainless steel are released. The ambient temperature in the reactor cavity at time of release from the experiment facility is assumed to be 873K.

2. The thin Zircaloy and aluminum clads [at the lateral surfaces of the 361-element core and forming the 324 cooling channels, 3/8 in. (9.5 mm) square and 8 ft (2.4 m) long, which will absorb heat from the gas-aerosol mixture leaving the experiment] weigh 228 kg and 122 kg, respectively.
3. Values of the specific heats chosen are:

Material	Specific Heat (cal/g-°C)
Na	0.30
Na_2O	0.28
O_2	0.22
N_2	0.25
Zr	0.08
Al	0.25
fuel	0.09
SS	0.15
SS oxide	0.17

4. It is estimated that the building air contains ∿790 kg O_2 and 2960 kg N_2 at 300K.
5. The original ambient temperature in the reactor cavity at the time of release from the experiment is 873K.

B. Acceptable Release for Given Meterological Conditions

Calculations were made to provide a preliminary evaluation of the impact on experiments using 19 advanced mixed-oxide pins when the 150-g limit was removed, and meterological limits were retained. The assumptions in Appendix M of the TREAT operating instructions and for MPBB, breathing rate, bone-retention factor and release fraction were used. Calculations were done for distances of 760 m (TREAT control building), 1300 m (EBR II Complex), and 15,000 m (ARA). These calculations were performed for stability conditions A, B, C, and D. For wind blowing directly to a receptor at each of the three locations, allowable releases are low at TREAT control and EBR II, compared

with an assumed 1500-g ^{239}Pu equivalent for 100% release of the plutonium in the 19 pins. As a receptor moves off the center of the release plume by angle $\Delta\theta$, the dose decreases relatively rapidly. As shown in part II of Table A-5.2, a wind direction 15° off the TREAT control building is sufficient to permit a release of 1500 g ^{239}Pu equivalent for a wind speed of 1 m/s or more. A slightly smaller angle is sufficient for EBR II. For the assumed release of 1500 g ^{239}Pu equivalent, a "No-No" receptor sector of 270°-330° wind direction is adequate to keep the receptor dose below limits at TREAT control and EBR II. The "No-No Sector" for 15000 m (ARA) is 50°-70° for wind speeds of <12.9 kw/s. EBR II meteorlogical data show that the acceptable conditions occur approximately 90% of the daytime.

TABLE A-5.2 Maximum Allowable Releases of Plutonium

I. Breathing Rate = 3.45×10^{-4} m^3/s
Bone-retention Factor = 0.2
Receptor on Plume ℄
Nonoccupational MPBB = 0.0625 μg ^{239}Pu (equiv)

Stability Type	x = 760 m g ^{239}Pu at	g Pu-239 at 1300 m	g Pu-239 at 15000 m
As*	96.9	562.	11891
Aw	96.9	303	2558.5
Bs	29.3	100	8288.5
Bw	29.3	100	2014.4
Cs	11.2	27.3	2086.4
Cw	11.2	27.3	1409.0
D	4.50	9.69	385.58

*"S" denotes spring and summer, while "w" denotes fall and winter.

TABLE A-5.2 Maximum Allowable Releases of Plutonium (Contd.)

II

To perform an experiment with 100% release of 1500 g β^9Pu (equiv) would require a value of $\bar{u}\ F_\theta$ = 33 @ 760 m, 155 @ 1300 m, 389 @ 15000 m.

$\bar{u}$ = Wind Speed,	$\Delta\theta$ required, degrees		
km/s	760 m	1300 m	15000 m
1.6	14.7	13.3	4.8
4.35	13.5	12.1	2.5
7.56	12.7	11.3	0
11.6	12.1	10.6	0